LOCKHEED MARTIN ENERGY RESEARCH LIBRARIES
3 4456 0513734 9

CENTRAL RESEARCH LIBRARY

ORNL-TM-4340

cy. 1

WATER RESEARCH PROGRAM

FINAL REPORT COVERING THE PERIOD MARCH 15, 1966, TO OCTOBER 31, 1972

CORROSION STUDIES for the OFFICE OF SALINE WATER U.S. Department of the Interior

OAK RIDGE NATIONAL LABORATORY
CENTRAL RESEARCH LIBRARY
DOCUMENT COLLECTION
LIBRARY LOAN COPY
DO NOT TRANSFER TO ANOTHER PERSON
If you wish someone else to see this document, send in name with document and the library will arrange a loan.
UCN-7969
(3-67)

OAK RIDGE NATIONAL LABORATORY
OPERATED BY UNION CARBIDE CORPORATION • FOR THE U.S. ATOMIC ENERGY COMMISSION

This report was prepared as an account of work sponsored by the United States Government. Neither the United States nor the United States Atomic Energy Commission, nor any of their employees, nor any of their contractors, subcontractors, or their employees, makes any warranty, express or implied, or assumes any legal liability or responsibility for the accuracy, completeness or usefulness of any information, apparatus, product or process disclosed, or represents that its use would not infringe privately owned rights.

ORNL-TM-4340

Contract No. W-7405-eng-26

WATER RESEARCH PROGRAM FINAL REPORT

Covering the Period March 15, 1966, to October 31, 1972

CORROSION STUDIES

The Corrosion of Copper and Copper Alloys in High-Temperature Sodium Chloride Solutions

J. C. Griess, Jr., A. L. Bacarella, and E. G. Bohlmann
Reactor Chemistry Division

For the
OFFICE OF SALINE WATER
F. H. Coley, Materials Division
U.S. DEPARTMENT OF THE INTERIOR
OSW-AEC INTERAGENCY AGREEMENTS 14-01-0001-937 and 14-30-2536

OCTOBER 1973

OAK RIDGE NATIONAL LABORATORY
Oak Ridge, Tennessee 37830
operated by
UNION CARBIDE CORPORATION
for the
U.S. ATOMIC ENERGY COMMISSION

LOCKHEED MARTIN ENERGY RESEARCH LIBRARIES
3 4456 0513734 9

Owing to budgetary considerations, a minimum number of copies of this report has been reproduced. If you do not require a copy permanently, the return of this copy to Virginia Lee, Room E-28, 4500N, would be appreciated.

James S. Johnson, Jr.

James S. Johnson, Jr.

TABLE OF CONTENTS

	Page
Preface	iv
Abstract	1
Introduction	3
Weight Loss Data	4
Experimental Procedures	4
Results	9
Effect of Additives	9
No Additive	9
Cystine Addition	9
Sulfur Additions	12
Oxygen Additions	15
Sulfite Addition	16
Corrosion of Other Alloys	16
Effect of Temperature	17
Effect of Velocity	19
Effect of Surface Area to Volume Ratio	27
Electrochemical Data	29
Experimental Procedures	30
Results of Anodic Polarizations	36
Copper	36
Nickel	38
Copper-Nickel Alloys	38
Other Alloys	49
Effect of Sulfide Additions	53
Anodic Passivation of 70-30 CuNi	55
Results of Cathodic Polarizations	63
Loop Data	63
Laboratory Data	72
Discussion	82
Acknowledgement	104
References	105
Appendix; Papers published in the Open Literature	107
"Crevice Corrosion of Titanium in Aqueous Salt Solutions," J. C. Griess, Jr.	108
"Analysis of Protective Oxide Films on Copper-Nickel Alloys by Photoelectron Spectroscopy," L. D. Hulett, A. L. Bacarella, L. LiDonnici and J. C. Griess	123

PREFACE

The Water Research Program at the Oak Ridge National Laboratory, sponsored by the Office of Saline Water, U.S. Department of the Interior, was authorized in March 1962 and has operated interagency agreements between the Department of the Interior and the U.S. Atomic Energy Commission. Results of the work carried out under this program have been reported on a regular basis to the Office of Saline Water (see page ii for the list of reports), and completed portions of the work were published in the open literature.

Work in the Program concerned with corrosion, supported by the OSW Materials Division under Dr. Francis H. Coley, has been reported in the first biennial progress report (March 15, 1962 to March 15, 1964), ORNL-CF-67-8-55 (OSW R & D Progress Report 302) and for the second biennium (March 15, 1964 to March 15, 1966) in combination with the biennial report for "Reactions and Transport Phenomena at Surfaces" because the work in these fields was so closely related; a joint report (ORNL-TM-4097) is in preparation. The present final report covers work in "Corrosion Studies" from the third biennium (starting March 15, 1966) to October 31, 1972, which was the termination date of work in this category under support of the Office of Saline Water.

Most of this report deals with the corrosion of copper and copper alloys under conditions of interest in desalination by distillation, that is, in high-temperature sodium chloride solutions. Other work in the program, mainly carried out early in the period covered by this report, has been concerned with the corrosion of aluminum and titanium, and the crevice corrosion of titanium. For completeness of presentation in this final report, direct reproduction of journal articles reporting these phases of the program are included in the Appendix. We are grateful to the Elsevier Publishing Company, 52 Vanderbilt Avenue, New York, New York 10017, for permission to reprint the complete texts of these articles. A notation of the source appears at the head of each reprinted article. Support of work cosponsored by the U.S. Atomic Energy Commission is acknowledged in the individual articles.

The desalination program at the Oak Ridge National Laboratory has two branches: the Water Research Program directed by K. A. Kraus up to July 12, 1971 and since that time by J. S. Johnson, Jr., and the Nuclear Desalination Program directed by R. P. Hammond. This report is the final report of the Water Research Program, Corrosion Studies, which has been coordinated by E. G. Bohlmann.

THE CORROSION OF COPPER AND COPPER ALLOYS IN HIGH TEMPERATURE SODIUM CHLORIDE SOLUTIONS: FINAL REPORT TO THE OFFICE OF SALINE WATER

J. C. Griess, Jr., A. L. Bacarella, and E. G. Bohlmann

ABSTRACT

During the past six years a program concerning the corrosion of copper and copper alloys was conducted for the Office of Saline Water, U.S. Department of Interior, at Oak Ridge National Laboratory. This program was recently terminated for lack of funding. The present report summarizes the important results obtained while this program was in existence. Although much new information was developed which yields new insights into the corrosion mechanisms of the copper-nickel alloys in saline waters, questions whose resolution require further work remain, and the results and their interpretation are incomplete.

The experimental program consisted of two parts: a determination of weight losses of specimens exposed under given conditions of temperature, flow rate, and various additives; and an electrochemical investigation of corrosion mechanisms.

Corrosion rates of a variety of copper alloys were determined by exposing specimens in deaerated 1 m NaCl flowing between 3 and 15 fps at temperatures as high as 200°C. At lower temperatures the copper-nickel alloys had lower corrosion rates than the brasses and copper, but at 175 and 200°C the reverse was generally true. Addition of oxygen to the solution at 125°C (the only temperature investigated) resulted in very high rates for Admiralty brass but had little effect on the general corrosion of 70-30 and 90-10 CuNi and Monel 400. (Copper was not exposed.) However, in the presence of oxygen 70-30 CuNi underwent crevice attack and Monel 400 pitted. The presence of low levels of sulfide had a detrimental effect on all alloys tested except Admiralty brass which corroded no more in the presence of sulfide than in its absence. Within the range investigated no significant effect of velocity was noted with either sulfide or oxygen. On the other hand, cystine produced a detrimental

effect on all materials, and the corrosion rate was higher the higher the flow rate.

The effect of very high velocities on 90-10 and 70-30 CuNi in deaerated 1 m NaCl was investigated at 125°C. Over the range of 20 to 100 fps no clearcut effect was found, but when oxygen was added to the system copper deposited on the leading edges of the coupons. A similar effect was noted in one test with Admiralty brass.

Both anodic and cathodic polarizations were performed with several copper-nickel alloys, copper, and nickel. At temperatures up to 175°C (the highest temperature investigated) anodic Tafel slopes for pure copper were equal to 2.3 RT/F. At a fixed potential the anodic current was dependent on the solution velocity, indicating diffusion control. A simple kinetic expression based on the Nernst Equation and Fick's First Law was derived which was in excellent agreement with the experimental results. Nickel, on the other hand, dissolved anodically under activation control, and consequently its dissolution rate was independent of velocity; Tafel slopes were equal to 2/3(2.3 RT/F). Copper-nickel alloys containing from 70 to 10% copper exhibited the same Tafel behavior as copper up to some temperature between 125 and 150°C; at 150°C and above the slopes were the same as for pure nickel. The Tafel slope for 80-20 CuNi changed between 150 and 175°C, but with 90-10 CuNi the slope was the same as that for pure copper at 175°C. No theoretical explanation for the change in mechanism from diffusion to activation control at high temperatures has been obtained to this time.

At sufficiently high anodic current densities the copper-nickel alloys and nickel demonstrated a passive-type behavior. Passivation also occurred spontaneously with sufficient oxygen in the solution. Examination of surface films formed on 70-30 CuNi in the passive region showed a significant enrichment of nickel over copper in the films.

Cathodic polarization curves were obtained with copper and 70-30 CuNi and cathodic processes involving the reduction of oxygen, protons, $CuCl_2^-$, and water were studied. The kinetic order for proton reduction and the activation energy for the reduction of protons and water were determined.

INTRODUCTION

The presence of low levels of certain impurities in aqueous environments can have a profound influence on the behavior of metals and alloys exposed to these environments. For example, only a few parts per billion of heavy metal ions in water or other aqueous solutions can produce severe pitting on aluminum,[1] and only a few parts per million of chloride ions can cause disastrous failures in austenitic stainless steels.[2] Similarly it is a well established fact that certain materials in saline waters, some the result of man made pollution, can produce enhanced corrosion of copper and copper alloys.[3] Thus an evaluation of the effects of impurities on corrosion is an essential part of any corrosion investigation.

This report summarizes the results obtained during the last six years from a study aimed at evaluating the effects of selected impurities in saline waters on the corrosion of copper and copper alloys. Basic to a determination of impurity effects is a determination of the behavior of the materials in the absence of impurities. Therefore considerable experimentation was carried out in pure solutions to establish base-line information and to determine the effects of other variables such as temperature and solution flow velocity on corrosion.

This study, which was sponsored by the Office of Saline Water, U.S. Department of the Interior, consisted of two related parts: a determination of weight losses of specimens exposed to controlled environments, and an electrochemical investigation of electrode processes. The first type of investigation gives direct information on the extent and type of corrosion whereas the latter type yields information about corrosion mechanisms. Although the two parts are complementary, for convenience the results are treated separately in this report. Although funding of this program was terminated with many questions outstanding, we have developed much useful and significant information about the behavior or copper and copper alloys, and to a lesser extent nickel, in sodium chloride solutions at temperatures as high as 200°C, and these results are presented in this report. It should be noted here that pure sodium chloride solutions, to which specific impurities were added when desired, were used in all cases. Thus the reported results, particularly those obtained by exposing specimens and determining weight changes, cannot be interpreted as being directly applicable in sea water.

WEIGHT LOSS DATA

Experimental Procedures

All of the experiments carried out in this part of the program were conducted in two pump loops in which all surfaces exposed to the circulating solution were titanium. These loops were designed and built for another program and had been used for many thousands of hours to circulate uranyl sulfate solutions at temperatures up to 300°C prior to their use with sodium chloride solutions. Each loop was constructed of 1½-in. sch. 80 titanium pipe, and a 100 gpm canned motor pump circulated the solution.

Each loop contained three parallel flow channels in which corrosion specimens were exposed. The flow through the channels could be individually controlled by use of calibrated orifice plates. The loops were operated completely full and a pulse pump and let-down valve allowed the solution in the loop to be replaced without interrupting the run. The volume of each loop was about 25ℓ and in the tests reported here the solution was continually refreshed at the rate of 1ℓ/hr. Electrical heating elements cast in aluminum around portions of the piping allowed heating of the loop solution to any desired temperature. Although the loops were capable of operation as high as 300°C, temperatures did not exceed 200°C in this program. The loop pressure was maintained by the let-down valve, and in the experiments described in this report the pressure was usually set about 100 psi above the solution vapor pressure.

The test specimens in most tests were small cylinders 1.38 in. long and 0.20 in. dia. and were mounted in a holder as shown in Fig. 1. The individual specimens were electrically insulated from the titanium holder with Teflon sleeves and the two halves of the holder were clamped together with titanium bands. Two assembled holders were fitted into each of the parallel flow channels of the loop. Special gaskets centered the holders in the pipe sections and forced the flow through the rectangular flow channel of the holder. In most tests a variety of different specimens was exposed in the same holder.

All of the materials from which the specimens were machined were obtained from commercial vendors. The compositions of the alloys are shown in Table 1. Although the principal purpose of this program was to obtain data on copper alloys, in a few runs other materials were exposed

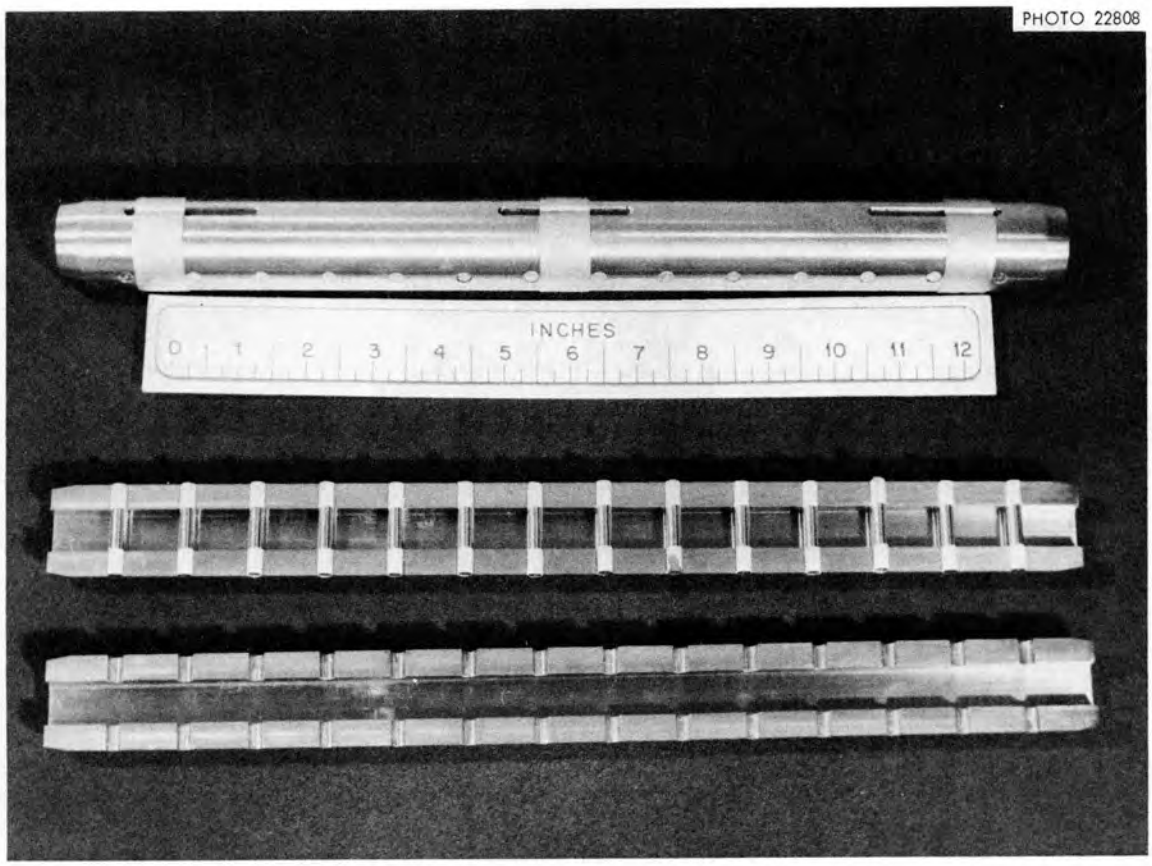

Fig. 1. Pin-Type Test Specimens in Pin Holder and Fully Assembled Holder.

to determine their corrosion resistance in some environments.

Table 1. The Composition of the Alloys Tested in Weight Percent

Alloy	Cu	Ni	Zn	Fe	As	Cr	Mo	W	Al
90-10 CuNi[a]	bal.	10.1	0.10	1.47	--	--	--	-	--
70-30 CuNi[a]	bal.	29.9	0.10	0.67	--	--	--	-	--
Adm. Brass[a]	70.7	--	bal.	0.01	0.05	--	--	-	--
Al Brass	bal.	--	22	--	0.04	--	--	-	2
CDA-194	bal.[b]	--	0.1	2.5	--	--	--	-	--
Monel 400	30	bal.	--	1.4	--	--	--	-	--
Inconel 600	--	bal.	--	7	--	16	--	-	--
Hastelloy C	--	bal.	--	6	--	17	17	5	--
316 SS	--	12	--	bal.	--	17	2.5	-	--
304 SS	--	9	--	bal.	--	19	--	-	--

[a]Certified mill analysis
[b]Contained also 0.025P

Specimen preparation consisted of degreasing the machined specimens in acetone, drying and weighing before mounting in the holders. Occasionally at intermediate times the test was interrupted, the samples were removed, rinsed in deionized water, dried at 100°C, weighed, and then returned to test. Also at times some of the specimens were removed and replaced with new specimens of the same alloy. At the completion of a test all specimens were defilmed, dried and weighed and corrosion rates were calculated from the observed weight loss and exposure time. Defilming was accomplished by immersion in either 10% H_2SO_4 solution at 80°C or 10% KCN solution at room temperature. Those specimens which developed sulfide scales could only be defilmed in the latter solution, whereas the other specimens were quickly descaled in either solution.

The procedure for conducting a test consisted of placing the specimen holders in flanged pipe sections and closing the loop. The loop was then evacuated and filled with the test solution contained in a 55-gal plastic-lined drum by means of the pulse pump. Once full the circulating pump was turned on and the feed rate was reduced to 1ℓ/hr. The let-down solution was discarded.

In all tests the feed solution was 1m NaCl prepared from reagent grade salt and deionized water (sp. resistivity > 10^6 ohm-cm) and the pH ranged from 6.3 to 6.7. In those tests where the solution is reported to be "deaerated" the solution in the feed tank was sparged with pure nitrogen overnight before filling the loop and continuously during the test. Several different analyses of the solution by a modified Winkler method showed oxygen concentration between 30 and 50 ppb. When sodium sulfide was added to the loop the same procedure as above was used except an additional small pulse pump was used to inject about 50 mℓ/hr of a relatively concentrated sulfide solution which was not sparged with nitrogen but only blanketed with it. Sparging such solutions removed much of the sulfide as H_2S. A similar procedure was used when sodium sulfite was the additive. In those tests in which H_2S was added the entire feed tank was continuously sparged with a mixed gas containing a nominal 0.5% H_2S in nitrogen. Under our conditions this resulted in an H_2S concentration of 10 to 15 ppm in the let-down stream. Sparging the feed tank with filtered air resulted in an oxygen concentration of 6 ppm and this was the solution used when the solution contained added oxygen. In those runs where cystine was an additive to the solution, the appropriate amount of cystine was dissolved in the nitrogen-sparged 1m NaCl solution. Cystine is a component of human

waste and is sometimes found in polluted sea water. Its formula is $[-S-CH_2-CH(NH_2)-COOH]_2$.

RESULTS

The constancy of the corrosion rate with time in all cases was established by removing and weighing specimens at intermediate times. In all cases except when the solution contained sulfide the quantity of film developed on the specimens was nearly insignificant so that the true specimens weight losses could be approximated without defilming the specimens at the intermediate times.

Effect of Additives - The effects of several individual additives on the corrosion of selected copper alloys were determined at 3, 7, and 15 fps at 125°C. At least three specimens of each alloy were exposed under each condition. In all cases the time of exposure was about 1500 hr except with oxygen present when the time was only 730 hr. Table 2 shows the corrosion rates calculated from the measured weight losses. Of the two values shown, the first is the average corrosion rate at 3 fps and the second is that at 15 fps; in nearly all cases rates at 7 fps were between the values shown. The effect of the individual additives is discussed below.

No Additive - In deaerated 1m NaCl all corrosion rates were low and the agreement between replicate specimens was excellent. Only on Admiralty brass was a significant velocity effect noted from the weight loss data, but visually attack looked uniform on all pins. All specimens were covered with uniform tarnish-like films and no evidence of any form of localized attack was noted.

Cystine Addition - The addition of 10 ppm cystine to deaerated 1m NaCl increased the corrosion rate of all alloys, and it was particularly

Table 2. The Corrosion[a] Rates of Copper Alloys in 1m NaCl Containing Various Additives at 125°C

Alloy	No Additive	10 ppm Cystine	40 ppm Cystine	10 ppmS as Na_2S	10 ppmS as H_2S	6 ppm O_2	10 ppm[b] $SO_3^=$
70-30 CuNi	0.1-0.3	2.8-5.6	8.4-26	9-16	5.8-4.7	0.7-1.1	0.10-0.15
90-10 CuNi	0.8-0.7	2.8-5.6	22-59	7-20	11.6-9.9	1.2-1.2	0.16-0.28
Adm. Brass	2.2-3.3	2.8-5.6	18-110	0.8-1.7	3.3-3.1	39-42	0.14-0.19
Monel 400	0.1-0.1	2.8-5.6	6.4-31	1.9-1.3	2.3-2.5	1.0-1.5	0.08-0.14

[a]First rate at 3 fps, second at 15 fps; rates at 7 fps were between values shown, mpy.
[b]CDA-194 also exposed in this run; rates were 0.21-0.29 mpy.

interesting to note that all four alloys behaved in the same manner. At 3 fps all specimens showed no visible evidence of a velocity effect except two Admiralty brass specimens which at the end of the run appeared to have less film on the leading edge of the pin than on the rest of the surface, and two other specimens which had a few random pits. At 7 fps there was no evidence of a velocity effect but a few small pits were noted on one Admiralty brass specimen. The average corrosion rate of each alloy was 4.1 mpy. At 15 fps all Admiralty brass specimens showed visual evidence of a velocity effect toward the end of the run and clearly had thinner corrosion product films on the front and trailing surfaces than on the rest of the surface. Also one 90-10 CuNi specimen showed a similar effect. On all other specimens both the amount of film and corrosion were uniform.

The above data indicated that near the end of the 1500-hr run velocity effects were becoming apparent which were not evident during examinations at intermediate times. For that reason a second 1500-hr test was conducted and in this run the cystine concentration was arbitrarily increased to 40 ppm. As indicated in Table 2 much greater attack was noted than when the cystine concentration was 10 ppm. At 3 and 7 fps all specimens had thinner films on the leading surfaces of the specimens than on the rest of the surfaces and showed the greatest attack in that region, although after defilming it was obvious that attack had occurred to an appreciable extent over the entire surfaces. Those specimens exposed at 15 fps showed clear-cut velocity effects but the extent of attack varied from specimen to specimen indicating that film breakdown occurred at random times during the run. In all cases attack appeared to originate on the leading edges and in some cases extended over most of the surfaces. Except for greater corrosion on the leading edges attack was mostly uniform. Only a few shallow pits were noted on Admiralty brass specimens and on a few Monel specimens. Although all specimens were heavily attacked, 70-30 CuNi and Monel 400 showed better corrosion resistance than Admiralty brass and 90-10 CuNi.

The addition of either 10 or 40 ppm cystine to the 1m NaCl produced no changes in pH of either the feed or let-down solution. Although the solutions were not completely analyzed for cystine or other degradation products, no evidence of sulfide was present in the let-down stream. However x-ray diffraction patterns obtained from a film scraped from the surfaces of a 90-10 CuNi specimen showed the presence of both Cu_2S and Ni_3S_2. The quantity of film on the surfaces of the specimens was quite

small; certainly, the amount of sulfide in the film represented no more than a very small amount of the total sulfur in the cystine added to the loop.

Sulfide Additions - In addition to the data shown in Table 2 a series of 4 runs was made in which the sulfide-containing solution was circulated at four different temperatures for about 600-hr periods. The solution was deaerated 1m NaCl which contained nominally 10 to 15 ppm sulfide as Na_2S. At the time these runs were made, we did not have a rapid method for determining the sulfide concentration and the above concentration was based on a feed solution of a known concentration and an approximate feed rate. Hence the actual sulfide concentration may have been appreciably different. However since the same method was used in each case, the sulfide concentrations should have been nearly the same in all four runs. The corrosion rates calculated from average weight losses are shown in Table 3. Perhaps the most surprising features of the data in Table 3 are the high corrosion rate of 90-10 CuNi at 50°C and the relatively low corrosion rate of Admiralty brass at all temperatures. At 50°C all 90-10 CuNi specimens experienced very uniform attack and developed heavy black films, much of which spalled from the specimens on room-temperature drying. All other specimens developed only very thin films. At temperatures above 50°C both 90-10 and 70-30 CuNi corroded to about the same extent and developed heavy films. The 90-10 CuNi specimens developed large diameter, shallow pits at 100°C and above, but localized attack was not found on the other alloys.

Under all conditions Admiralty brass developed only thin adherent films and showed very low corrosion rates which were not greatly influenced by temperatures between 100 and 150°C. While Monel had the lowest

Table 3. Corrosion Rate of Four Copper Alloys in 1m NaCl Containing Nominally 10 to 15 ppm Sulfide Added as Na_2S

Temp. °C	Time hr	Alloy	Corrosion Rate, mpy 3 fps	7 fps	15 fps
50	600	90-10 CuNi	9.0	20	43
		70-30 CuNi	0.28	0.44	0.35
		Adm. Brass	0.29	0.42	0.43
		Monel 400	0.06	0.09	0.06
100	600	90-10 CuNi	5.9	12	26
		70-30 CuNi	5.9	8.3	14
		Adm. Brass	0.94	1.3	1.4
		Monel 400	1.6	2.4	2.7
125	640	90-10 CuNi	8.7	9.4	11
		70-30 CuNi	7.6	10	11
		Adm. Brass	1.0	2.0	2.3
		Monel 400	4.3	4.2	4.6
150	620	90-10 CuNi	16	16	15
		70-30 CuNi	11	12	16
		Adm. Brass	0.85	0.73	1.3
		Monel 400	7.0	7.5	8.5

corrosion rate at 50°C, its rate continued to increase with temperature so that at 100°C and above its corrosion rate was greater than that for Admiralty brass. The films formed on Monel were glossy and tightly adherent and showed no tendency to spall even on drying at 100°C. Particularly with the cupronickels, and to a lesser extent with the other two alloys, effects of velocity decreased as the temperature increased.

By the time the data presentedin Table 2 were obtained, a specific ion electrode which responded to sulfide ions had been acquired. The sulfide concentration in the let-down stream was monitored, and the feed rate was adjusted when the sulfide concentration deviated from 10 ppm. Thus those data shown in Table 2 were obtained under conditions as

specified. The corrosion results obtained with 10 ppm sulfur as Na_2S, however, are in reasonably good agreement with those shown in Table 3 at 125°C. Generally the appearance and corrosion rates were the same indicating that either the sulfide concentrations were the same or that sulfide concentration above some lower level has relatively little effect on the observed corrosion rates.

Since Na_2S is extensively hydrolyzed, the room-temperature pH of the solutions used in the above test was about 10. Thus the corrosion results could have been influenced not only by the presence of sulfide but also by the pH of the solution. Furthermore the form in which the sulfur exists in solution (H_2S, HS^-, or $S^=$) is pH dependent with H_2S predominating in acid or neutral solutions and HS^- and $S^=$ increasing as the solution becomes more basic. In view of the above considerations a second 1500-hr run was made in which H_2S instead of Na_2S was added to the solution. At the concentrations used H_2S produced no detectable change in the pH of the solution. The results of this test are shown in Table 2.

The appearance of the specimens was the same as in the runs in which Na_2S was added. The 90-10 CuNi specimens developed shallow pits and all other specimens experienced only uniform attack. There was a slight indication that 90-10 and 70-30 CuNi corroded at lower rates in the presence of H_2S, but in both of the runs there was an appreciable spread in weight changes of replicate specimens, and it was concluded that there was no significant difference in corrosion rates of the cupronickels between the two runs. X-ray diffraction patterns obtained from the scale on the cupronickel specimens showed the presence of both Cu_2S and Ni_3S_2. Both Admiralty brass and Monel 400 corroded at somewhat higher rates in the run

with H_2S than in similar runs with Na_2S and this may be a reflection of the pH difference. It was interesting to note that average corrosion rates were independent of velocity in this run whereas with Na_2S corrosion rates were higher the higher the flow rate.

Oxygen Additions - Comparison of the corrosion rates with and without oxygen in Table 2 shows that the presence of 6 ppm oxygen increased the corrosion rates of all materials but the effect was most apparent on Admiralty brass. Most of the Admiralty brass specimens corroded uniformly, but a few large-diameter pits were noted on the surface of some of the specimens. There was no evidence of a velocity effect and the specimens had the appearance of a heavily acid-etched surface. No significant crevice attack was noted between the Teflon insulation and the brass where the specimens were clamped into the holder.

The 70-30 CuNi specimens developed only very thin films on the surfaces exposed to the flowing solution and showed insignificant attack. However all of the specimens underwent significant crevice attack under the Teflon insulation. The attack was localized in that some areas under the Teflon were completely free of attack whereas adjoining areas underwent relatively heavy attack. Some localized crevice corrosion was observed on each of the 18 specimens. Since the corrosion rates listed in Table 2 are based on total weight loss which includes crevice attack, the true corrosion rates on the exposed surface areas were even lower than those shown in Table 2.

In contrast to the 70-30 alloy, 90-10 CuNi showed no susceptibility to crevice corrosion or any other form of localized attack. Monel 400 was subject to random and sometimes very severe pitting on the exposed surfaces.

In addition crevice attack was sometimes observed under the Teflon, but the extent of attack was less than with 70-30 CuNi. Except for the pits the surfaces of the Monel pins were covered with a smooth, thin, dark film.

Sulfite Addition - As noted previously the deaerated solution contained between 30 and 50 ppb O_2 and it was of interest to determine the corrosion rates of the alloys shown in Table 2 in the complete absence of oxygen. The results indicate that scavenging the last traces of oxygen with sulfite addition had very little effect on 70-30 CuNi and Monel 400, some effect on 90-10 CuNi, and the largest effect on Admiralty brass. Comparison of the results from the runs with no additive (30-50 ppb O_2) and with 6 ppm oxygen with the present run clearly shows that of the four alloys Admiralty brass was most influenced by the oxygen concentration. All alloys developed only very thin films and no form of localized attack was observed.

Corrosion of Other Alloys - Several other alloys were exposed to the 1m NaCl solutions in the runs with no additive and in the runs to which sodium sulfide was added. This included the two runs shown in Table 2 and most of the runs shown in Table 3. In those runs Hastelloy C was essentially immune to attack. Under the microscope the surfaces showed only a very lightly etched appearance and there was no sign of crevice attack under the Teflon insulation. Within the weighing accuracy weight losses could not be detected. Inconel 600 as well as 304 and 316 stainless steel also underwent negligible attack on the exposed surfaces but all three showed a tendency to undergo crevice attack under the Teflon. The frequency and severity of attack was greater on Inconel 600 than on the stainless steels.

The titanium loops showed no effect of the many thousands of hours of use with the solutions indicated in Tables 2 and 3. Particularly in the runs with 6 ppm O_2 severe crevice corrosion was anticipated and for that reason the run was continued for a lesser time than the others. Examination of the loop after the run with oxygen showed no evidence of crevice corrosion on the loop itself; however, severe crevice corrosion was noted on the clamping bands and on the few titanium pins exposed during the run. The results indicated that the protective film developed on the titanium loop during years of service with uranyl sulfate solutions greatly minimized or eliminated crevice attack, whereas in the absence of such a film on the new pins and clamping bands heavy crevice attack occurred. Light crevice attack was occasionally observed on the pins and clamping bands in the runs with "deaerated" solutions including those in which cystine was present, but attack of titanium was totally absent in the runs with sulfide and sulfite present. The latter two additives scavenge the last traces of oxygen from the solutions. Since crevice corrosion has its origin in a differential aeration cell,[4] the complete removal of oxygen should prevent crevice corrosion and this was indeed observed.

Effect of Temperature - In addition to the results shown in Table 2 a series of about 1500-hr loop runs was made to determine the effect of temperature on the corrosion rate of several copper alloys in deaerated 1m NaCl. The tests were conducted in the same manner as before and most runs were interrupted two or three times during the exposure to verify the constancy of the corrosion rates. The results are shown in Table 4.

Table 4. The Corrosion Rate of Copper and Copper Alloys in Deaerated 1m NaCl Flowing at 3, 7, or 15 fps

Material	Corrosion Rate, mpy 100°C	125°C	150°C	175°C	200°C
70-30 CuNi	0.08	0.2	0.4	1.7	3.8
90-10 CuNi	0.17	0.8	1	1.7	5.9
Adm. Brass	0.35	2.8	3	1.3	7.6
Aluminum Brass	0.39	-	-	-	12
Monel 400	0.07	0.1	0.3	2.2	2.4
CDA-194	0.39	-	4	1.6	4.6
Copper	0.33	-	-	1.0	3.0

Only at 125°C was a velocity effect apparent; at all other temperatures no significant difference existed among the weight losses for the pins of the same alloy exposed at 3, 7, or 15 fps. For that reason the average corrosion rate for each alloy is given in Table 4. However, at 150°C the spread among the replicate specimens was relatively large and the corrosion rate is reported to only one significant figure.

In all cases only uniform corrosion occurred and all specimens developed only very thin films which were easily removed. At 100°C all rates were very low. Both 70-30 and 90-10 CuNi and Monel 400 showed continually increasing corrosion rates with increasing temperatures while CDA-194 and Admiralty brass showed minimum rates at 175°C. Although copper was not exposed at 125 or 150°C it is probable that it would have behaved like CDA-194. In all tests except the one at 200°C the pH of the feed and let-down solution was in the range 6.3 to 6.7. At 200°C the pH of the feed solution was in that range but the pH of the let-down solution was 5.5 at the start of the run and gradually increased to about 6.0 after about 20 days. It is probable that the low pH contributed to the relatively high

corrosion rates at 200°C. No logical explanation can be given for the low pH at the highest temperature in spite of various efforts to ascertain one.

The most interesting aspect of the results was that the nickel alloys were considerably more resistant to corrosion than the other alloys at low temperatures, but above 150°C they were no more, and probably even less, resistant than copper and CDA-194. In fact at 175°C copper had the lowest corrosion rate of any material tested.

Effect of Velocity - Most of the data obtained with the pin-type specimens indicated little if any significant effect of the velocity of the flowing stream on the corrosion rates of the copper alloys. Only when cystine was in the solution was there visual evidence of attack which appeared to be attributable to high velocity. These observations were based on cylindrical specimens mounted across a flowing stream so that at all velocities the degree of turbulence was high. In an attempt to investigate the effect of velocity further a different type of holder which had been designed for another program and in which bulk solution velocities in excess of 100 fps could be achieved was used. Figure 2 is a photograph of a set of 10 flat specimens mounted in half a holder (titanium) and a fully assembled holder ready to be inserted in one of the bypass lines of a titanium loop. Each coupon was 1.40 x 1.38 x 0.20 in. and the edges were insulated from the holder with Teflon. The outside dimensions of the holder were the same as the pin-type holder. The flow channel in the holder was symmetrically tapered so that the highest velocity was at the axial midpoint with uniformly decreasing bulk velocities in either direction. In the tests described here the bulk flow through the holder was constant; the velocity range over the specimens was 20 to 102 fps. In the first

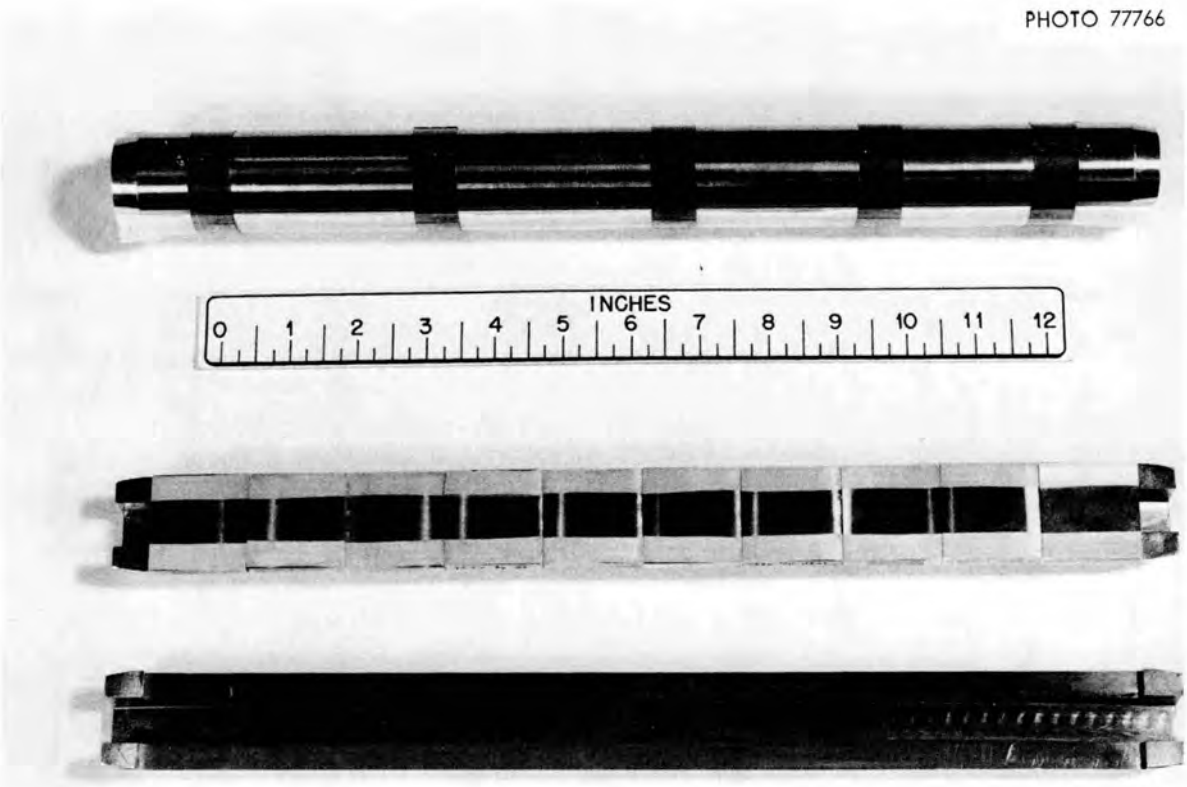

Figure 2. Corrosion Specimens Used for Velocity Studies and an Assembled Holder.

several runs five 90-10 CuNi specimens were in the front half of the holder, followed by five 70-30 CuNi specimens. The results obtained in deaerated 1m NaCl on the plain coupons are shown in Table 5. Also shown in the same table are the results obtained when an intentional flow disturbance was present on each coupon and in a run in which carbon steel was corroding in the system. In the former case a 1/16 in. diameter hole was drilled through each coupon near the leading edge and a pin of the same alloy was inserted through the hole so that it extended 1/16 in. beyond the surface of the coupon on each side. In the latter case smooth coupons were used but a pin holder containing a number of carbon steel pins (total surface area = 36.5 cm^2) was placed immediately upstream from the coupons.

Table 5 shows that in no case was a velocity effect noted. Excluding the first and last coupon in the holder, corrosion rates were generally no higher in the velocity range of 90 to 102 fps than at substantially lower velocities. Excessive attack on the lead and sometimes on the last coupon is frequently observed as is noted with the first run shown in Table 5. Why this effect is sometimes seen and other times not is not clear. The presence of the projections also made no difference either in corrosion or in visual appearance. While the presence of ferrous corrosion products in the solution significantly inhibited the corrosion rate of both alloys, no velocity effects were apparent on the specimens. As removed from the loop all were covered with a uniformly thin reddish black film. It has been reported that in saline waters the presence of ferrous corrosion products produces a film of lepidocrocite ($\gamma FeO \cdot OH$) on copper surfaces which inhibits corrosion.[5,6] It was interesting to note that such a film was able to form even at the highest flow rate and diminished the corrosion rate

Table 5. The Corrosion Rates of 90-10 and 70-30 CuNi Coupons in Deaerated 1m NaCl at 125°C

Velocity Range fps	Corrosion Rate, mpy					
	Plain Coupons		with Projections		with Carbon Steel	
	90-10 CuNi	70-30 CuNi	90-10 CuNi	70-30 CuNi	90-10 CuNi	70-30 CuNi
20-28	13	11	3.5	0.71	0.24	0.20
28-42	2.3	0.82	2.3	0.87	0.32	0.41
42-64	2.1	1.2	2.4	1.2	0.44	0.41
64-90	2.8	1.2	2.3	1.6	0.59	0.35
90-102	2.0	1.4	2.3	1.6	0.68	0.41

of both cupronickel alloys. Based on the weight loss of the carbon steel specimens and assuming a constant corrosion rate, the rate of addition of iron to the solution was 6.6 mg/hr.

It has been reported[7] that velocity effects on copper alloys in saline water are more severe at temperatures lower than 125°C and for that reason a 1098-hr test was conducted at 58°C. The test was made with deaerated 1m NaCl using coupons with turbulence promoters. The results showed no evidence of a velocity effect either visually or from weight changes. The 90-10 CuNi coupons corroded at an average rate of 1.0 mpy and the 70-30 coupons at 0.38 mpy.

Because cystine appeared to cause a velocity effect with pin type specimens another run identical to those above was made in which 10 ppm cystine was added to deaerated 1m NaCl solution. Also the effect of adding individually ∿ 5 ppm cuprous ions or 6 ppm oxygen was evaluated in other runs. These results are shown in Table 6.

Table 6. The Corrosion Rates of 90-10 and 70-30 CuNi Coupons in 1m NaCl Containing Various Additives at 125°C

Velocity Range fps	Corrosion Rate, mpy					
	10 ppm Cystine		6 ppm O_2		5 ppm Cu^+	
	90-10 CuNi	70-30 CuNi	90-10 CuNi	70-30 CuNi	90-10 CuNi	70-30 CuNi
20-28	22	13	67	1.3	1.0	0.49
28-42	26	9.1	8.3	1.8	1.0	0.31
42-64	23	15	5.8	6.0	1.0	0.48
64-90	16	9.8	15	26	1.5	0.72
90-102	13	11	12	15	2.0	0.94

Although the corrosion rates varied from run to run, the data showed no consistent trend of increasing corrosion rate with increasing velocity. Those specimens exposed to the cystine-containing solution all had black films similar to those noted on the pin-type specimens (Table 2). Attack was higher on all coupons than was observed on pin-type specimens in comparable runs. However since the corrosion rate of the pins increased with velocity up to 15 fps (Table 2), the fact that the corrosion rate was higher on the coupons (20-102 fps) was not surprising. The specimens exposed to the solution containing cuprous ions had only thin films identical to those observed in deaerated solutions, but the observed corrosion rates were somewhat lower than those in the deaerated solutions, probably because the cuprous ions removed essentially all of the oxygen from the solution.

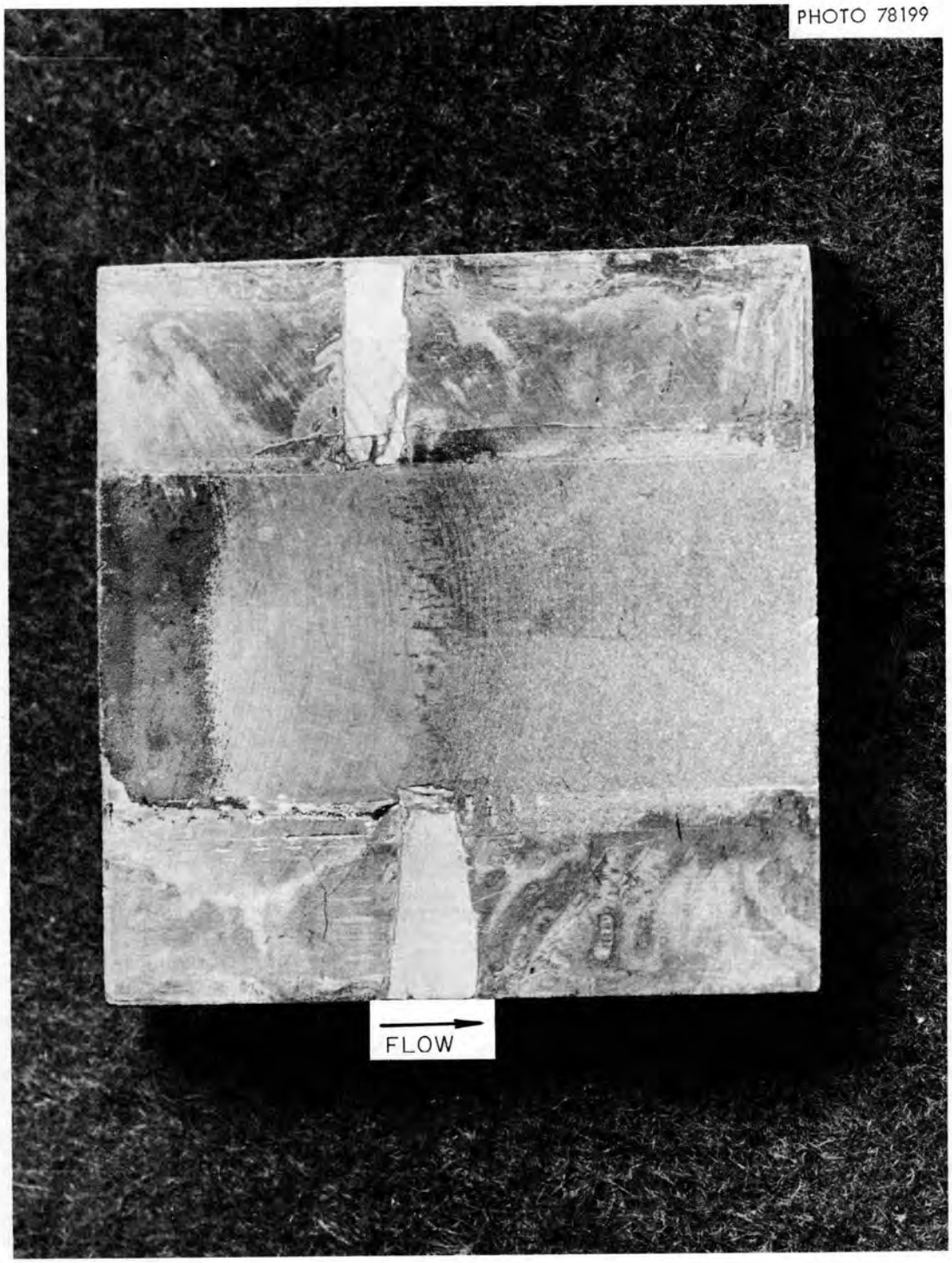

Fig. 3. Photograph of a 70-30 CuNi Specimen Showing Copper Deposit on Leading Edge. Specimen Dimensions 1.400 x 1.380 x 0.200 in.

The specimens exposed to the oxygen-containing solution were distinctly different from any others reported to this time. Except for the first and last coupons in the holder, the leading edge of each coupon was plated with a deposit of metallic copper, the amount of which was greater the higher the bulk solution velocity. Figure 3 is a photograph of the 70-30 CuNi coupon exposed in the highest velocity range. In this particular run the first five specimens in the holder were 70-30 CuNi so that the solution velocity over each specimen was highest at the trailing edge; with the 90-10 specimens the velocity was highest at the leading or upstream edge. Thus the location of the copper deposit was independent of the direction of the velocity gradient over the coupon surface and was on the leading edge of the coupon.

As removed from test all coupons had a thin dark film on their surfaces except for the copper which appeared to be film-free. Immersion in 10% H_2SO_4 failed to remove the film, indicating that it was not Cu_2O but probably CuO. A quick dip in 10% KCN solution completely dissolved the film. The specimen shown in Fig. 3 had been subject to this treatment. Examination of Fig. 3 shows that the downstream (or high velocity in this case) half of the coupon was attacked; this was followed by an area of no apparent attack at lower velocities and at the lowest bulk velocity copper was deposited. The copper deposit was tapered being heaviest near the end of the specimen. Using a sharp knife-edge the entire coherent deposit of copper could be pried from the surface, exposing a dark film which looked like the original film on the rest of the surface. The thickness of the copper on the specimen was 1 to 3 mils. For some reason, unknown at this time, the trailing end of the coupon was anodic to the leading end. On

the 90-10 CuNi coupons the reverse was true; that is, the attack was on the low velocity end and the copper deposit was on the high velocity end. The corrosion observed on the trailing end of the coupon was not characteristic of impingement attack but was very uniform.

Several experiments similar to the one described above were carried out and in every case some copper deposition was observed. The location of the deposit was always the same but the quantity of copper deposited varied widely. A similar experiment at 100°C yielded the same result as did one in which Admiralty brass instead of the cupronickels was exposed. With Admiralty brass in the aerated solution corrosion was much greater than with the cupronickels, and in addition to deposition on the lead ends of the coupons some copper crystals formed at random on all the coupon surfaces.

The mechanism by which copper deposited has not been determined. It did appear that the presence of oxygen in the solution was a necessary condition. Oxygen in solution increased the corrosion rates of most copper alloys and presumably resulted in a greater concentration of copper corrosion products in solution. However when an appreciable concentration of cuprous ions ($\sim$ 5 ppm) was added to the deaerated solution, deposition was not observed, indicating that oxygen plays some other, undefined role.

This series of experiments indicated that in the range of 20 to 102 fps velocity was not an important variable. In no case was there evidence of impingement or cavitation attack. Only uniform attack was observed even when turbulence promoters were built into the specimens. These data suggest that the localized attack usually observed downstream from obstructions in evaporator tubes must be due to causes other than, or in

addition to, pure solution turbulence.

Effect of Surface Area to Volume Ratio - In the case of some materials the corrosion rate depends on the ratio of the surface area of metal exposed to the volume of the test solution.[8] To determine if such an effect existed with copper alloys in saline water three loop runs were made in which the test conditions were the same but the total surface area of specimens was varied. The solution chosen was deaerated 1m NaCl at 175°C because the agreement among replicate specimens of the same alloy was better at this temperature than at any other. The results of the run made with 72 pins are shown in Table 4. Additional runs were made with 18 and 9 pins. The plane surface area of each pin was 4.8 cm^2 so that the total surface areas of copper and copper alloys exposed were 346, 86, and 43 cm^2, respectively, for the 72, 18, and 9 pins. In each run the proportionate number of specimens of each material was approximately the same. The run with 18 pins was continued for 1552 hr and the run with 9 pins lasted only 503 hr. However it had been established that the corrosion rate was constant, and the length of the run was unimportant.

Table 7 shows the average corrosion rates for the materials exposed in the three runs. The data indicate that as the surface area decreased the corrosion rates generally increased. The only two cases where this was not true were for copper and CDA-194 in the two runs with the smaller surface areas.

The reason why the corrosion rates of all the materials shown in Table 7 increased as the surface area of specimens decreased is not completely certain. The most probable reason is related to the availability of oxygen in the system. In all three runs the amount of oxygen added per

Table 7. Average Corrosion Rates of Copper and Several Copper Alloys in N_2-Sparged 1m NaCl at 175°C

Material	Corrosion Rate, mpy		
	346 cm^2	86 cm^2	43 cm^2
70-30 CuNi	1.7	4.0	4.5
90-10 CuNi	1.7	4.5	5.6
Adm. Brass	1.3	3.7	4.9
Monel 400	2.2	2.3	5.2
Copper	1.0	3.1	2.6
CDA-194	1.6	5.6	5.2

hour should have been approximately the same. If one assumes that the oxygen concentration of the solution used to fill the loop and that continuously added was 50 ppb and that there was no consumption of oxygen due to corrosion of the titanium loop itself, then it can be shown that the total amount of metal corroded was greater in all cases than could be accounted for by the oxygen present. The percentages of the total corrosion that complete reduction of oxygen could account for were 23, 38, and 67.5%, respectively, for the runs containing 346, 86, and 43 cm^2 exposed areas. These calculations were based on the fact that nickel and zinc corrosion products are divalent whereas that of copper is monovalent and that the oxygen was reduced to water. If the further assumptions are made that the effect of oxygen is proportionately the same for all materials at the very low oxygen concentrations and that the corrosion attributable to oxygen can be subtracted from the total corrosion, the corrosion rates shown in Table 8 are obtained. Based on the above assumptions these are the rates that would be expected if the solutions were completely free of oxygen and the cathodic corrosion process consisted of the reduction of molecular water to hydrogen. The

agreement between the runs with the highest and lowest exposed surface area is reasonably good, but the corrosion rates in the 86-cm^2 run are considerably higher. If the oxygen concentration in this run had been 80 instead of 50 ppb, the agreement among the three runs would be quite good.

Table 8. Corrosion Rates of Copper and Several Copper Alloys in 1m NaCl at 175°C After Subtracting Corrosion Attributable to Oxygen

Material	Corrosion Rates, mpy		
	346 cm^2	86 cm^2	43 cm^2
70-30 CuNi	1.3	2.5	1.4
90-10 CuNi	1.3	2.8	1.8
Adm. Brass	1.0	2.3	1.6
Monel 400	1.7	1.8	1.7
Copper	0.8	1.9	0.8
CDA-194	1.2	3.2	1.7

Thus under the conditions of these tests the apparent differences in corrosion rates when the exposed surface-area-to-volume ratio was varied seem to be related to the availability of oxygen in the solution. While not completely conclusive, these data indicate that a surface area-to-volume effect, *per se*, either does not exist or is small.

ELECTROCHEMICAL DATA

In the previous section the actual type and extent of corrosion observed on copper alloys in saline solutions was presented. In this section electrochemical data obtained with some of the same alloys under similar conditions are presented. Corrosion is an electrochemical process, and by proper interpretation of electrochemical polarization data corrosion

mechanisms can be inferred. We have obtained such data in the laboratory as well as in flowing streams up to 200°C. Even though anodic and cathodic processes are of equal importance in corrosion, most of our efforts have been on the anodic process. It was our intention to study cathodic processes in greater detail than we did, but as mentioned previously the funding for this program was terminated before completion of this project. Although data that we have obtained are not complete, they shed new light on the corrosion mechanisms of copper and copper alloys in saline environments.

Experimental Procedures

Electrochemical studies were conducted in two different types of cells: conventional laboratory glass cells and a cell mounted in a recirculating pump loop which was constructed of Hastelloy C. In the glass cells temperatures up to atmospheric boiling were investigated, and in the loop temperatures were as high as 200°C. Zone-refined copper was used in the laboratory studies whereas standard electrical-conductor grade copper was used in the loop study. In the zone-refined material all metallic impurities were below the level of detection by emission spectrographic analysis. Based on the same method of analysis the electrical-conductor grade copper contained 300 ppm Ag, 90 ppm Fe, and 40 ppm Ni as the major impurities. In the studies described here no detectable difference between the two materials was apparent. All alloys that were investigated were either from commercial heats or were made for us by the Metals and Ceramics Division of ORNL. The nickel specimens were made from Nickel-270 (International Nickel Co.) with a nominal nickel content of 99.97%.

All solutions were prepared from reagent grade chemicals without further purification. In the laboratory studies the chemicals were dissolved in triply distilled water and for the loop studies deionized water with a specific resistivity of > 10^6 ohm-cm was the solvent. Again the quality of the solvent made no apparent difference. Solutions were saturated with the appropriate gas by sparging for several hours before use.

Both constant current and constant potential polarizations were carried out. All measurements were taken at steady state which was generally achieved within relatively few minutes after changing either the current or potential. An electronic potentiostat designed and built at Oak Ridge National Laboratory and an Anotrol Model 4700 potentiostat were used in these studies. Both instruments also included provisions for galvanostatic operation. In all cases currents were measured as potential drops across precision resistors with Keithley Model 600A battery-operated electrometers, the outputs of which were recorded with Hewlett-Packard Model 7100B dual channel recorders.

Most of the laboratory experiments were performed in a 3-liter flask which had ground glass necks for admission of a test electrode, a polarizing electrode, a Haber-Luggin capillary probe, a tube for gas entry, a mercury thermoregulator, and a condenser. The condenser was equipped with a water-bubbler trap to prevent back diffusion of atmospheric oxygen. Heat was applied with an electric mantle activated by a mercury thermoregulator through an electronic relay. All potentials were measured with reference to a saturated calomel electrode (SCE) in an external vessel at room temperature ($\sim$ 29°C) connected to the cell via a Haber-Luggin capillary. In the laboratory cells the electrodes were mounted on conventional

Teflon holders and either platinum or graphite served as the polarizing electrode. Gentle stirring was provided by means of a magnetic stirrer in the bottom of the cell.

Polarizations in the Hastelloy C pump loop were carried out in a cell mounted in a bypass line of the loop. Figure 4 is a schematic drawing of the cell which consisted of a 1½ in. dia. schedule 80 titanium pipe with six welded fittings through which the electrodes were inserted. A heavy-walled Teflon tube with a 1 cm diameter flow channel fitted snugly inside the pipe section. The ends of the pipe and the caps (also titanium) were threaded, and flat Teflon gaskets prevented leakage between the liner and the caps. The cell was mounted in the bypass line with flanges (not shown in Fig. 4) attached to the caps.

Figure 5 shows the manner in which a specimen was mounted in the cell. The Teflon liner was drilled and threaded as shown and Teflon seal B was inserted. This seal was permanently bonded to the liner with Chemgrip (Chemplast Inc., Wayne, NJ). The specimen was pushed through the opening, and Teflon seal A was then slid over the specimen. Tightening the gland nut sealed the specimen in the vicinity of the junction of the two seals. The four graphite polarizing electrodes were mounted in nearly the same manner. The diameter of the graphite was 0.64 cm, and the ends were shaped so that they could be mounted flush with the inner surface of the Teflon liner. In contrast to the specimen mount, the liner was threaded throughout its thickness as was the graphite. Both the graphite and the lower Teflon seal were permanently bonded to the liner. Threaded into the short length of graphite was a 3 mm diameter copper wire so that the remainder of the assembly was identical to that shown in Fig. 5. During

ORNL-DWG 68-6703R

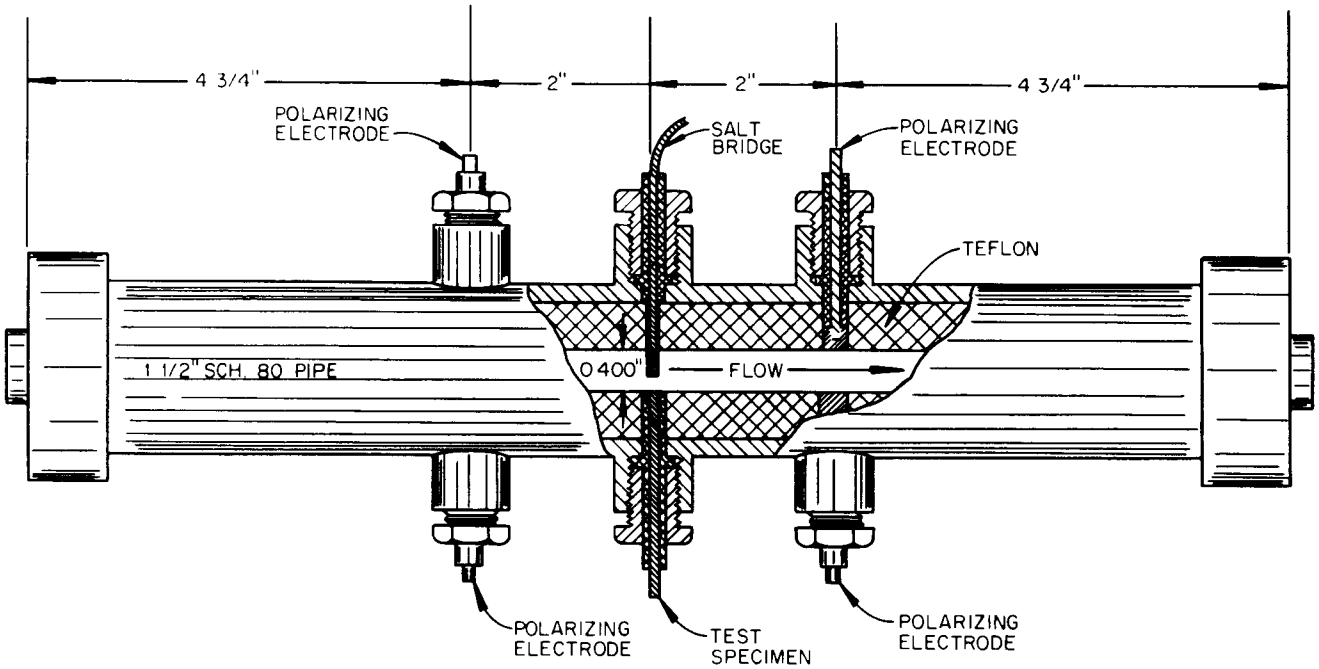

Fig. 4. Drawing of Polarization Cell Used in Hastelloy C Pump Loop.

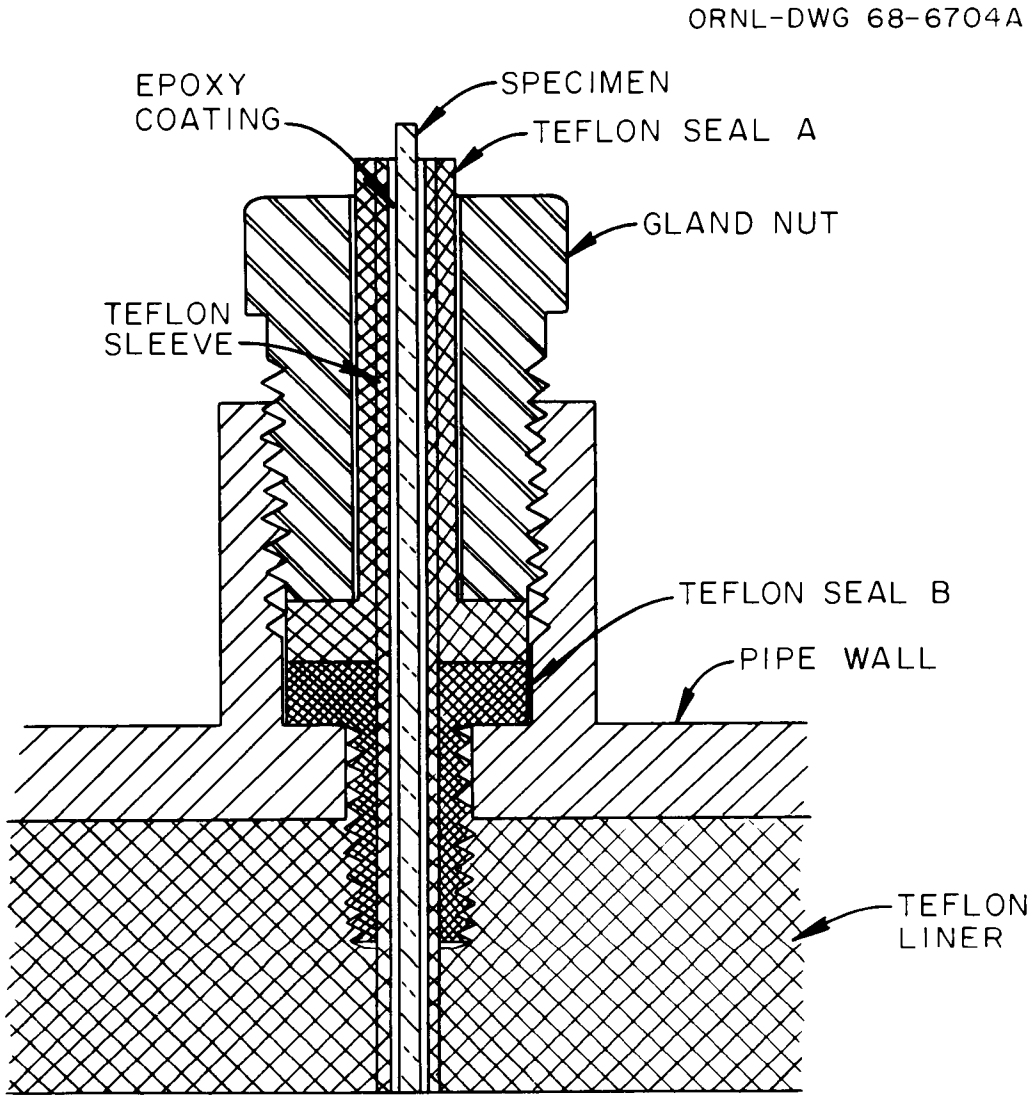

Fig. 5. Sketch of Test Specimen Mounted in Polarization Cell.

polarizations, the four graphite electrodes were connected in parallel. The reference electrode was in an external vessel and was connected to the cell by a salt bridge. The end of the salt bridge extended into the flow channel and ended a short distance (1 to 2 mm) from the specimen. At the current densities used no IR corrections were necessary.

The specimens used in the loop were made from 3.2 mm diameter rods which were coated with epoxy cement (Epoxi-Patch, Hysol Div., Dexter Corp., Olean, NY), and enclosed in a Teflon tube. The end of the rod to be inserted into the cell was ground flat so that the exposed surface area of the specimen was its cross sectional area, 0.08 cm^2. The surface of the test electrode was essentially flush with the Teflon liner. In some early experiments the specimen was not coated with epoxy cement and the specimen extended about 1/4 in. into the flow channel. With this arrangement solution could enter the crevice between the specimen and the Teflon. In some cases the results appeared normal but in other cases spurious results were obtained, probably because of corrosion within the crevice. Results obtained with this early type specimen are indicated in the text.

The loop was constructed of Hastelloy C and a nominal 25 gpm Hastelloy C pump driven by a variable speed motor circulated the solution. In these studies the flow rate of solution past the specimen was either 4, 8, or 12 fps. In all loop tests the solution was 1m NaCl with a pH between 6.3 and 7.0. The total volume of solution in the loop was 3.7 liters, and this was refreshed at the rate of 1ℓ/hr by means of a pulse pump and letdown valve. Loop pressure was maintained at about 200 psig in most cases. Heat was applied to the loop by electric heaters on the pipe walls and temperature was maintained within $\pm$ 2°C by pneumatic

controller operated from a thermocouple upstream from the cell.

Results of Anodic Polarizations

Copper - The results obtained with pure copper have been published[9] and only a brief summary will be given here. Anodic polarization curves obtained with copper in deaerated 1m NaCl in the Hastelloy C pump loop are shown in Fig. 6. The procedure consisted of obtaining the curve at the lowest temperature and the lower flow rate, then disconnecting the cell and increasing the flow rate. After the electrode reached a steady-state open-circuit potential, the curve at the higher flow rate was obtained. The temperature was then raised to the next higher level and the procedure was repeated. Thus all of the curves shown in Fig. 6 were obtained with the same electrode without removing it from the loop. All other polarization curves obtained in the loop were obtained in the same manner. Copper showed Tafel behavior (E vs. log i plots were linear) out to the highest current densities investigated. The Tafel slopes were very close to 2.3 RT/F (59, 69, 79, 84, and 89 mv/decade at 25, 75, 125, 150, and 175°C, respectively). The reproducibility from specimen to specimen was good. Both at 4 and 8 fps the flow was turbulent and the Reynolds Number was directly proportional to velocity. Thus the data shown in Fig. 6 indicates that at a fixed potential the current density increased at about the 0.8 power of the Reynolds Number. The velocity dependence of the anodic process indicates diffusion control.

Using laboratory equipment it was shown that the anodic process was independent of pH (0 to 9) and that the current density depended on the square of the chloride ion concentration. Thus the corrosion product was $CuCl_2^-$; no evidence of solid corrosion product formation was observed.

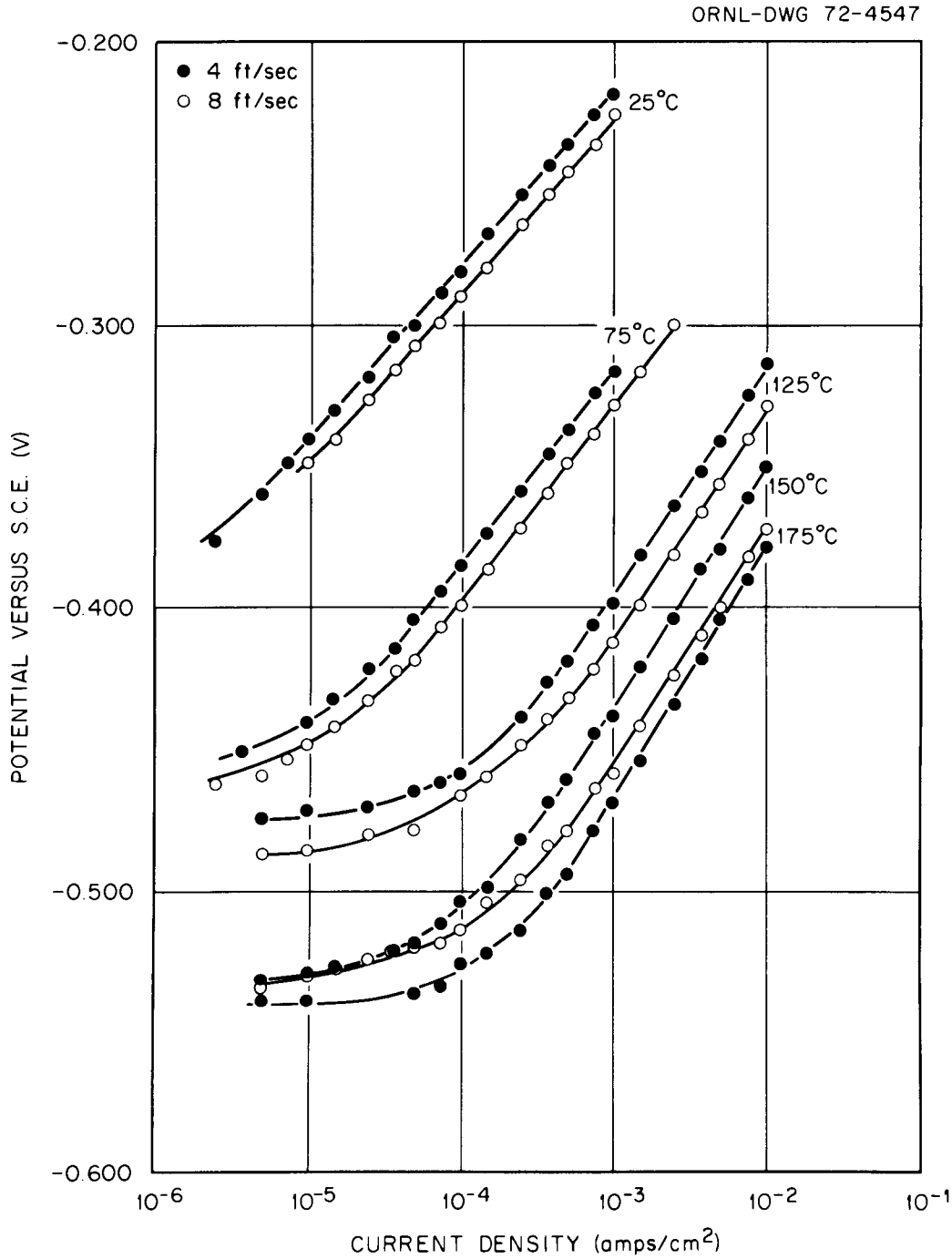

Fig. 6. Anodic Polarization Curves Obtained with a Copper Electrode in Deaerated 1m NaCl.

It was further shown that the temperature dependence of the standard redox potential dE^o/dT for the half reaction,

$$Cu + 2\ Cl^- = CuCl_2^- + e,$$

was -0.4 mv/deg.

We derived the following kinetic expression which was in agreement with our data over the entire temperature range of 25 to 175°C.

$$\log i = \log \frac{zFD_o}{\delta} + 2 \log (Cl^-) - \frac{\Delta H_D^*}{2.3\ RT} + \frac{F\eta}{2.3\ RT} .$$

In this expression, i is the current density, z is the charge on the diffusing species, D_o is a constant related to the diffusion coefficient, δ is the diffusion layer thickness, ΔH_D^* is the apparent activation energy for diffusion transport, η is the overvoltage defined as $E - E^o$ at the appropriate temperature, and the other terms have their usual meaning.

Nickel - At 25°C nickel was passive in the 1m NaCl; that is, current densities of only a few microamps/cm^2 caused large increases in potential. However, at 75°C and all higher temperatures Tafel behavior was observed before the onset of passivation. Figure 7 shows the results. In contrast to copper the current density was independent of solution flow rate and the Tafel slopes were equal to 2/3(2.3 RT/F). Thus the anodic dissolution of nickel is controlled by electrochemical activation rather than by diffusion. Two different specimens were exposed and the results were in excellent agreement.

Copper-Nickel Alloys - Anodic polarization curves were obtained with 6 different copper-nickel alloys in the Hastelloy C pump loop. The copper concentrations were 90, 80, 70, 50, 40 and 10 weight percent. The 90 and 70% copper alloys were from commercial heats whereas all other compositions were prepared from pure elements by the Metals and Ceramics Division

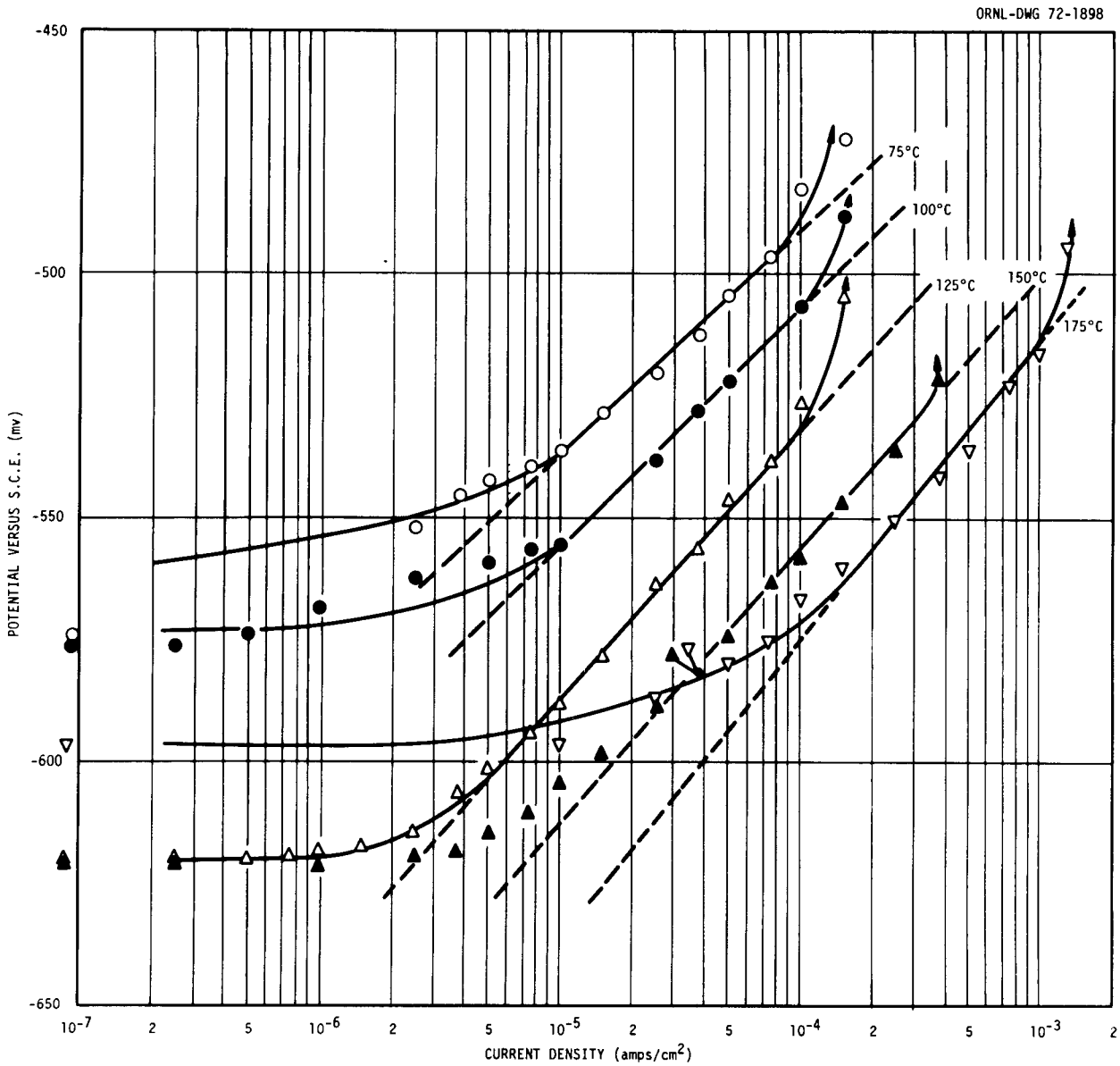

Fig. 7. Anodic Polarization Curves Obtained with a Nickel Electrode in Deaerated 1m NaCl Flowing at 4 fps.

of ORNL.

Figure 8 shows the anodic polarization curves obtained with 90-10 CuNi. At all temperatures Tafel behavior was observed, but at sufficiently high current densities the onset of an apparent passivation process was observed. As with copper the current density was velocity dependent up to 125°C and the magnitude of the velocity dependence was essentially the same as that for copper. It was not possible to maintain loop temperature above 4 fps at temperatures above 125°C with the heaters on the loop at the time these tests were run. A duplicate 90-10 CuNi specimen was run but in this case only at 4 fps. The corresponding curves were displaced only 5 to 10 mv from the curves shown in Fig. 8. At all temperatures the Tafel slopes were equal to 2.3 RT/F, and in fact the curves were nearly identical to those for copper. At 150 and 175°C an additional anodic process at about -0.525V vs SCE appeared to be indicated from the curves. As subsequent data will show this same behavior at the higher temperatures was noted with nearly all nickel alloys.

Figure 9 shows data obtained with 80-20 CuNi. These curves are similar to those for both copper and 90-10 CuNi, but in this case the temperature was extended to 200°C. The velocity dependence appeared to be less than in the case of the other two materials but the Tafel slopes up to and including 150°C were approximately equal to 2.3 RT/F. At 175 and 200°C the Tafel slopes were equal to 2/3(2.3 RT/F), that is the same slope observed with nickel.

A duplicate specimen was run for the purpose of verifying the change in slope at 175°C and above. Unfortunately part of the loop heaters was lost and the maximum temperature attained was 150°C. However the slope

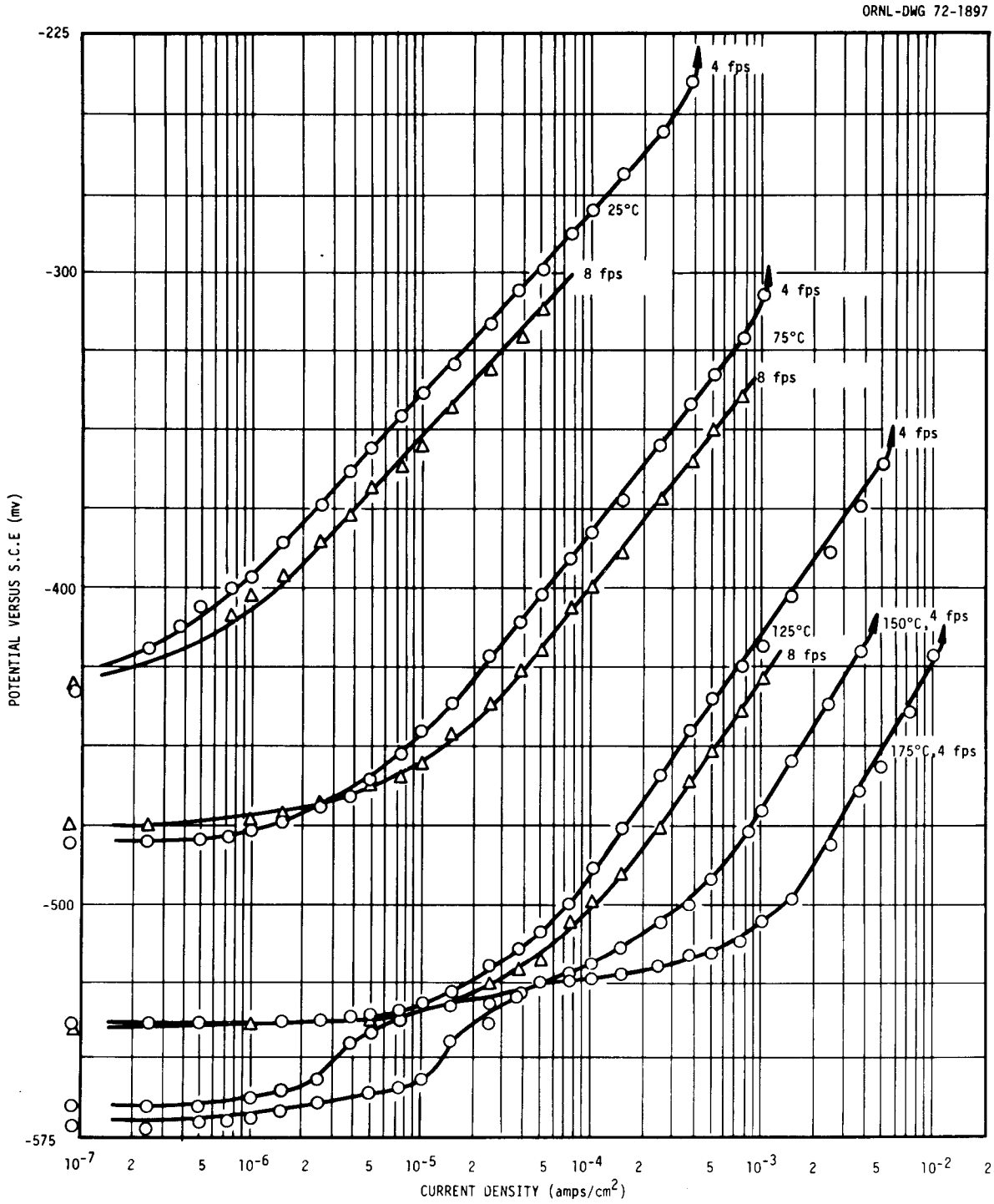

Fig. 8. Anodic Polarization Curves Obtained with a 90-10 CuNi Electrode in Deaerated 1m NaCl.

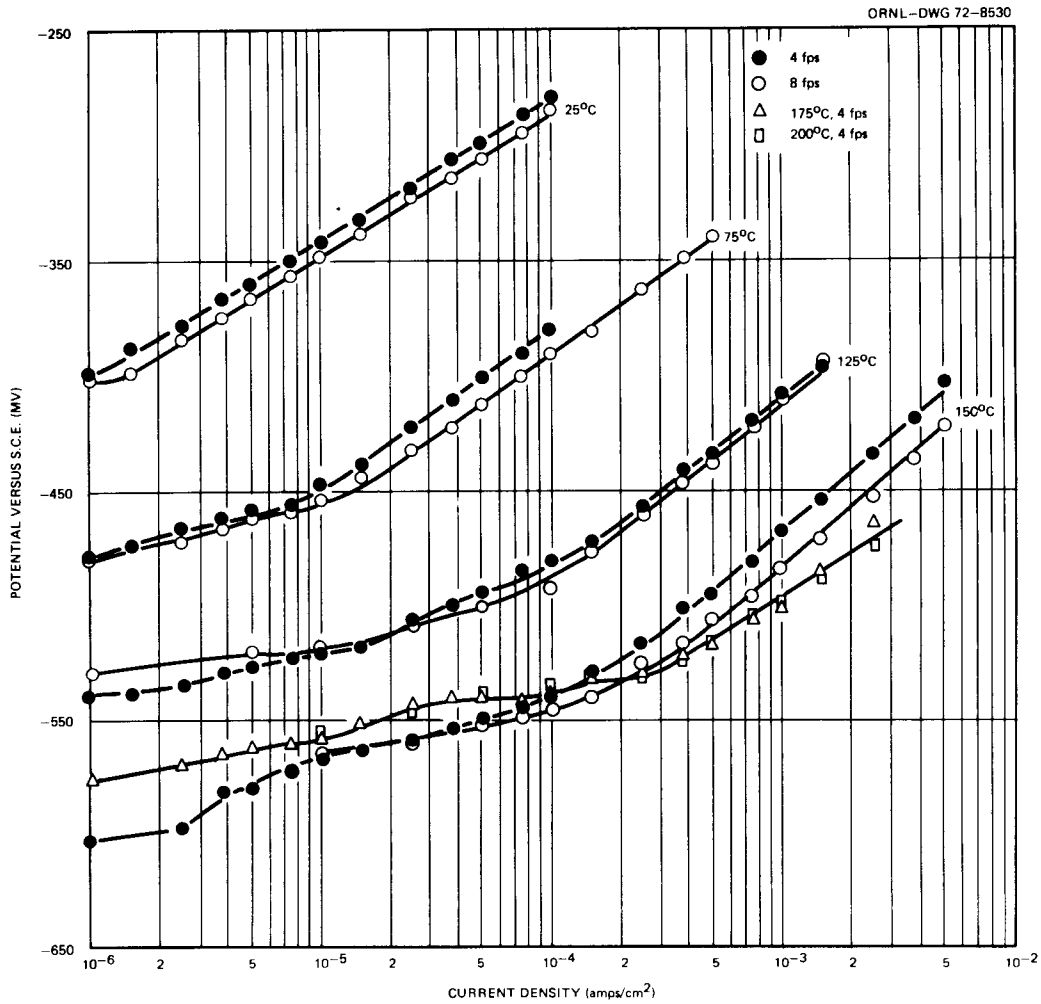

Fig. 9. Anodic Polarization Curves Obtained with an 80-20 CuNi Electrode in Deaerated 1m NaCl.

at 150°C was 89 mv, 5 mv higher than 2.3 RT/F. The effect of velocity was determined in this case by changing the velocity at a single fixed current density and noting the change in potential. At 30°C increasing the velocity from 4 to 8 fps caused a potential change of -5 mv; at 75°C the change was -6 mv; and at 125°C, -1 mv. These results were in reasonable agreement with those shown in Fig. 8.

Figure 10 shows one set of anodic polarization curves obtained with a 70-30 CuNi specimen. At 24, 75 and 125°C clearly defined Tafel lines with slopes equal to 2.3 RT/F were obtained before the onset of passivity. At 155°C the slope was 59 mv. Another specimen was run only at 150°C to determine the slope of the Tafel line. A slope of 58 mv/decade was obtained, in agreement with the curve shown in Fig. 10 at 155°C. A third specimen was run to determine the effect of velocity. At 28°C changing the velocity from 4 to 8 fps caused a change of -5 mv; at 75°C no difference was found between the curves at 4 and 8 fps, but on increasing the velocity to 12 fps a -9 mv change was observed; at 125°C changing from 4 to 8 fps resulted in a potential change of -12 mv, and on going from 8 to 12 fps the change was an additional -12 mv. The slopes and locations of the curves were in good agreement with those shown in Fig. 10. At 150 and 175°C curves were obtained only at 4 fps. In both cases the Tafel slopes were equal to 2/3(2.3 RT/F). While the above experiment indicated that up to 125°C the anodic process was velocity dependent, the velocity dependence was not as clearly defined as was the case with copper and 90-10 CuNi.

All of the data concerning the copper-nickel alloys presented above was obtained in the Hastelloy C pump loop. Considerable experimentation

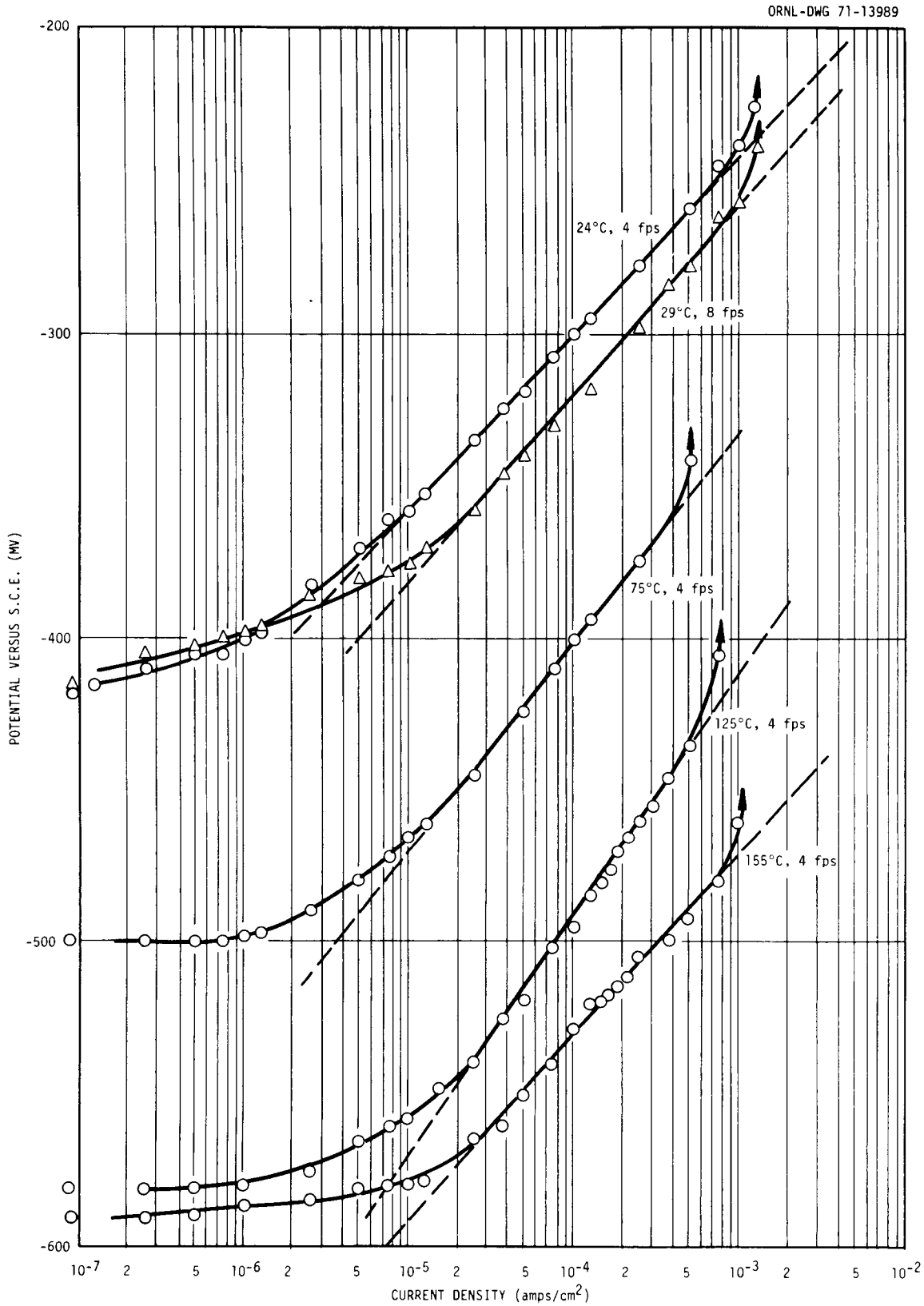

Fig. 10. Anodic Polarization Curves Obtained with a 70-30 CuNi in Deaerated 1m NaCl.

was also conducted with 70-30 CuNi, and to a lesser extent with 90-10 CuNi, under very carefully controlled laboratory conditions. In general the laboratory and loop data were in good agreement. However in about half of the cases Tafel slopes obtained in the laboratory were about 10 to 15 mv greater than 2.3 RT/F at all temperatures between 30 and 100°C. In other cases under presumably the same condition slopes exactly equal to 2.3 RT/F were obtained. Fewer tests were conducted with 90-10 CuNi but the same variance was observed. In contrast similar experiments with pure copper always yielded the 2.3 RT/F slope. As indicated above Tafel slopes obtained in the loop at temperatures between 25 and 125°C were usually equal to 2.3 RT/F or deviated from that value by only a few millivolts. The explanation for the rather frequent deviation in Tafel slopes in the laboratory tests is not obvious at this time. In addition laboratory tests at 100°C showed that at a fixed potential in the active region the current density of a 70-30 CuNi specimen depended on the square of the chloride ion concentration as was observed with copper.

Anodic polarization curves obtained with a 50-50 CuNi specimen are shown in Fig. 11. Curves were obtained at a greater number of temperatures than in the previous cases and at the three lower temperatures curves were obtained at 4 and 8 fps. Table 9 shows both the experimentally determined and the calculated Tafel slopes (2.3 RT/F up to 140°C and 2/3 that value at higher temperatures). The agreement between the two is quite good. With this alloy the change in slope occurred between 140 and 150°C. Increasing the velocity from 4 to 8 fps caused potential shifts of -12, -7, -4, and 0 mv at 28, 50, 75 and 100°C, respectively.

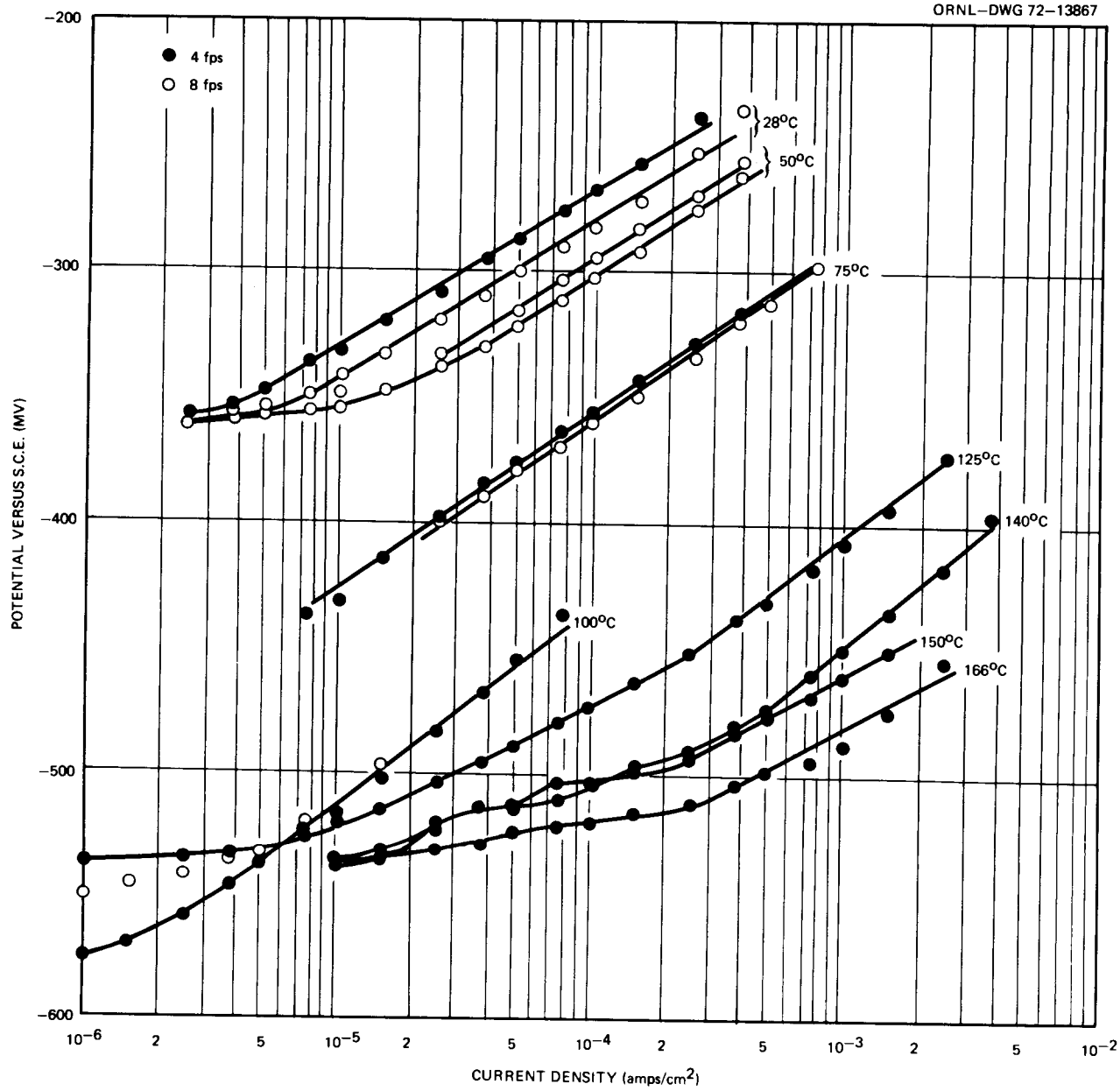

Fig. 11. Anodic Polarization Curves Obtained with a 50-50 CuNi Electrode in Deaerated 1m NaCl.

Table 9. Experimental and Calculated Tafel Slopes Obtained with 50 Cu-50 Ni in 1m NaCl

Temperature °C	Tafel Slopes, mv/decade Experimental	Calculated
28	61	60
50	65	64
75	70	69
100	78	74
125	77	79
140	84	81
150	54	57
166	54	57

A duplicate 50-50 CuNi specimen was run at only 4 fps and the results were similar to those reported above except in this case it was not possible to activate the specimen at 25°C; current densities of a few μamps/cm^2 caused large changes in potential. At all other temperatures the specimen appeared active and well defined Tafel lines were obtained before passivation began. At 75 and 125°C Tafel slopes were 2.3 RT/F and at 150 and 175°C slopes were 2/3(2.3 RT/F).

Figure 12 shows anodic polarization curves obtained with 40-60 CuNi. At 30, 50, 75, and 100°C Tafel slopes were equal to 2.3 RT/F, and at 125 and 150°C slopes were equal to 2/3(2.3 RT/F). At 175 and 200°C the curves were complex and Tafel behavior was not apparent. At temperatures as low as 100°C additional anodic processes were indicated at low current densities. Velocity effects were determined at 30, 50 and 100°C by changing the velocity from 4 to 8 fps. The shifts amounted to -11, -5 and -1 mv at 30, 50 and 100°C, respectively. In a duplicate test it was noted that at 125°C the slope of the Tafel line was 2.3 RT/F but at 140°C the slope had changed to 2/3(2.3 RT/F). Thus the results indicated that the shift in

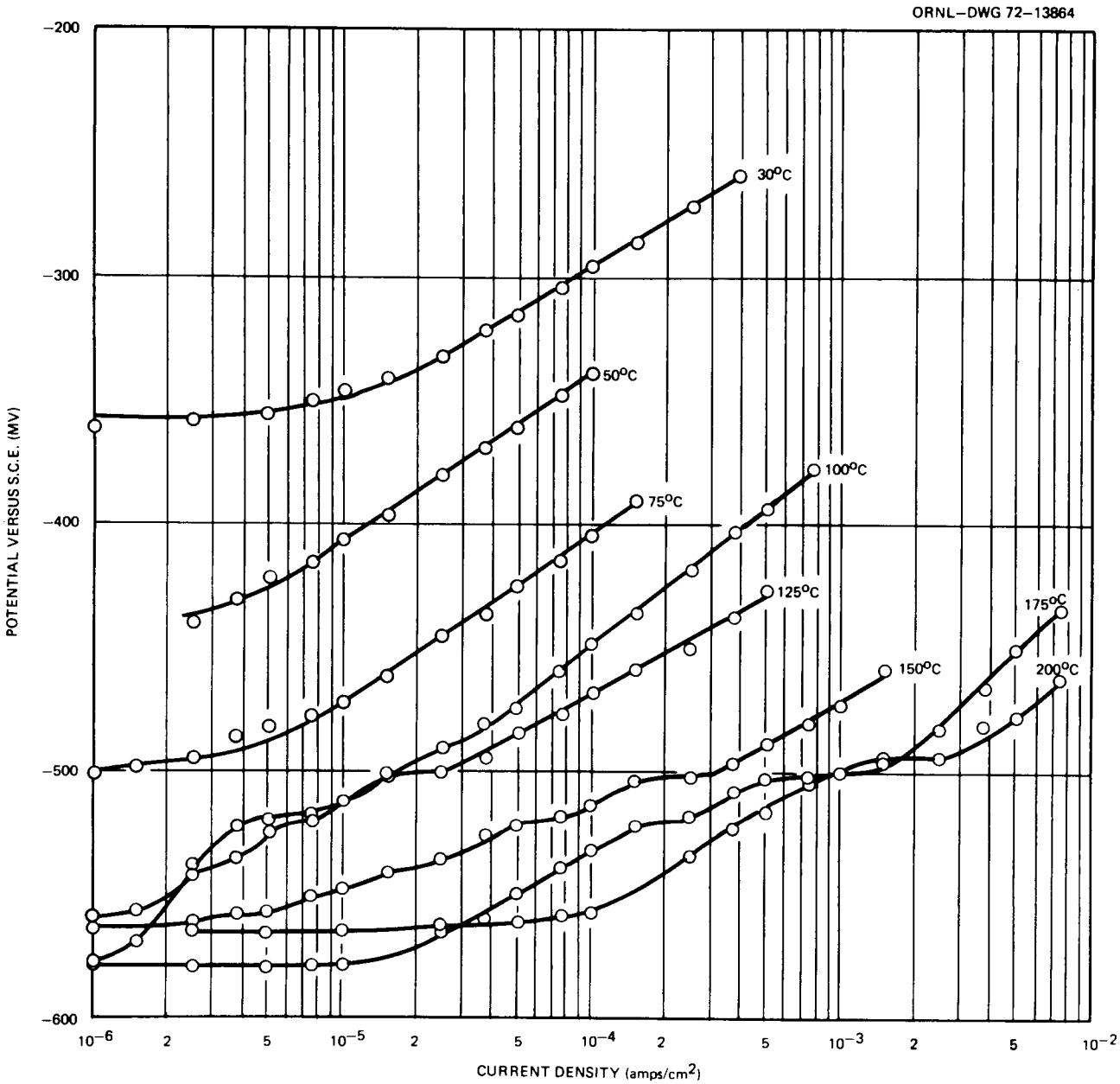

Fig. 12. Anodic Polarization Curves Obtained with a 40-60 CuNi Electrode in Deaerated 1m NaCl.

Tafel slope occurred at a somewhat lower temperature with this alloy than with the other alloys.

Results obtained with the alloy containing the highest nickel content, 90%, are shown in Fig. 13. At 28°C the curves at 4 and 8 fps were separated by about 6 mv and both slopes were equal to 66 mv, 6 mv higher than expected. At 75 and 125°C the expected slopes (69 and 79 mv respectively) were observed and at 75°C the curves at 4 and 8 fps were identical. At 150 and 175°C the Tafel slopes were 2/3(2.3 RT/F). In a duplicate experiment the results obtained at 28°C were in good agreement with those shown in Fig. 13, but at 75°C a Tafel region with a 100-mv slope was obtained, possibly indicating the presence of a film on the electrode at the start of the polarization. At 125, 150 and 175°C Tafel slopes of 2/3(2.3 RT/F) were obtained. Thus as with the 40-60 alloy there was a suggestion that the change in Tafel slope occurred at a somewhat lower temperature than with the alloys containing 50 or less percent nickel.

Other Alloys - Polarization curves were obtained with only two other alloys using the epoxy-coated specimen. These were aluminum brass and Monel 400. The results obtained with aluminum brass are shown in Fig. 14. The slopes of the Tafel lines were equal to 2.3 RT/F and the positions of the curves were similar to those for copper and the copper-nickel alloys. It is probable that the current density was velocity dependent although this point was not investigated.

Polarization curves obtained with Monel 400 are shown in Fig. 15. At 25°C the Tafel slopes were 60 mv/decade and a velocity dependence was noted. At 75°C the slopes of the curves were 46 mv in contrast to the expected 69 mv, and a slight velocity dependence was observed. At 125 to

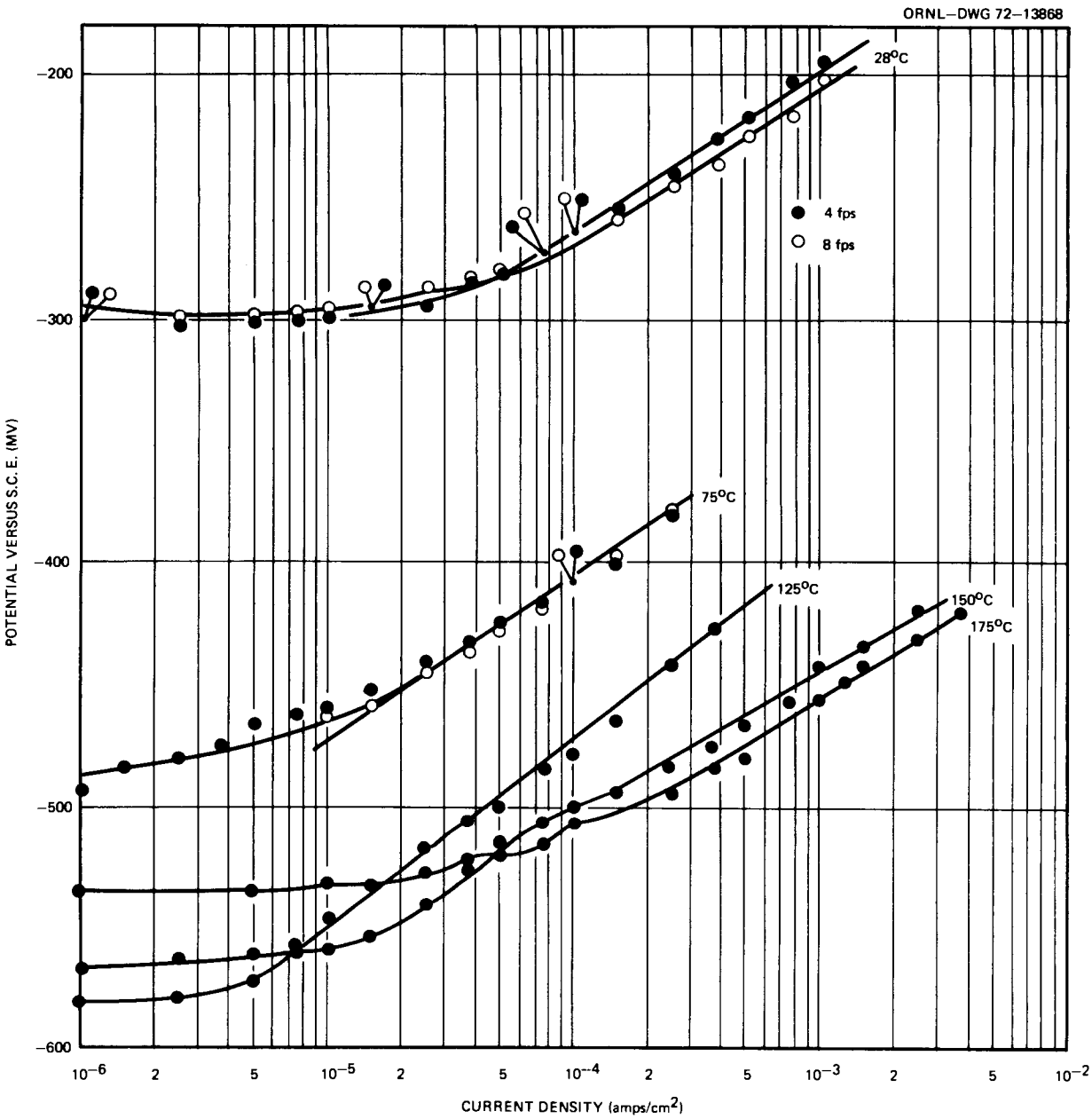

Fig. 13. Anodic Polarization Curves Obtained with a 10-90 CuNi Electrode in Deaerated 1m NaCl.

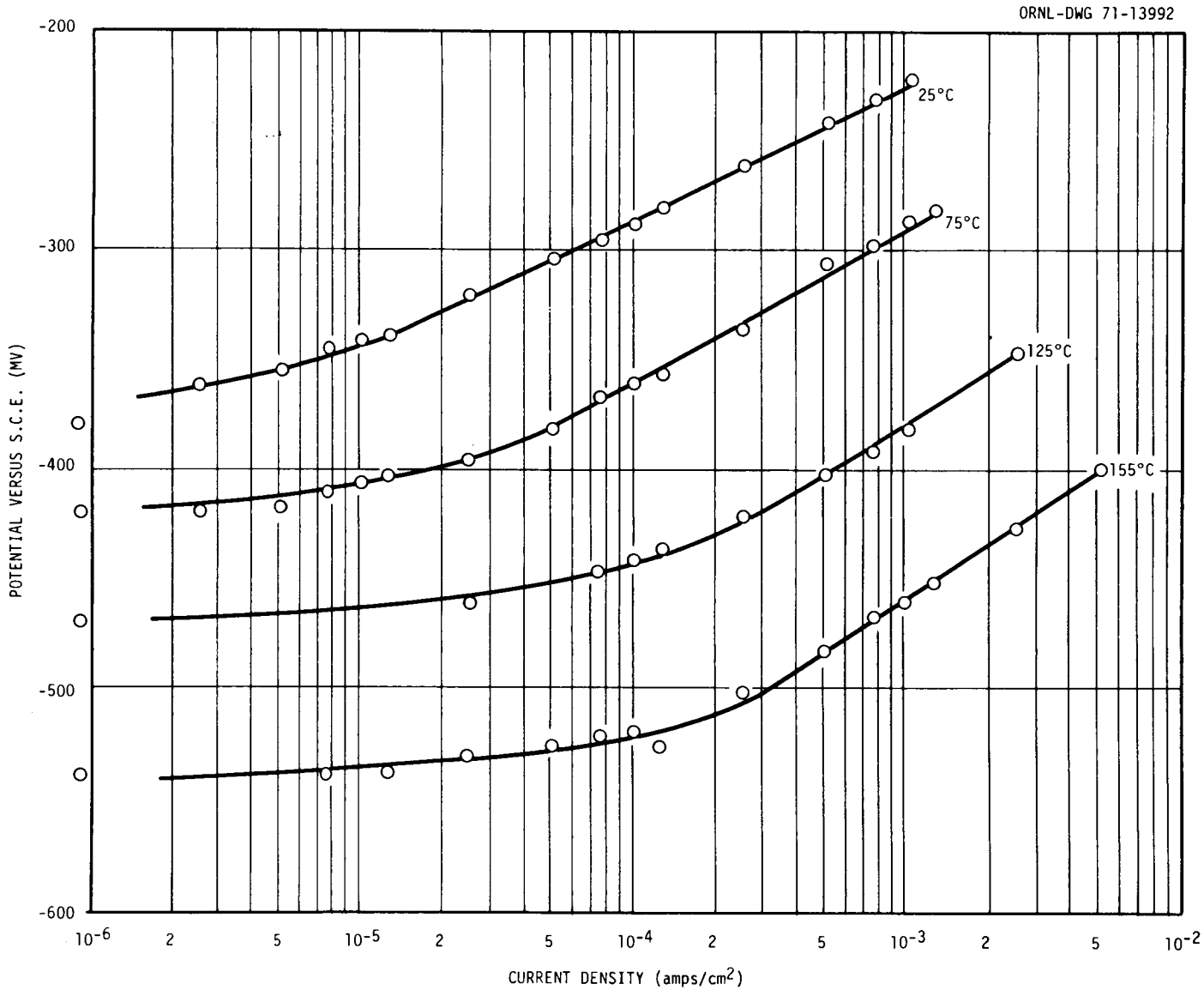

Fig. 14. Anodic Polarization Curves Obtained with an Aluminum Brass Electrode in Deaerated 1m NaCl.

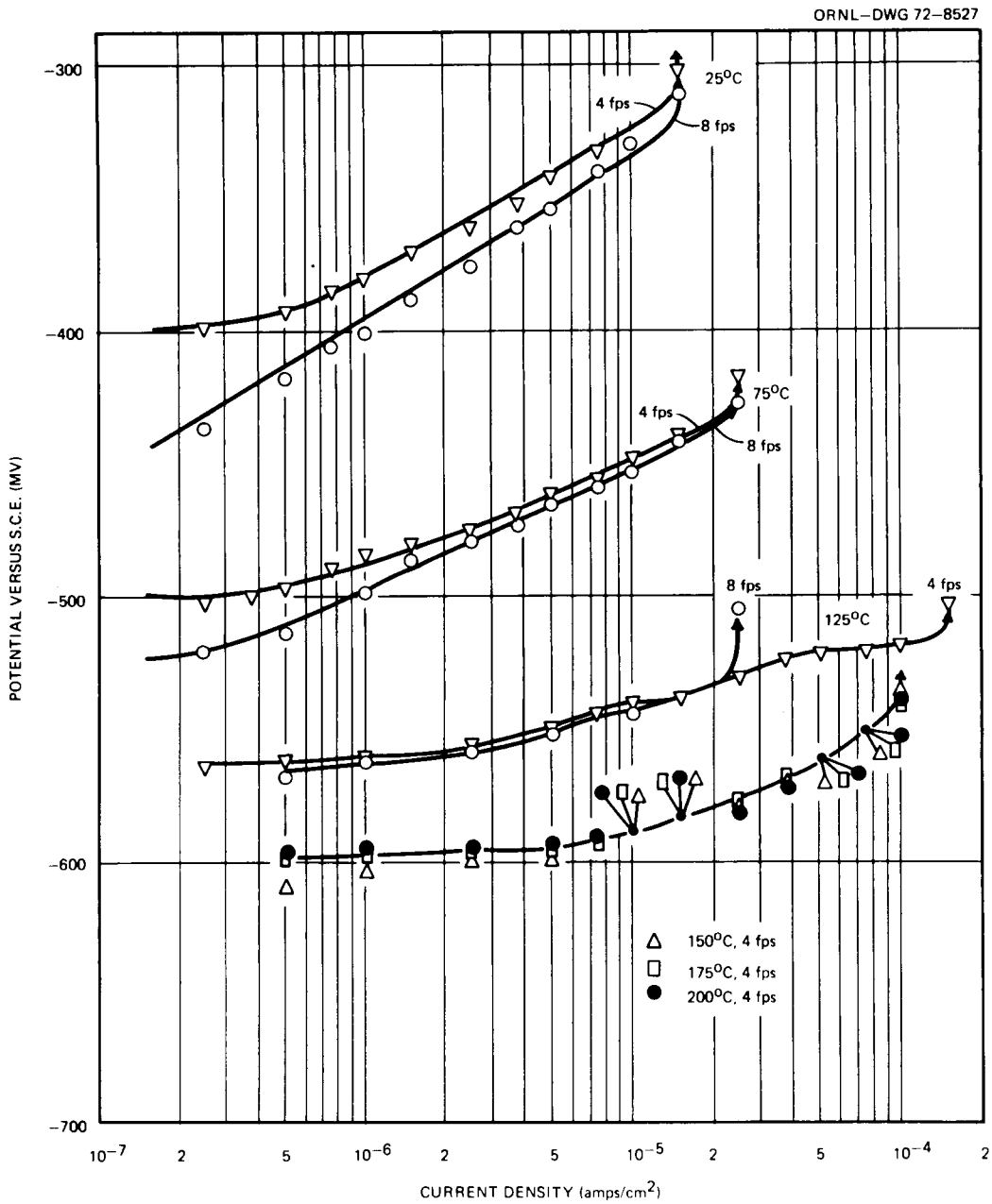

Fig. 15. Anodic Polarization Curves Obtained with a Monel 400 Electrode in Deaerated 1m NaCl.

200°C the alloy was not very polarizable and no evidence of a Tafel region was noted. At the three highest temperatures the curves appeared to be independent of temperature. In view of the similarity of this alloy to 40-60 CuNi (see Table 2) the results were surprising and perhaps indicate some unknown defect in the experiment. Unfortunately time did not permit a repeat of this experiment.

Both Admiralty brass and CDA-194 were anodically polarized using the uncoated type specimen. At low temperatures the results in both cases appeared to be similar to those for copper but spurious results were usually obtained at higher temperatures. At times clear evidence of attack was noted in the crevice region and in some cases deposits of Cu_2O were also found there. Curves were also run with 90-10 and 70-30 CuNi using the uncoated specimens and similar results were observed. Because of this unpredictable behavior, the epoxy-coated specimen was developed.

Effect of Sulfide Additions - A few anodic polarization curves were obtained with some of the alloys when low concentrations of sodium sulfide were added to the 1m NaCl. All of these results were obtained at 125°C using the uncoated type of specimen. Figure 16 shows the results. In all cases the addition of sodium sulfide depressed the potential substantially and all anodic curves showed an apparent diffusion limited current density. The concentrations of sulfide in the solution was determined with a sulfide ion specific electrode on a sample of the letdown stream. (In all cases the solution to be analyzed was made 0.1m in NaOH before the determination.) Since the concentrations were not the same in all cases, the curves are not directly comparable. For that reason the effect of sulfide concentration on the limiting current density was evaluated in the follow-

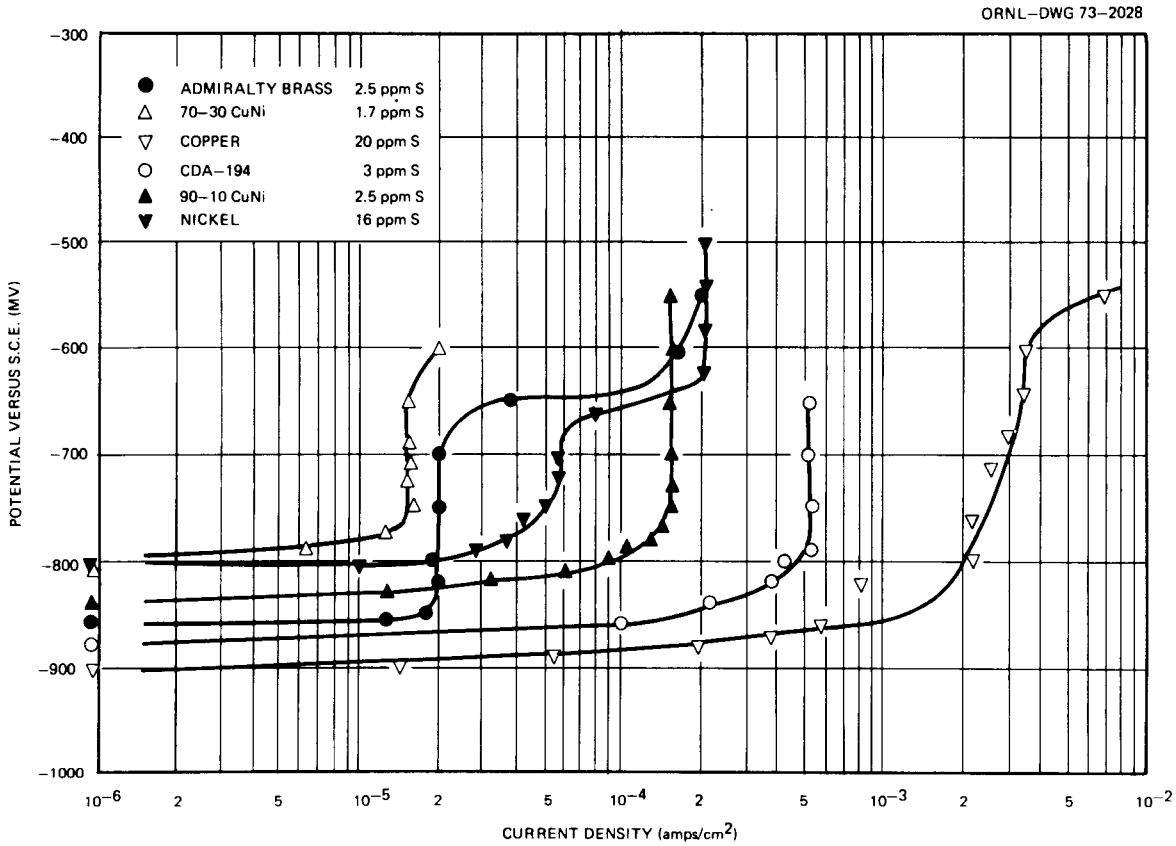

Fig. 16. Anodic Polarization Curves Obtained with Various Alloys in 1m NaCl Containing Added Sulfide at 125°C. Flow Rate - 4 fps.

ing manner. The potential of the test electrode was fixed at a potential in the limiting current density range and enough sodium sulfide solution was injected into the loop to give a concentration of about 100 ppm sulfide. The sulfide concentration was diluted as sulfide-free sodium chloride was continuously pumped into the loop. Periodically the sulfide concentration was determined and the current noted.

The results are shown in Fig. 17 from which it can be seen that at a given sulfide concentration copper and CDA-194 had a much greater limiting diffusion current density than 90-10 CuNi, and 90-10 CuNi had a greater current density than 70-30 CuNi. The lines for both cupronickels and copper fit the points reasonably well. The data points for CDA-194 were so few and so scattered that no line was drawn through the points. The significance of the slopes of the lines is obscure. It should be noted, however, that as the sulfide concentration decreased, the pH (measured at room temp.) also decreased. As an example in one case when the solution contained 2.5 ppm sulfide the pH was 10.2 and with 94 ppm the pH was slightly greater than 11. Since the ionic form in which sulfur exists (H_2S, HS^-, $S^=$) is pH dependent, it is probable that the data reflect in part the relative concentrations of the various species at the different pH values.

Anodic Passivation of 70-30 CuNi - All of the curves shown in the previous figures were obtained galvanostatically and any tendency for an alloy to passivate was reflected by a constantly increasing potential. Figure 18 shows a series of anodic polarization curves obtained potentiostatically with a 70-30 CuNi specimen. Each point on the curves represents an apparent steady-state value. In fact, the first point after the passive

ORNL-DWG 69-4007

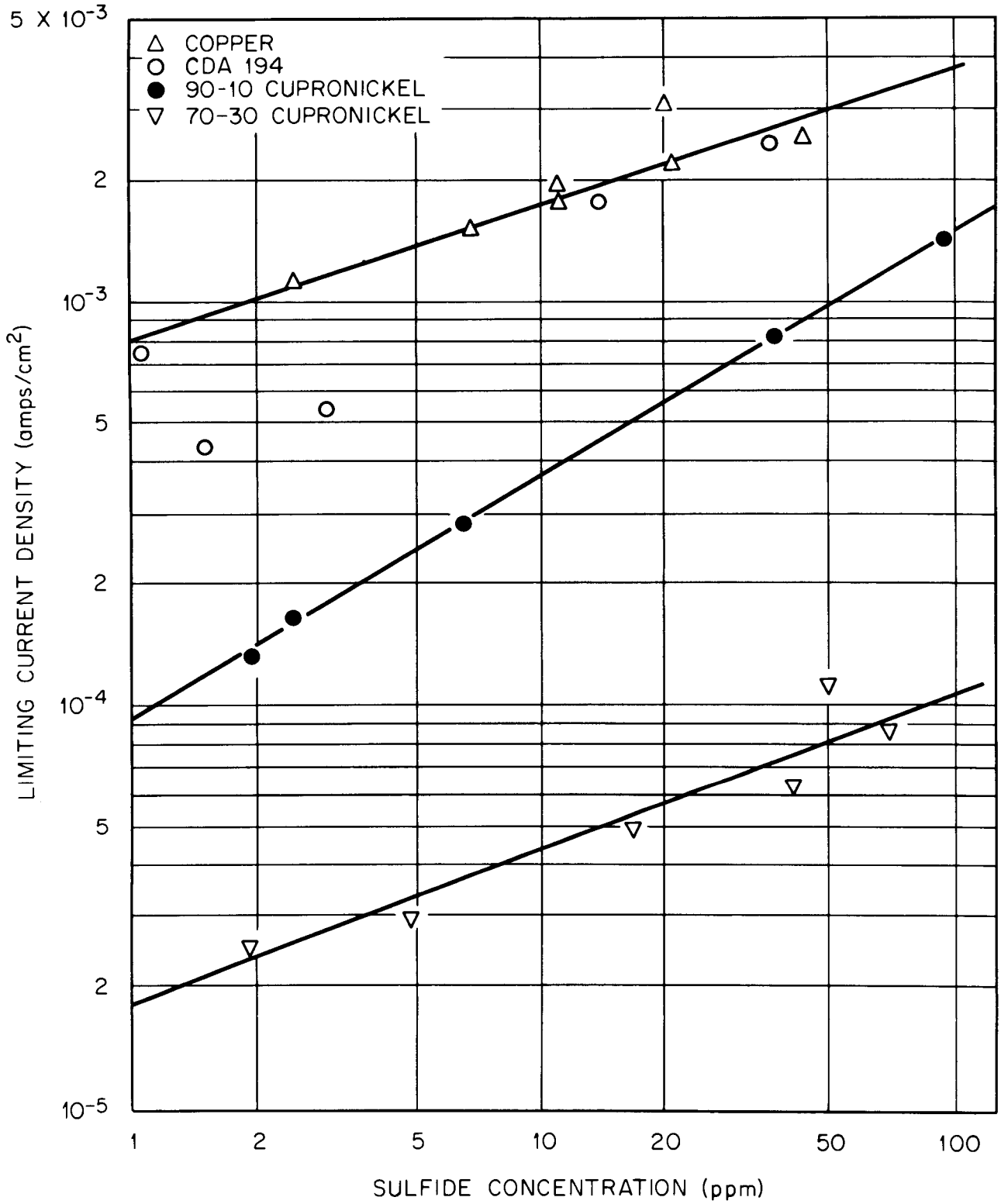

Fig. 17. The Effect of Sulfide Concentration on the Limiting Anodic Diffusion Current Density in 1m NaCl at 125°C. Flow Rate - 4 fps.

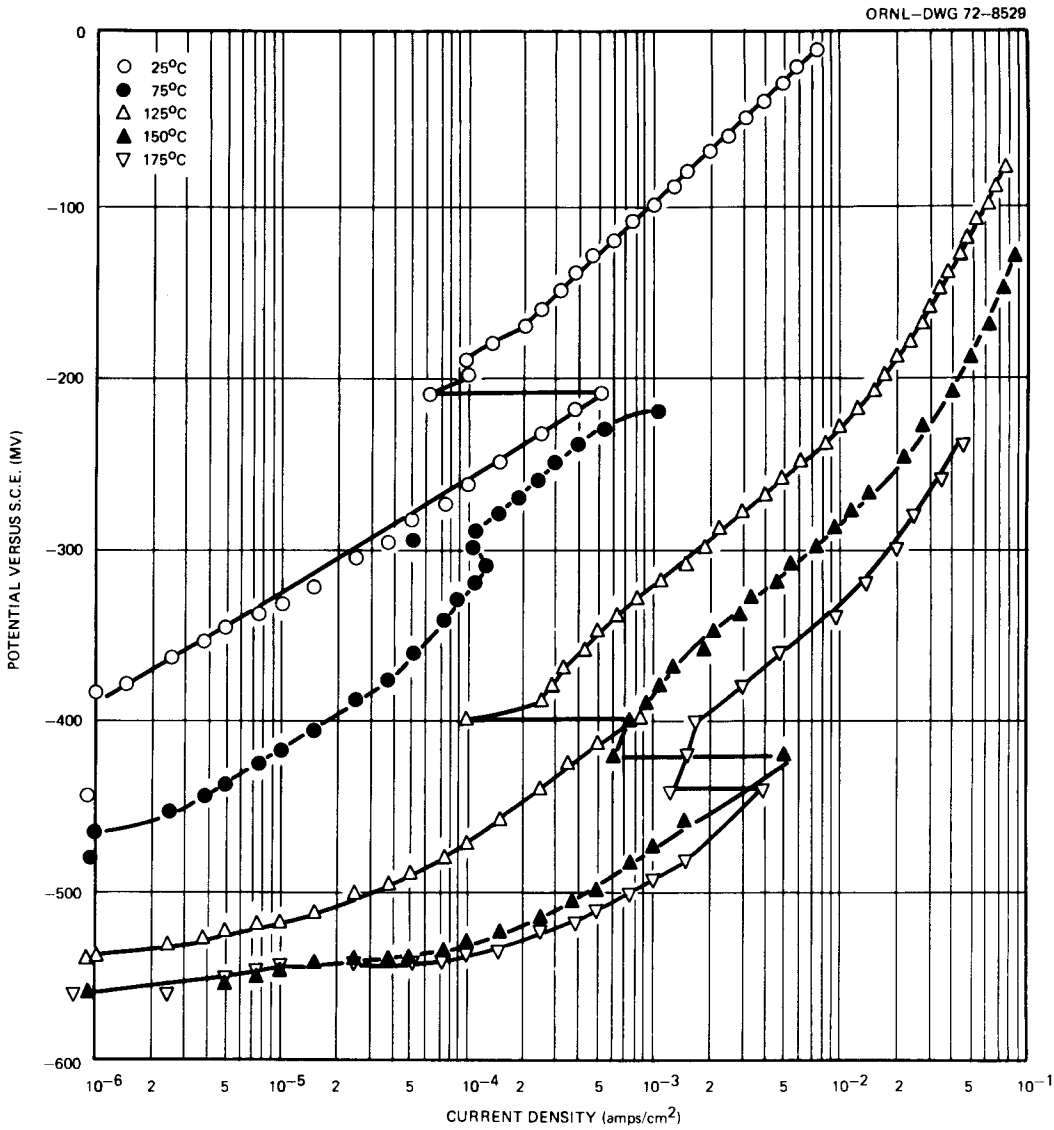

Fig. 18. Anodic Polarization Curves Obtained with a 70-30 CuNi in Deaerated 1m NaCl. Flow Rate - 4 fps.

potential was usually obtained after the potential remained constant at that potential overnight. At the passive potential the current density slowly decreased until it was a factor of 3 to 10 lower than at the slightly lower potential. At potentials greater than that required for passivation Tafel behavior was again observed. The curvature in the polarization curves at current densities greater than 10^{-2} amps/cm^2 was due to IR drop included in the potential measurements. Corrected post-passive slopes were: 105 mv at 25°C; 83 mv at 125°C; 86 mv at 150°C; and 93 mv at 175°C. The significance of the post-passive lines, if any, is not known. None of the curves gave any indication of a pitting potential and no pits were noted on the specimen at the end of the test. However in some laboratory tests polarizations into the regions shown in Fig. 18 have indicated pitting potentials (potential of unpolarizability) and pits developed on the electrode.

The passive phenomenon on 70-30 CuNi was investigated more thoroughly in laboratory tests using boiling 1.24m NaCl. In one experiment the potential of the specimen was slowly increased potentiostatically until a further slight increase in potential caused a decrease rather than an increase in current. The potential of the specimen and the pH of the solution were noted, the pH was changed, and the process was repeated. The potential where the current began to decrease as a function of pH is shown in Fig. 19. The solid point on the curve represents the average potential of passivation noted with several other specimens in neutral solution. The equation of the curve drawn through the points is

$$E = 0.19 - 0.076 \text{ pH}.$$

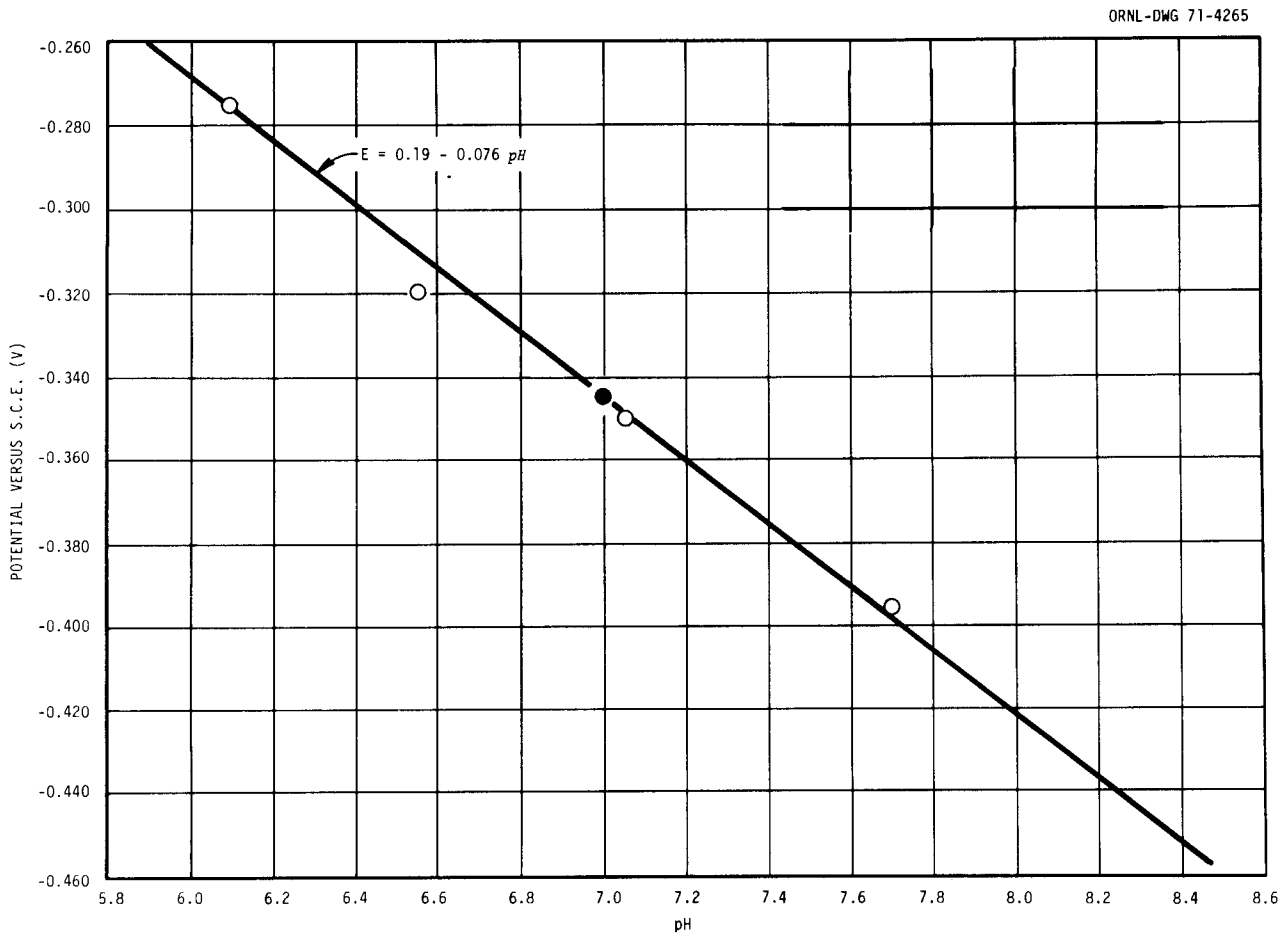

Fig. 19. The pH Dependence of the Passivation Potential for 70-30 CuNi in H_2-Saturated Boiling 1m NaCl.

Regarding the above equation it is interesting to note that Sato and Okamoto[10] reported the standard potential for the reaction

$$3NiO + H_2O = Ni_3O_4 + 2H^+ + 2e$$

to be 0.24V vs SCE. Assuming a temperature coefficient of -0.4 mv/°C, the Nernst Equation for the above reaction is

$$E^{100°C}_{Ni_3O_4} = 0.21 - 0.074\ pH$$

which is in reasonable agreement with the experimental results. However data reported by Pourbaix[11] indicate that the potential of formation of Ni_3O_4 should be substantially above that reported by Sato and Okamoto. Thus the agreement of the equation given above with that of Sato may be coincidental.

In other laboratory tests it was shown that at, or slightly above, the passive potential the current decreased by factors as large as 10^3 or 10^4 over a period of several hours. As indicated above (Fig. 18) the comparable factor in the loop was seldom greater than a factor of 10 and was usually less. In many cases the only apparent difference in test conditions between the laboratory and loop experiments was that in the loop the specimens were exposed to a highly turbulent solution whereas in the laboratory the specimens were exposed under semi-static conditions. Thus there is at least an indication that velocity influences the protectiveness of the passive film.

Thermodynamic data indicate that $Ni(OH)_2$ (or NiO) should be stable at potentials substantially below the passive potential.[12] For example the potential of formation of NiO (based on $E_{NiO} = -0.14 - 0.074\ pH$) is -0.58V vs SCE at pH = 6, a value well below the passive potential. However

the above experiment indicated that if it was present, it had no discernible effect on the anodic process. On the other hand, general experience indicates that the copper-nickel alloys have better corrosion resistance than pure copper in saline environments which may indicate that NiO is present and affects cathodic processes. It should be noted that in the above experiment polarization of the electrode was obtained by an outside source; that is, cathodic processes normally associated with a freely corroding metal were suppressed.

The potential of passivation should also be obtained if sufficient oxygen (or some other oxidizing agent) is present in the solution to polarize the anodic process to the potential of passivation; that is, if the limiting current density for reduction of oxygen exceeds the current density required for passivation. If the oxygen concentration is such that the limiting diffusion current density is less than the current density at the passive potential, passivation would not be expected and the corrosion rate would remain constant, provided $Ni(OH)_2$ did not form and interfere with the cathodic process.

Based on the above line of reasoning experiments were carried out in 1.24m NaCl at 90°C. Both the pH and oxygen concentration were varied and periodically brief polarizations were carried out to determine whether the anodic or cathodic process was affected. The results, while not completely unambiguous, indicated that under conditions where the limiting diffusion current density for the reduction of oxygen exceeded the current density for passivation, both anodic and cathodic processes were affected. With oxygen concentrations such that the limiting diffusion current density was close to but less than the current density for passivation, only

the cathodic process appeared to be affected; at a constant oxygen concentration the limiting diffusion current density decreased with time. At lower oxygen concentrations neither the anodic nor cathodic process was affected. Although these data are insufficient to answer all questions, it seems probable that the interference with the cathodic process only was associated with the formation of $Ni(OH)_2$ whereas at the passive potential the formation of some other, perhaps higher, nickel oxide or hydroxide was responsible for inhibition of both the anodic and cathodic process.

An attempt was made to determine the nature of the films formed on 70-30 CuNi at various potentials using photoelectron spectroscopy. With this technique the surface to be examined is exposed to soft x-rays and the energy of the ejected electrons, which is characteristic of the element, is determined. The ejected electrons escape from depths of only 10 to 20 atom layers so that the spectrum is not complicated by subsurface materials if the film is at least 20 layers thick. For these experiments 70-30 CuNi specimens were anodized at potentials both below and above the passivation potential in deaerated 1.24m NaCl at 100°C and the specimens were examined. The detailed results of this study have been reported[13] and only the major result is given here. At a potential below the passive potential either no film or a film containing copper and nickel in the same ratio as the alloy existed on the alloy surface. At the passive potential, -0.350V vs SCE in this case, the spectrum of the passive film indicated primarily nickel oxide and was very similar to the spectrum obtained from a pure nickel specimen passivated in the same environment.

Results of Cathodic Polarizations

Loop Data - All of the cathodic polarizations performed in the Hastelloy C loop were carried out with the old type specimen, that is the type without the epoxy coating. Even though the results obtained with this type specimen may be open to question, some of the data are presented here because we believe them to be at least qualitatively correct. The procedures used to obtain the cathodic curves were identical to those used with the anodic curves.

Figure 20 shows cathodic curves obtained with a copper specimen in "deaerated" 1m NaCl at four temperatures. As explained previously "deaerated" means sparged with nitrogen and such solutions usually contained 30 to 50 ppb oxygen. It was interesting to note that as the temperature was increased the copper became less polarizable. At the two highest temperatures there appeared to be regions of unpolarizability where some reductive process occurred. There also appeared to be a limiting diffusion current density which was at least partially caused by the reduction of oxygen. Curves for all other alloys investigated were similar although the magnitude of the limiting current density appeared to vary from alloy to alloy.

The reduction of oxygen on copper was investigated at 50 and 100°C and the results are shown in Fig. 21. The feed solution was sparged with the gas indicated on the figure at room temperature (∿ 25°C). With 2% oxygen in argon the oxygen concentration in the solution should have been about 0.6 ppm; with air, 6 ppm; and with oxygen, 30 ppm. Chemical analyses for oxygen were not made. With all three runs the galvanostatic polarizations began at the open-circuit potential and continued stepwise in a

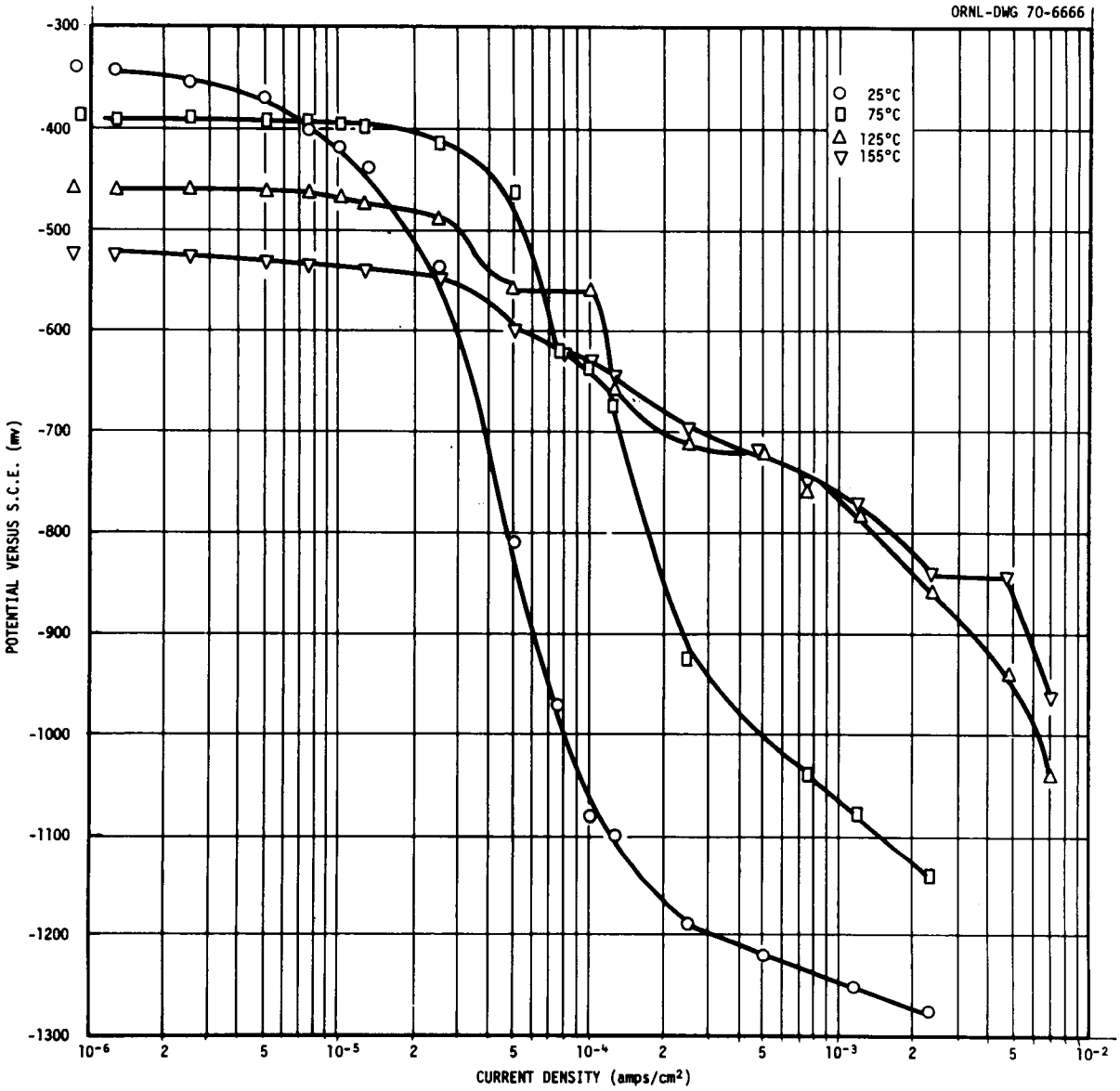

Fig. 20. Cathodic Polarization Curves Obtained with a Copper Electrode in Deaerated 1m NaCl. Flowing at 4 fps.

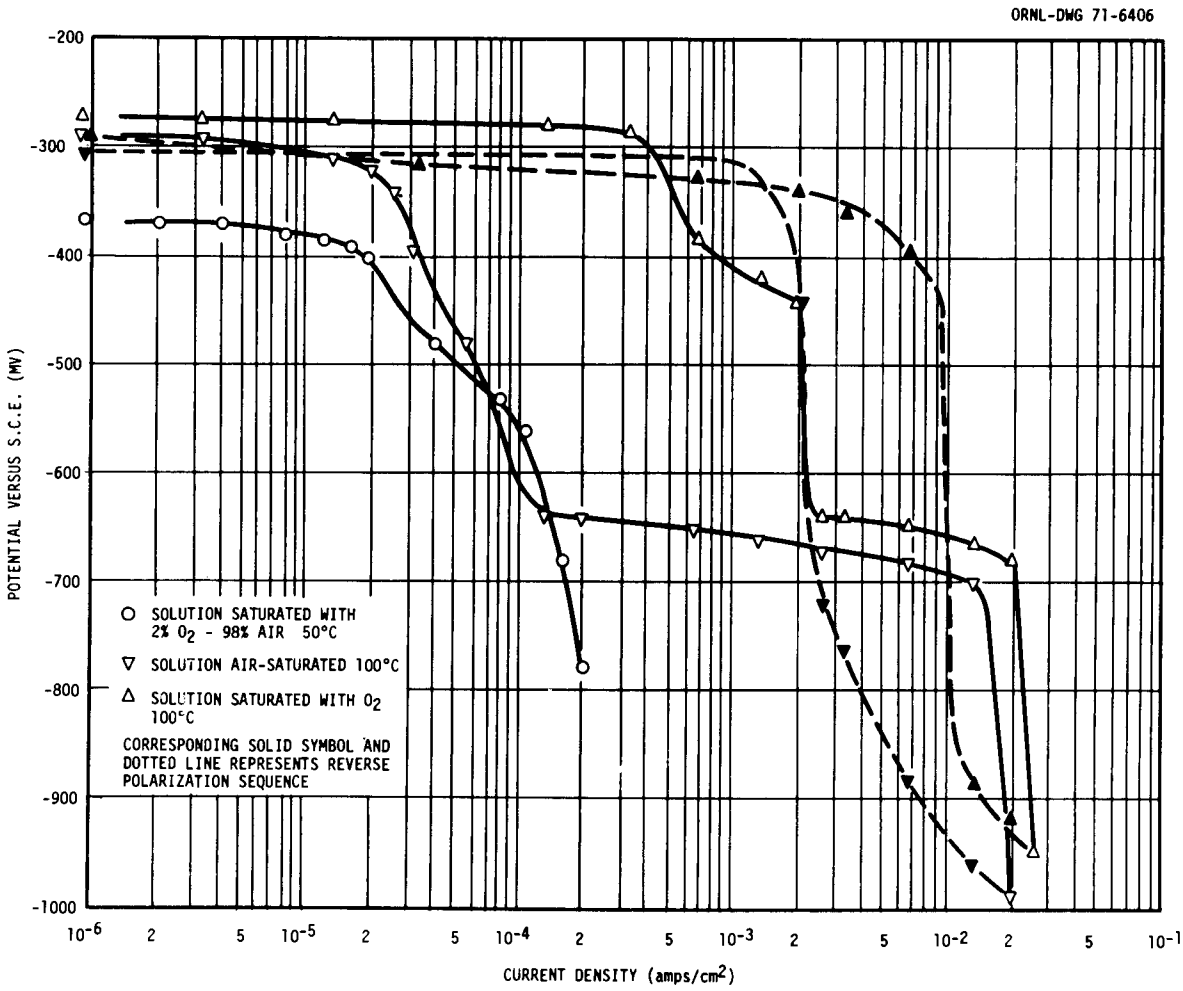

Fig. 21. Cathodic Polarization Curves Obtained in O_2-Containing 1m NaCl Flowing at 4 fps.

cathodic direction. At 100°C after potentials of between -900 and -1000 mv vs SCE had been obtained, the polarization sequence was reversed and a second curve was obtained. Unfortunately only a forward curve was obtained at 50°C. At both oxygen levels at 100°C there appeared to be two regions where some reductive processes occurred on the forward curves and both were absent on the reverse curve. On the forward curves there appeared to be an "overshoot", that is the steady-state potential values were probably not obtained before the current was increased. The reverse curves at 100°C showed limiting diffusion current densities in correct proportion to the oxygen concentration. We interpret the data to indicate that at potentials near the open-circuit the oxygen reduction reaction was limited by the presence of some substance on the copper, part of which was reduced at about -400 mv and the rest at about -650; the reverse curve represented the reduction of oxygen on a "clean" electrode. Whether this is the correct interpretation is not certain, but most other alloys showed similar behavior.

Figure 22 shows cathodic curves obtained with five different alloys in 1m NaCl containing about 6 ppm O_2 at 125°C. These curves were obtained in a normal direction only and several of them showed evidence of reduction processes; had the reverse curves been obtained, it is probable that most, if not all, of the inflections in the curves would have been eliminated and a single limiting current density would have been observed. It was of interest to note, however, that the limiting current densities were different for the different materials, being the smallest for 70-30 CuNi and the largest for copper. Of those alloys exposed for weight loss measurements in a similar solution (see Table 2), the order of corrosion resis-

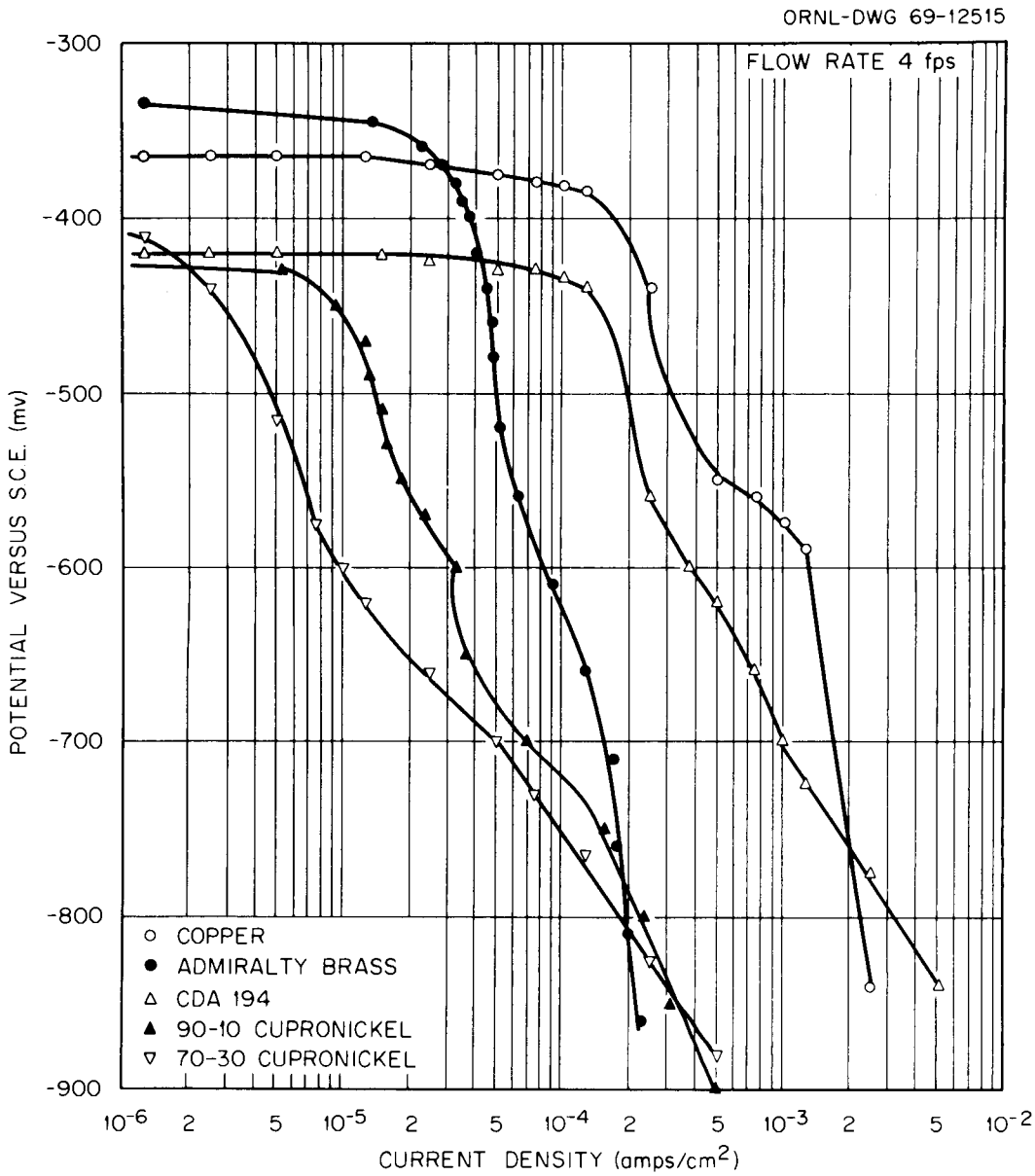

Fig. 22. Cathodic Polarization Curves Obtained with Five Different Materials in 1m NaCl Containing ∿ 6 ppm O_2 at 125°C.

tance was the same as the order of the limiting diffusion current density. Thus 70-30 CuNi had the lowest corrosion rate, followed by 90-10 CuNi; Admiralty brass had the highest corrosion rate. Copper and CDA-194 were not exposed for weight loss determination.

Most cathodic curves conducted in "deaerated" solutions showed evidence of a limiting diffusion current density which appeared to be related to traces of oxygen in the solution. To be sure that this was the case several polarizations were made with about 50 to 60 ppm $SO_3^=$ as sodium sulfite added to the solution. These curves are shown in Fig. 23. The diffusion limited process seemed to be replaced by an activation controlled process. The slopes of the Tafel lines on the different materials ranged between 85 and 95 mv. The cathodic process corresponding to the Tafel behavior is not known for certain, but it has been reported that reduction of sulfite occurs at about -0.7V vs SCE at a dropping mercury electrode.[14] At a pH of 6.0 the following reactions were proposed:

$$HSO_3^- + 2H^+ e \rightarrow HSO_2 + H_2O$$
$$2HSO_2 \rightarrow H_2S_2O_4 \rightleftarrows 2H^+ + S_2O_4^=$$

It seems probable that the same or a similar process occurred on the copper alloys.

In the above cathodic polarizations the cathodic reduction of water was generally obscured because other more easily reducible substances were present and at the potentials of interest the current corresponding to the reduction of water was small. However in sodium chloride solutions free of other reducible substances, the only cathodic process that can support corrosion is water reduction (see later section). In runs with sodium sulfide, which is also an oxygen scavenger and is not itself reducible,

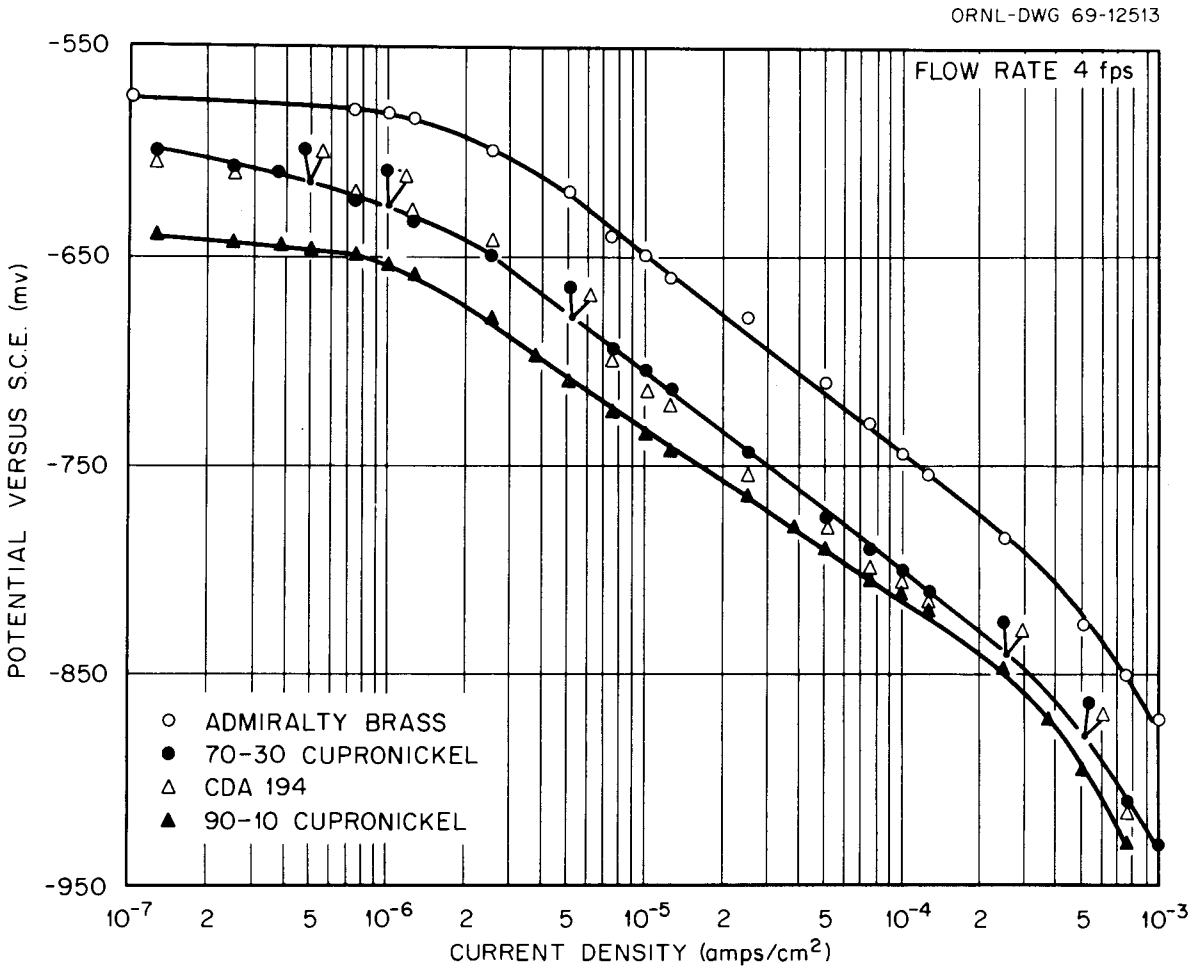

Fig. 23. Cathodic Polarization Curves Obtained in 1M NaCl Containing Sodium Sulfite at 125°C.

the only cathodic process available to support corrosion is the reduction of molecular water. Furthermore, since in the presence of sulfide the copper alloys achieve a very negative potential (close to the Cu/Cu_2S potential), reduction of water can proceed at an appreciable rate. This fact is illustrated in Fig. 24 in which both the anodic and cathodic curves for a 90-10 CuNi specimen are shown. A cathodic curve starting at the open-circuit potential and proceeding in a cathodic direction was obtained. After achieving a potential of about -1250 mv vs SCE the sequence was reversed and a second curve was obtained. On the forward curve there was first an apparent Tafel slope, followed by a region of unpolarizability, and this was followed by another Tafel region of about the same slope as the first. The reverse curve contained only a single Tafel region of the same slope as the other two. We believe that the first slope represents the reduction of water on a sulfide-coated (or maybe partially coated) surface. The region of unpolarizability represents reduction of a component on the surface (probably Cu_2S) and the last Tafel region represents the reduction of water on a clean (or cleaner) surface. The extrapolation of the first Tafel line to the corrosion potential results in a current density of about 10^{-5} amps/cm^2 which corresponds to a corrosion rate of about 8 mpy. This rate is in reasonable agreement with that observed from weight loss data (see Table 2).

Cathodic curves with other copper alloys were obtained in the presence of sulfide and all were similar to that shown in Fig. 24. At about -950 mv vs SCE a region of unpolarizability was observed on the forward curve which was absent on the reverse curve.

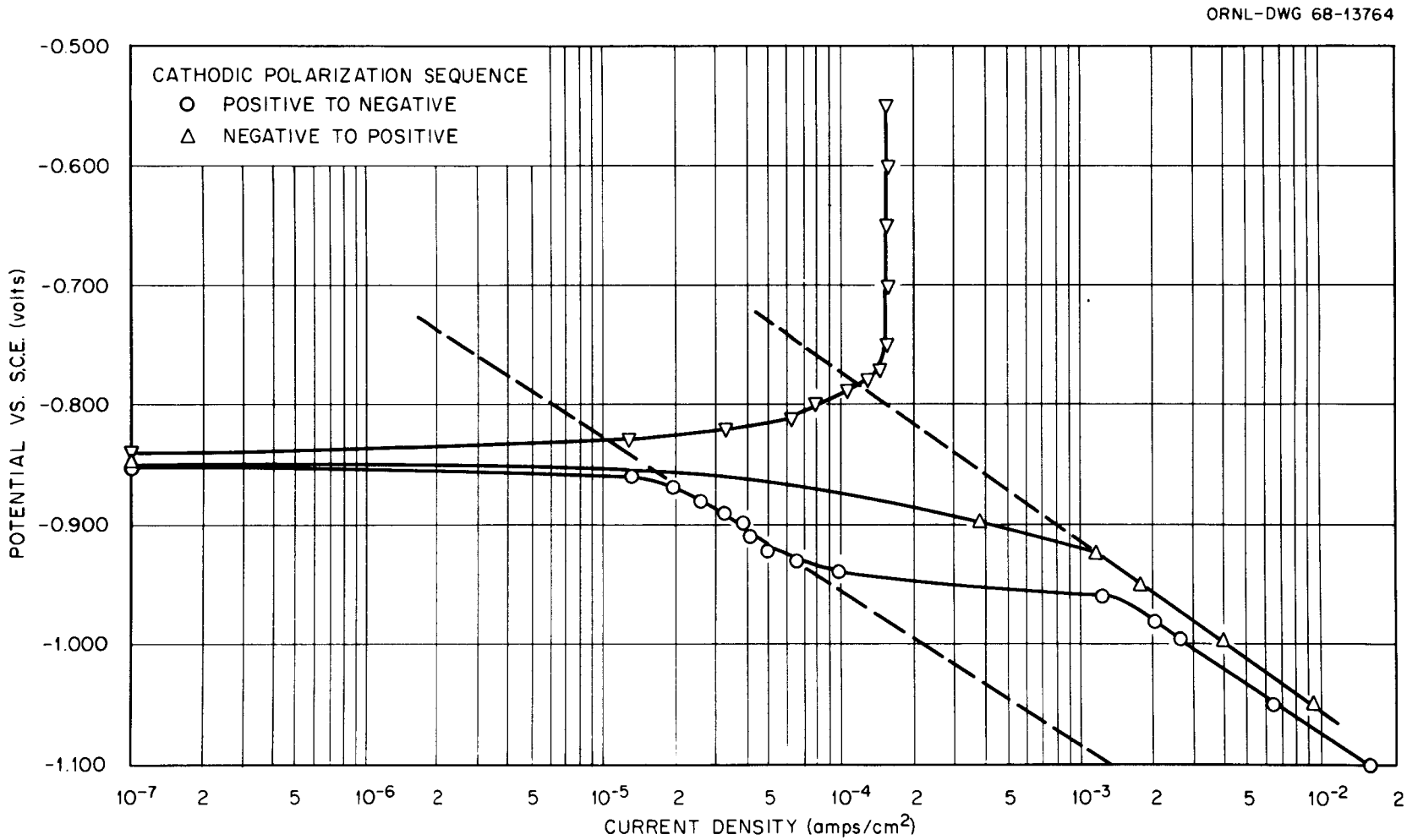

Fig. 24. Polarization Curves Obtained with a 90-10 CuNi Specimen in 1m NaCl Containing 2.5 ppm Sulfide at 125°C. Flow Rate - 4 fps.

Laboratory Data - One of the major difficulties in obtaining cathodic polarization data is adequate purification of the solution. In the loop experiments described in the preceding section, the possibility of contamination of the solution with air (O_2) during pumping of the solution into the loop and by corrosion products originating from the metallic system were ever present. Under laboratory conditions contamination and other variables are more easily controlled than in a loop.

A complete polarization curve obtained in boiling, deaerated 1.24m NaCl (pH = 7.6) is shown in Fig. 25. The major cathodic process is the reduction of molecular water to hydrogen. Analysis of the curve indicates in addition to the activation controlled process a limiting diffusion current of 5.3×10^{-7} amp for the 2.2 cm^2 electrode. An oxygen concentration of about 1 ppb would be sufficient to support this current. Also shown in Fig. 25 are similar data for 30°C. Based on the data shown, the corrosion rate of copper was about 0.2 mpy at 100°C and about 100 times less at 30°C.

Experiments were also conducted to examine the reduction of $CuCl_2^-$ and oxygen on copper. These experiments were conducted in deaerated 1.24m NaCl (pH = 7.4) at 90°C. The diffusion limited current expected can be calculated from Fick's First Law,

$$i_d = \frac{zFDc}{\delta} ,$$

where i_d is the current density (amps/cm^2), z is the number of electrons involved (1 for $CuCl_2^-$ and 4 for $O_2 \rightarrow H_2O$ or 2 for $O_2 \rightarrow H_2O_2$), F is the Faraday, D is the diffusion coefficient (cm^2/sec), c is the concentration (moles/cm^3), and δ is the diffusion layer thickness (cm). The diffusion coefficient for Cl^- is 7×10^{-5} cm^2/sec at 100°C[15] and the same value was

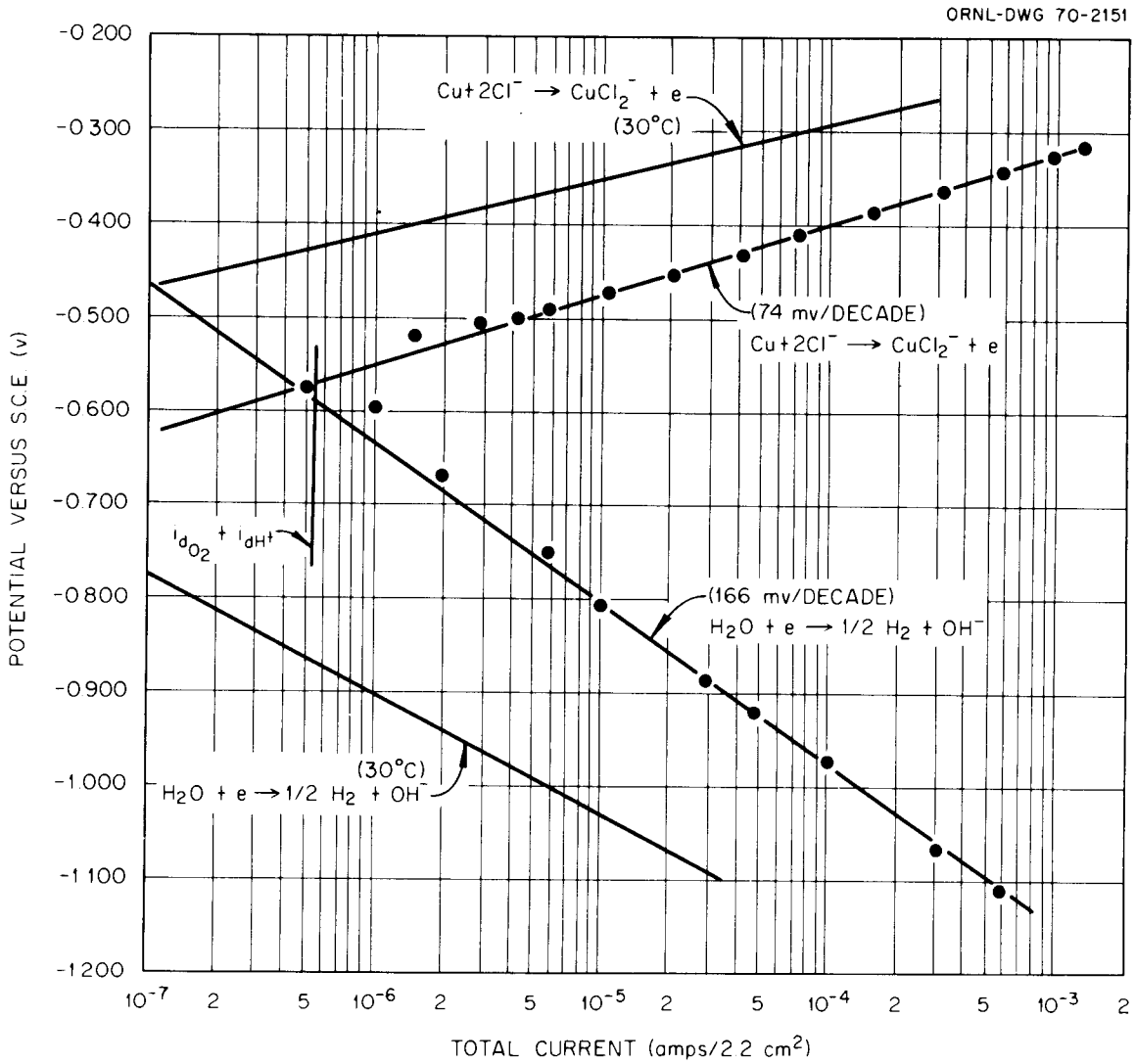

Fig. 25. Polarization Curves in Boiling 1m NaCl at 100°C pH = 7.6.

used for O_2 and $CuCl_2^-$ at 90°C. From other studies δ was determined to be 14×10^{-3} cm. Also from the Henry's Law Constant and from the oxygen partial pressure the oxygen concentration was calculated. The desired concentration of $CuCl_2^-$ was obtained by dissolving the correct weight of CuCl in the 1.24m NaCl solution.

Figure 26 shows the cathodic polarization curves obtained when the solution was saturated with O_2 at 90°C ($pO_2 + pH_2O = 1$ atm) resulting in a calculated oxygen concentration of about 6 ppm (1.9×10^{-4} m) and when the deaerated solution contained 2.63×10^{-5} m $CuCl_2^-$. The anodic curve was obtained when the solution contained only $CuCl_2^-$. The potential obtained upon extrapolation of the limiting diffusion cathodic current for $CuCl_2^-$ to the anodic Tafel line was identical to the observed open-circuit or corrosion potential, -0.409v vs SCE. Also the observed i_d of 3.3×10^{-5} amps agreed satisfactorily with that predicted from Fick's First Law, 2.9×10^{-5} amps.

In case of oxygen reduction the limiting cathodic diffusion current of 8×10^{-4} amps also agreed with the calculated value of 8.5×10^{-4} amps. However the open-circuit potential obtained upon extrapolation of the diffusion limited cathodic current to the anodic Tafel line was -0.303v compared with the observed value of -0.328v. In a repeat experiment under the same conditions the same result was observed. With 20% oxygen in the gas the discrepancy between the extrapolated and observed was also 25 mv.

The calculated diffusion limited cathodic current for oxygen assumed the reduction of oxygen to water, that is a 4 electron change, and this value agreed with the observed diffusion limited current. However if at low overvoltages (near the corrosion potential) oxygen was reduced to

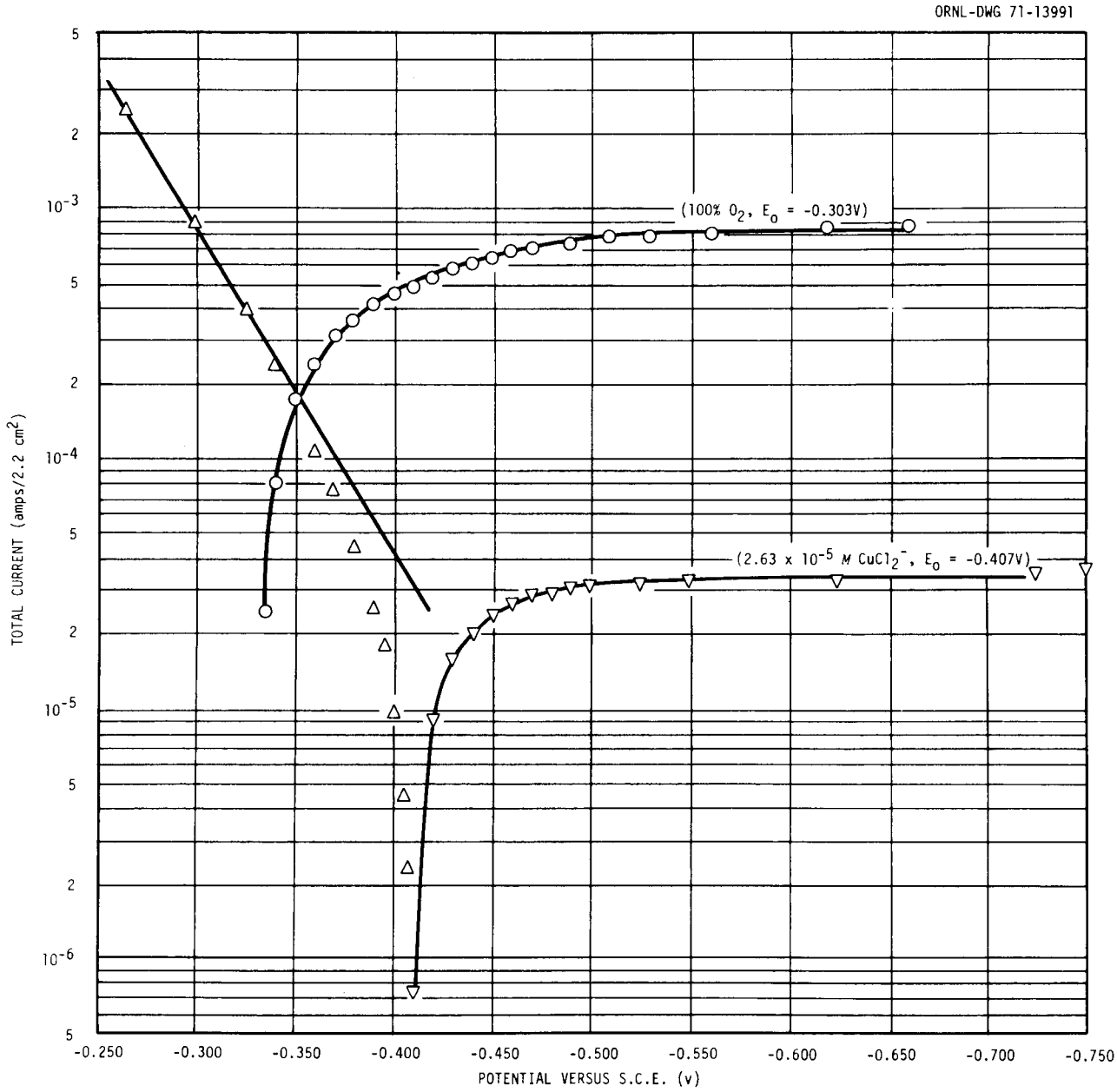

Fig. 26. Oxygen and $CuCl_2^-$ Reduction on Copper in 1.2 m NaCl at 90°C.

H_2O_2, then only two equivalents per mole of oxygen are required. Since the anodic Tafel slope, dE/dlog i, at 90°C is 72 mv, the difference in open-circuit potential would amount to 22 mv (72 log 4/2), a value in close agreement with the 25 mv observed. Another possible explanation for the discrepancy is that at low cathodic overvoltages oxygen reduction may be activation controlled. At present it is not possible to determine which, if either, of the above explanations is correct.

In deaerated acid saline solutions the reduction of protons becomes the predominant cathodic process as is illustrated in Fig. 27. These data were taken in 1.24m ($Na^+ + H^+$)Cl solutions at 100°C. Cathodic polarization curves were obtained with both copper and 70-30 CuNi in solutions with pH's ranging from 0.6 to 4.0. Under the above conditions the anodic polarization curves for both copper and 70-30 CuNi are the same and independent of pH. In Fig. 27 the solid cathodic Tafel lines are for hydrogen evolution on 70-30 CuNi and the dashed ones are for copper. The solid arrows locate the experimental corrosion potential for 70-30 CuNi at the given pH and the dashed arrows are those for copper. It should be noted that the corrosion potentials obtained from the intersection of the anodic and cathodic Tafel lines for 70-30 CuNi agreed within $\pm$ 5 mv with the experimental values at each pH. Only at the two lower pH's (0.56 and 1.6) were the extrapolated and experimental corrosion potentials for copper in agreement; at higher pH's there was an increasing deviation between the experimental and extrapolated corrosion potential. This deviation apparently occurred because of the increasing importance of another cathodic process (under diffusion control) relative to the reduction of protons. The origin of this current is not known. Actually the corrosion potential

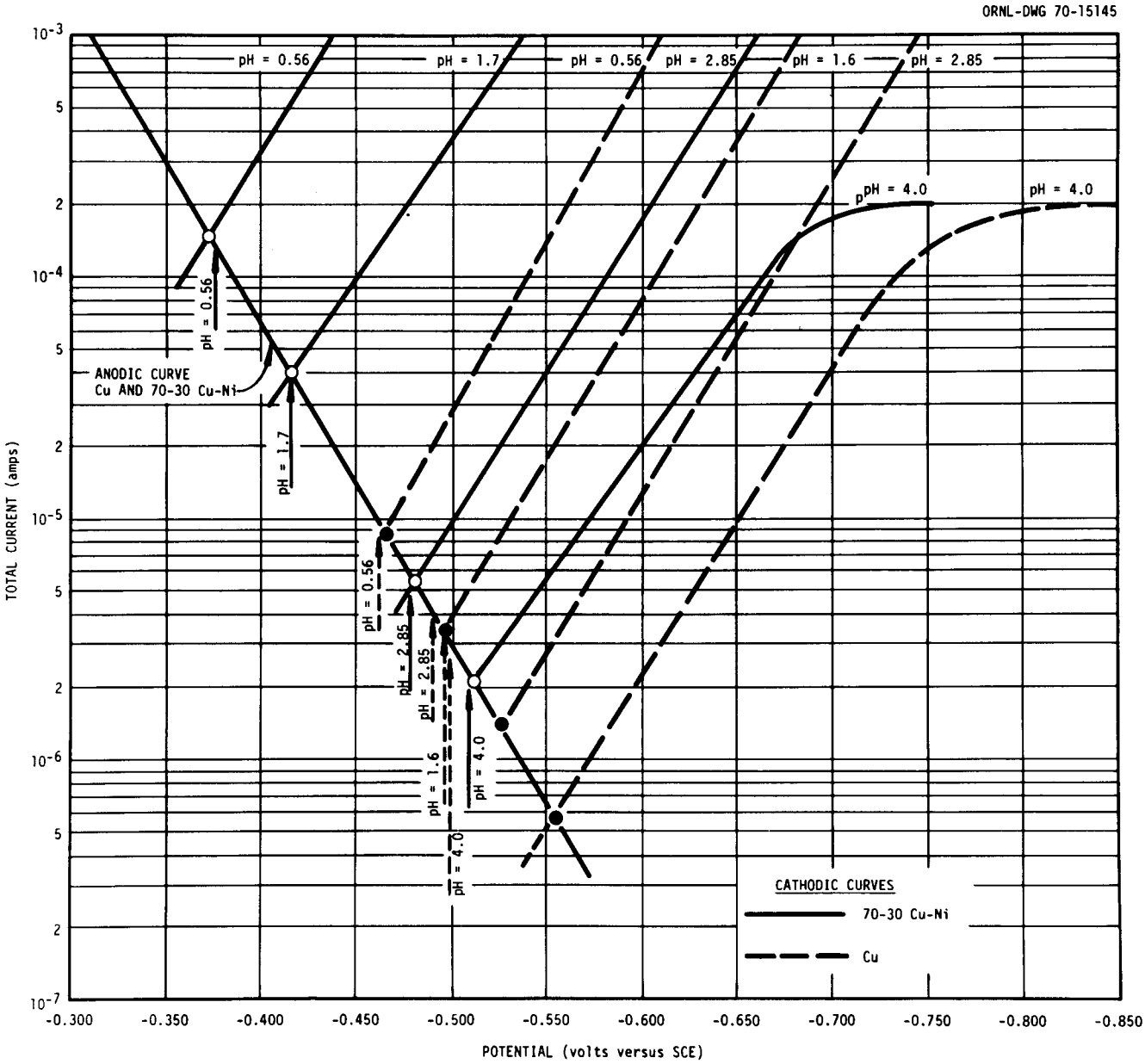

Fig. 27. Cathodic Polarizations for Hydrogen Evolutions from Protons in 1.24m Cl^- at 100°C as a Function of pH on Copper and 70-30 CuNi.

for copper from pH 1.6 to 9.0 was constant at -0.500 $\pm$ 0.010v vs SCE. At the pH's used in this study the diffusion limited process was not evident on 70-30 CuNi.

It should be noted in Fig. 27 that in the pH range of 0.56 to 4.0 the corrosion rate of 70-30 CuNi was higher than copper. However a closer examination reveals that at higher pH's the corrosion rate of copper would exceed that of the 70-30 alloy. This is best illustrated in Fig. 28 which shows that the kinetic order for proton reduction on copper is 0.72 and on 70-30 CuNi, 1.0. Thus the rate of hydrogen evolution decreases more rapidly with increasing pH on 70-30 CuNi than on copper.

From an analysis of the data presented in Figs. 27 and 28 it can be shown that the corrosion rate of the CuNi alloy would exceed that of copper up to a pH of about 8 if evolution of hydrogen from protons were the rate limiting reaction at this pH. It is known, however, that the dissolution rate of copper is higher than that for 70-30 CuNi even at a pH of 7 so obviously some other process was rate limiting. This process was most likely a diffusion limiting current on copper which maintained the corrosion current at about 1.5×10^{-6} amps/cm^2 and the potential at about -0.500v vs SCE. The above experiments give no indication why the diffusion limited process is apparent on copper and not on 70-30 CuNi.

An additional series of cathodic polarizations was conducted with copper in 1.24$\underline{m}$ $(Na^+ + H^+)Cl$ at pH's ranging from 0.04 to 3.95 over the temperature range of 30 to 101°C to study the evolution of hydrogen from protons. At pH values between 0.04 and 1.0 the cathodic polarization appeared to be independent of pH, and as at all other temperatures and pH values the Tafel slope was close to 2.3 RT/F. Analysis of the data showed

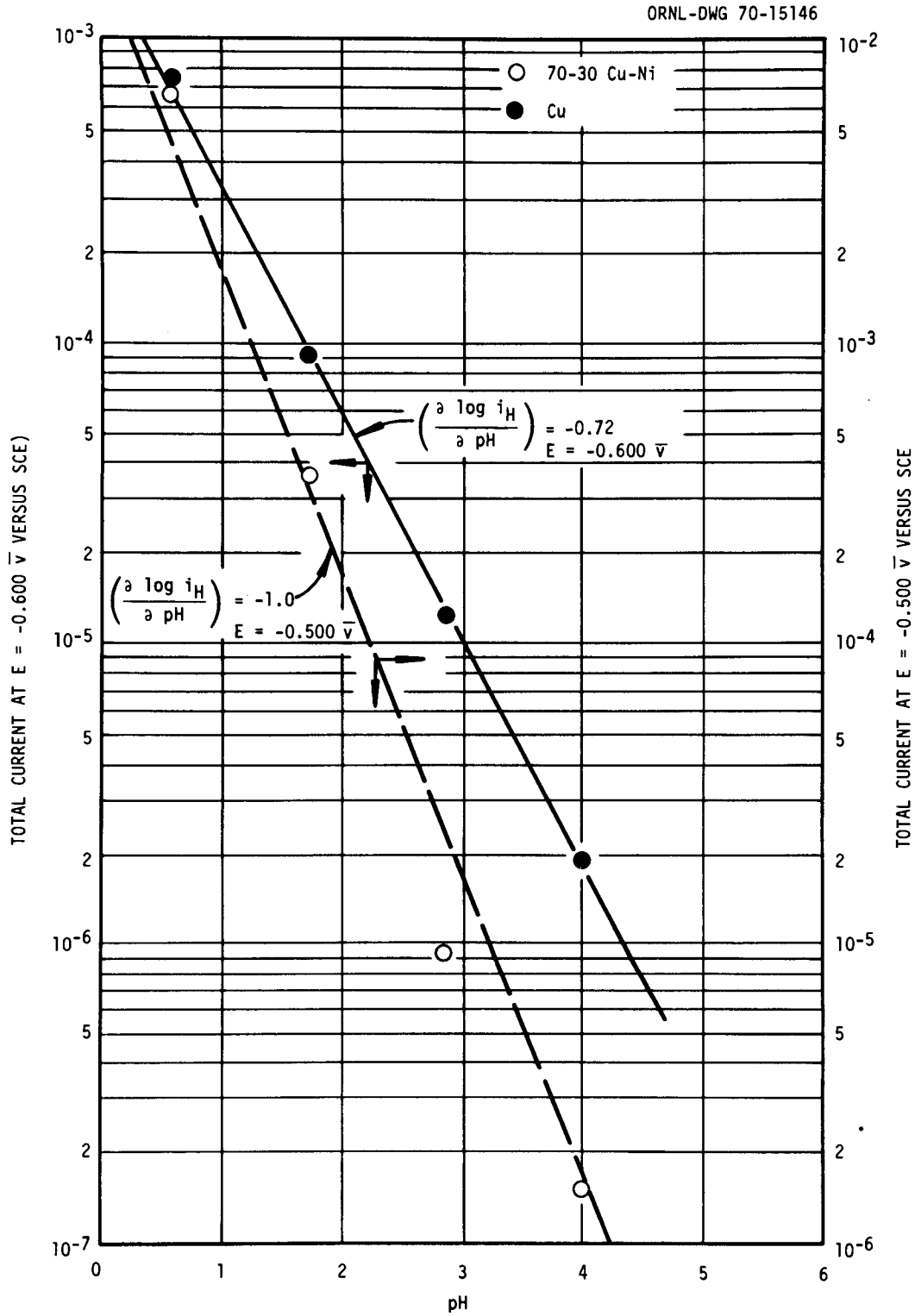

Fig. 28. Kinetic Order for Hydrogen Evolution from Protons on Copper and 70-30 CuNi in 1.24m at 100°C.

that at all pH values the temperature dependence was the same and corresponded to an activation energy of 16.9 $\pm$ 0.5 Kcal/mole at a potential of -0.550v vs SCE. The kinetic order with respect to pH, $(\partial \log i/\partial pH)_{T,E}$, was -0.6 at all temperatures, a value somewhat lower than that found in the previous study.

In a separate but similar study complete cathodic polarization curves were obtained in 1.24m NaCl with an adjusted pH of 3.95 at 29, 50, 75 and 101°C. The one obtained at 101°C is shown in Fig. 29. All others were similar. In Fig. 29 the open symbols are the experimental points and the closed points are those derived for the discharge of hydrogen from protons and from water.

To analyze or resolve the cathodic curve into its component parts it is necessary to consider also the anodic process at low current densities and for that reason the anodic polarization curve has been drawn on the figure. In the region near the corrosion potential the current due to hydrogen evolution from protons, i_{H^+} , is

$$i_{H^+} = i_N + i_A - i_{H_2O} - i_{D(x)}$$

where i_N is the experimental net cathodic current, i_A is the contribution from the anodic current (in the cathodic potential region), i_{H_2O} is the contribution from hydrogen evolution from water, and $i_{D(x)}$ is the contribution from an undetermined diffusion limited current (most likely O_2 at about 10 ppb). To obtain i_{H^+} both $i_{D(x)}$ and i_{H_2O} are needed. In the above case the contribution from i_{H_2O} was readily obtainable since $i_{H_2O} = i_N - i_{D(H^+)}$ in the region beyond the limiting diffusion current for proton reduction, 3×10^{-4} amp in Fig. 29. In this range i_A and $i_{D(x)}$ make negligible contributions to the net cathodic current. The assumed value for

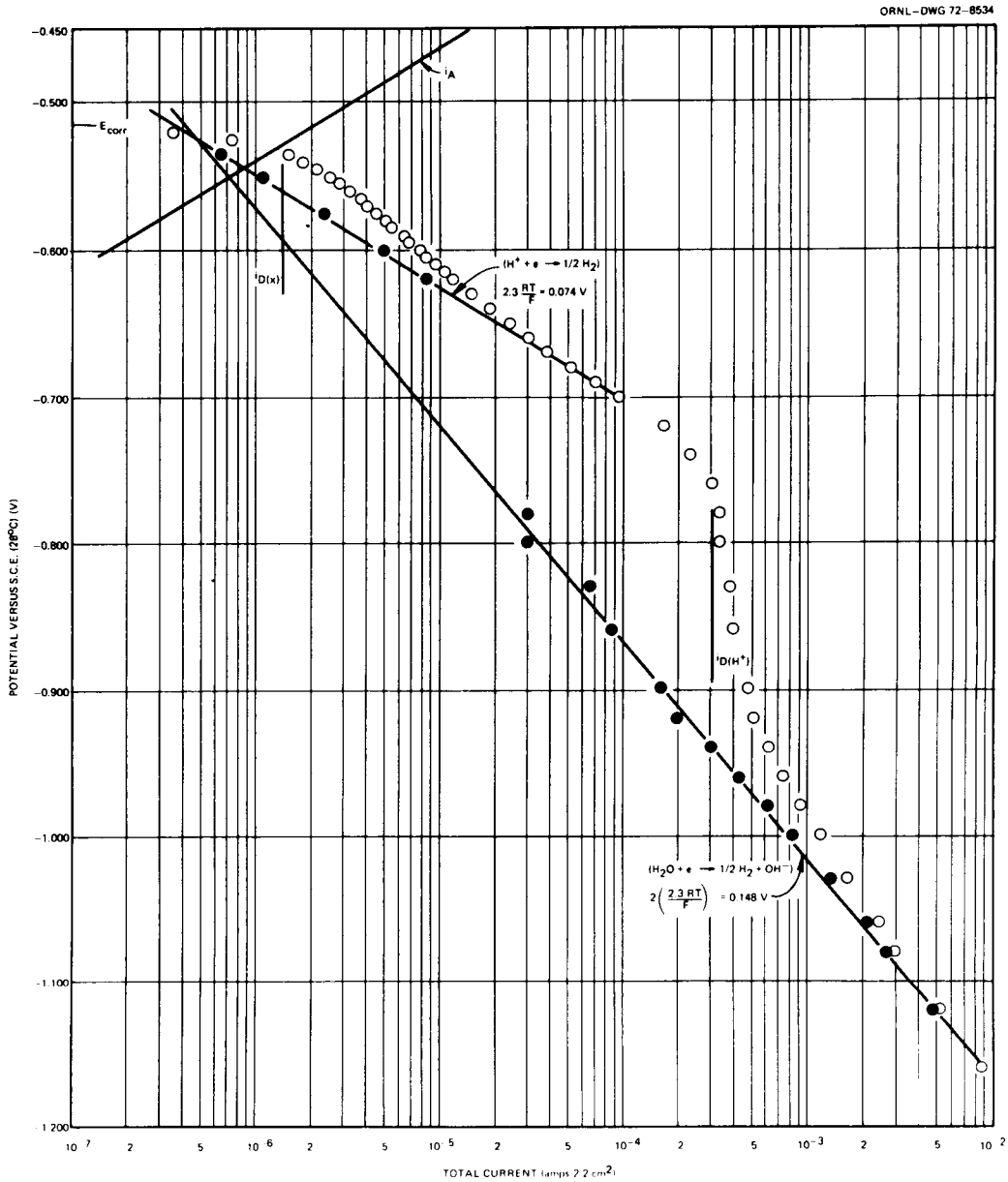

Fig. 29. Cathodic Polarization on Copper in 1.24m NaCl at 101°C and pH = 3.95.

$i_{D(x)}$ is then that value which gives the best Tafel line for i_{H^+}. Using the above procedure the solid symbols were calculated as being the Tafel lines for reduction of protons and reduction of water. As indicated in Fig. 29 $i_{D(x)}$ was 1.5×10^{-6} amps and $i_{D(H^+)}$ was 3×10^{-4} amps. The Tafel slope for reduction of protons was 0.074 mv (2.3 RT/F) and that for reduction of water, 0.148 mv [2(2.3 RT/F)].

The temperature dependence for the evolution of hydrogen from both protons and water is shown in Fig. 30. At a fixed potential of -0.550v vs SCE both processes had the same activation energy of 17.4 Kcal/mole.

Preliminary experiments in deaerated 1.24m NaCl at a pH of 6.0 indicated that the Tafel slope for the reduction of water was 2.3 RT/F near the corrosion potential and changed to 2(2.3 RT/F) at larger polarizations. Unfortunately time did not permit the verification of this observation, nor were we able to determine whether chloride concentration influenced water reduction; a few observations indicated that such might be the case.

DISCUSSION

The results of the weight-loss tests at 100 to 125°C were more or less in agreement with the generally accepted belief about the relative corrosion resistance of the materials tested. Thus, in essentially deaerated seawater 70-30 CuNi and Monel 400 were more resistant than 90-10 CuNi, and 90-10 CuNi was more resistant than Admiralty Brass. However, as the temperature was increased the advantage of the cupronickel alloys over brass or even pure copper disappeared; for example at 175°C the corrosion rate of copper was less than that of either 70-30 CuNi or Monel 400 during a 1500-hr test. At 200°C Monel 400 appeared to be slightly more resistant than copper and copper was more resistant than 70-30 CuNi. However, at

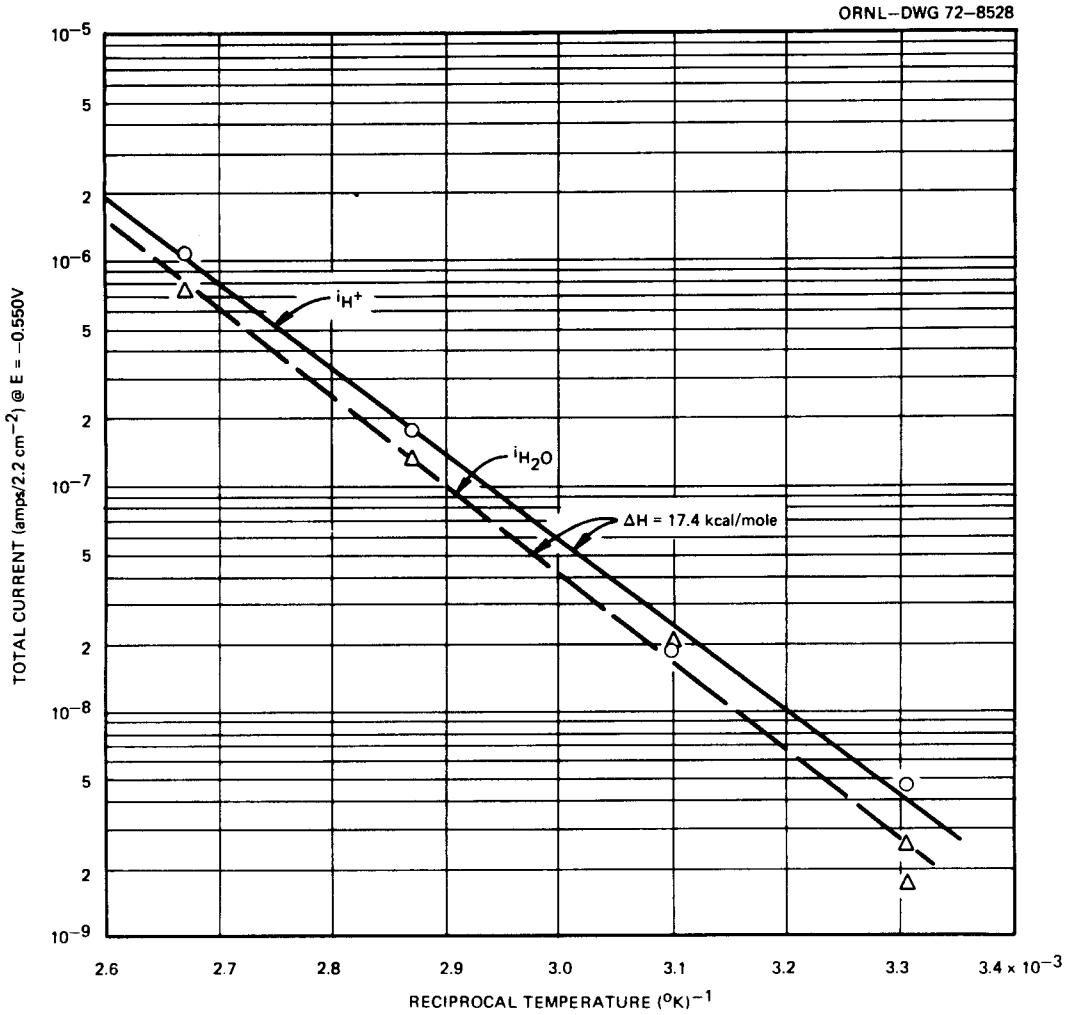

Fig. 30. The Temperature Dependence of Hydrogen Evolution on Copper from Protons and Water in 1.24m NaCl at -0.550v vs SCE. pH = 3.95.

the highest temperature the pH of the test solution (measured at room temperature) decreased slightly for unknown reasons and the results probably are not directly comparable with those obtained at lower temperatures.

It is generally recognized that the corrosion of copper and copper alloys in saline solutions is controlled primarily by cathodic processes and our results confirm this in most cases. Thus in the "deaerated" solution which contained in the range of 50 ppb oxygen some of the observed corrosion resulted from the oxygen in the solution. However if one assumes that the oxygen concentration of the feed solution was 50 ppb and was reduced to water in the corrosion process, a material balance shows that in every case the total amount of metal corroded was in excess of the total oxygen in the system. Thus at least a sizeable amount of the corrosion represented reduction of molecular water. Of course, the kinetics of the reduction of oxygen would not necessarily be the same with all alloys, so in our system with numerous specimens of different alloys how much oxygen was consumed by the different alloys cannot be determined. Comparing the data in Table 2 in runs with deaerated solution, air-saturated solution, and solution with sodium sulfite (an oxygen scavenger), it is obvious that of the materials tested Admiralty brass was much more susceptible to oxygen than were the other materials. Unfortunately copper, CDA-194, and aluminum brass were not exposed in these runs. It seems probable that these materials would have been as much, or more, affected by oxygen as was Admiralty brass.

The presence of 6 ppm oxygen in the 1m NaCl (125°C) produced some unexpected results, but subsequent electrochemical experiments provided a basis for explaining at least part of them. In the presence of 6 ppm O_2

it seems probable that the potential of passivation of the nickel-containing alloys was exceeded so that relatively low corrosion rates were experienced. In the case of 70-30 CuNi and Monel 400 the corrosion observed under the Teflon insulation could be rationalized on the basis of typical crevice corrosion which had its origin in a differential aeration cell, the oxygen concentration in the crevice being substantially lower than on the freely exposed surface areas. Presumably the oxygen concentration in the crevice solution was such that the alloys were in the active potential range whereas on the freely exposed surfaces the potential was in the passive range. Although fewer electrochemical experiments were conducted with 90-10 CuNi, those that were conducted indicated a passive behavior similar to 70-30 CuNi. Therefore the total absence of crevice corrosion on all 18 specimens of 90-10 CuNi and the presence of at least some attack on the 18 specimens of 70-30 CuNi was unexpected and is unexplained at this time. The presence of pits on some of the Monel 400 specimens indicates that the oxygen increased the potential up to the pitting potential. Similar behavior would be expected with 70-30 and 90-10 CuNi at sufficiently high potentials, and one can only conclude that the pitting potential of Monel 400 in 1m NaCl at 125°C is lower than that for 70-30 and 90-10 CuNi.

In the complete absence of oxygen, that is with excess sodium sulfite in the system, there was very little difference in the corrosion rates of any of the materials tested. At flow rates of 3 to 15 fps in 1m NaCl at 125°C all materials corroded at rates of less than 0.3 mpy. Based on cathodic polarization curves shown in Fig. 23 it appears that reduction of sulfite ions would constitute most of the cathodic process.

Sulfide ions are also scavengers for dissolved oxygen but in this case the presence of sulfide increased corrosion rates, particularly at temperatures of 100°C and higher. It was interesting to note that at 50°C 90-10 CuNi showed a significant effect of sulfide ions whereas 70-30 CuNi showed little or no effect. At all other temperatures, however, 90-10 and 70-30 NuNi showed similar high rates. Interestingly enough, Admiralty brass was essentially unaffected by the presence of sulfide and at 125°C actually showed lower corrosion rates with sulfide in the solution than in the deaerated solution (Table 2). Although industrial publications recommend the use of Admiralty brass in sulfide-containing saline water, no explanation for the better corrosion resistance of this alloy in the sulfide environment has been presented. Unfortunately we did not have time to conduct detailed electrochemical studies and to determine the composition of surface films with this alloy which might have been helpful in understanding the good corrosion resistance of Admiralty brass in sulfide-containing saline solutions.

Cystine under the conditions of test had a significant effect on the corrosion of 90-10 and 70-30 CuNi, Admiralty brass, and Monel 400. At a concentration of 10 ppm, the corrosion rates observed on all four materials were about the same at the same velocity and all showed increasing corrosion rates with increasing velocity. In a similar test with 40 ppm cystine the four alloys showed different corrosion rates and all showed a relatively large velocity effect. Some black corrosion product removed from one of the 90-10 CuNi specimens was examined by X-ray diffraction. The pattern indicated the presence of both Cu_2S and Ni_3S_2. Both of these compounds were also present in the film of a similar specimen exposed to

the solution containing 10 ppm sulfide (as Na_2S).

Cystine could presumably produce detrimental effects in three different ways: first, cystine is an alpha amino acid and as such can act as a chelating agent for metallic ions; secondly, degradation of the compound could produce ionic sulfide which has a detrimental effect, particularly on the cupronickels; and thirdly, degradation could produce ammonia which might accelerate corrosion of copper alloys. Complete degradation of cystine at a concentration of 10 ppm would produce 2.7 ppm sulfide and 1.5 ppm ammonium ion. That neither of these products was formed to any major extent was shown by the absence of odor and pH change in the letdown stream. Thus with the present data it is not possible to determine why cystine affects the corrosion of copper alloys.

One of the more puzzling aspects of our weight-loss data was the general absence of a significant velocity effect in the deaerated solutions. Failures in copper alloy condenser tubes usually result from localized attack in regions of high turbulence such as immediately downstream from an obstruction in a tube. In these cases the attack has a characteristic irregularly pitted appearance in the affected areas. No such form of attack was noted in any of our tests, even when protrusions were built into the specimens or at bulk solution velocities up to 100 fps. No good explanation is readily apparent to account for the absence of such an effect but two factors may be important. Our solutions were made with pure water and sodium chloride and contained no particulate matter such as probably exists in actual seawater. Thus it is possible that particulate matter could be the responsible agent for the attack observed in actual seawater. Another possibility may be that the pressure on our systems was too high

to permit cavitation, that is, the formation of vapor bubbles at regions of high velocity (low pressure) followed by subsequent collapse at lower velocities. Whether either of the above explanations is applicable or whether some other explanation must be found cannot be determined at the present time.

One of the more interesting observations made with regard to velocity effects was the selective deposition of metallic copper on the leading edges of flat coupons when the solution contained oxygen. Deposition was observed on 90-10 and 70-30 CuNi and Admiralty brass (the only materials examined). This observation was only noted at high bulk solution velocities (> 20 fps) and the location on the specimen was always on the leading edge, regardless of the bulk velocity gradient over the flat specimen. For these tests ten flat specimens were end-to-end in a holder with a symmetrically tapered Venturi flow channel. The specimens were separated from the holder and each other by wrapping the end with 2 to 3 mil thick Teflon tape so that each coupon was separated from its neighbors by 4 to 6 mils (see Fig. 2). It appears that the interruption between coupons in the flow channel produced localized turbulence immediately downstream from the interruption, and it was in this region where copper deposited. Downstream from the copper deposit on each coupon was an area which appeared to be totally unattacked and the rest of the specimen had a lightly and uniformly etched appearance. Why copper deposited where it did and why the presence of oxygen appeared to be a necessary condition is not understood at this time. With oxygen in the system both the anodic and cathodic processes should be diffusion controlled and an increase in turbulence should affect both processes to about the same extent.

The most complete electrochemical study was concerned with the anodic oxidation of pure copper. Although the results of this study have been reported,[9] the similarity of anodic processes on copper and all copper-nickel alloys investigated is striking and justifies repeating some of the interpretation of the copper data previously reported.

In the case of copper the anodic current density depended on the velocity indicating that the anodic process was diffusion controlled. Yet Tafel slopes equal to 2.3 RT/F were obtained. The explanation of this phenomenon is as follows. The reactions of importance are

$$Cu + 2Cl^- = (CuCl_2^-)_i + e \tag{1}$$

$$(CuCl_2^-)_i \xrightarrow{r.d.s.} (CuCl_2^-)_s \tag{2}$$

where the subscripts i and s refer to concentrations at the copper-solution interface and bulk solution, respectively. The rate determining step (2) is the diffusion transport of $CuCl_2^-$ from the interface to the bulk solution. The first step is assumed to be in equilibrium for which the Nernst equation,

$$E = E^o + RT/F \ln \frac{(CuCl_2^-)_i}{(Cl^-)^2}, \tag{3}$$

is applicable and from which $(CuCl_2^-)_i$ is obtained. Substituting $(CuCl_2^-)_i$ into the rate determining diffusion transport equation

$$i = \frac{zFD\,(CuCl_2^-)_i}{\delta} \tag{4}$$

$$i = \frac{zFD}{\delta}\,(Cl^-)^2 \exp \frac{F(E - E^o)}{RT} \tag{5}$$

In Eq. (5) z is the charge on the species undergoing mass transport, D is the diffusion coefficient for $CuCl_2^-$, δ is the diffusion layer thickness, and $(CuCl_2^-)_i >> (CuCl_2^-)_s$. Since the diffusion coefficient is temperature dependent

$$D = D_o \exp(-\Delta H_D^*/RT). \tag{6}$$

Equation (5) can be rewritten to include the apparent activation energy for diffusion transport, ΔH_D^*,

$$i = \frac{zFD_o}{\delta}(Cl^-)^2 \exp \frac{-\Delta H_D^*}{RT} \exp \frac{F(E - E^o)}{RT} \tag{7}$$

In the above expression E^o, the standard redox potential for Eq. (1) is temperature dependent. Defining overvoltage, η, as $E - E^o$ and expressing Eq. (7) in logarithmic form yields

$$\log i = \log \frac{zFD_o}{\delta} + 2 \log (Cl^-) - \frac{\Delta H_D^*}{2.3RT} + \frac{F\eta}{2.3RT} \tag{8}$$

which is the same equation shown on page 38. From Eq. (8) it can be seen that the current density is proportional to the square of the chloride ion concentration, to the activation energy for diffusion transport, and to an electrical work term, $F\eta$. Furthermore the slope of the Tafel line, $d\eta/d \log i$, is equal to 2.3 RT/F which is indeed what is found. Furthermore since η is defined as $E - E^o$ and since E^o as a function of temperature is known, it is possible to calculate the apparent activation energy for diffusion transport of $CuCl_2^-$ by measuring the current density at any value of E and evaluating the $F\eta$ term or by extrapolating the Tafel lines to a potential equal to E^o, that is $\eta = 0$. The apparent activation energy for diffusion transport of $CuCl_2^-$ was found to be about 4.5 Kcal/mole.

In the case of the alloys E^o values are not known. However comparison of the polarization curves for copper with those for the copper-nickel alloys shows them to be very similar up to and including 125°C. This point is illustrated in Table 10 where the potentials at an arbitrarily chosen current density of 10^{-4} amps/cm^2 are shown for 25, 75, and 125°C. The potential values were obtained from the Tafel lines obtained at 4 fps. In those cases where duplicate runs were made both values are given. Examination of the data in Table 10 reveals little difference among the values for all materials at the same temperature.

Another indication of the similarities among the above materials is the effect of temperature on the anodic process. To illustrate this point the current density at -0.450 and -0.550v vs SCE was plotted against the reciprocal of the absolute temperature and the best line was drawn through the points. From the slope of the line an apparent activation energy was calculated. In most cases the fit of the points to the curve was good. The apparent activation energies are shown in Table 11. Also shown is the activation energy for nickel.

The average value for copper and the copper-nickel alloys is 18.5 Kcal/mole with a standard deviation of 1.2 Kcal/mole at -0.450v vs SCE and 20.9 Kcal/mole with a standard deviation of 1.1 Kcal/mole at -0.550v vs SCE. Certainly within the experimental error the activation energies for copper and the copper-nickel alloys were the same. The activation energy for nickel dissolution was distinctly lower. In this case the dissolution process was independent of velocity and was controlled by electrochemical activation.

Although comparisons of the Tafel lines and the activation energies for copper and the copper-nickel alloys showed marked similarities, the effect of velocity on anodic polarization showed differences. For turbulent flow it has been reported that δ, the diffusion layer thickness, is proportional to the product of the Reynolds number to the -0.9 power and the Prandtl number to the -0.33 power.[16] The Prandtl number is independent of velocity and the Reynolds number is directly proportional to velocity. Since the diffusion current density is inversely proportional to δ, the increase in current density should be proportional to velocity to the 0.9 power. Our experimental results with copper showed that at a fixed potential the current density increased as about the 0.8 power of velocity which was in reasonable agreement with the expected value.

Table 10. Potential of Various Materials at a Current Density of 10^{-4} amps/cm^2 in Deaerated 1m NaCl Flowing at 4 fps

Material	Potential vs SCE		
	25°C	75°C	125°C
Copper	-0.285	-0.379	-0.486
	-0.276	-0.386	-0.478
90-10 CuNi	-0.280	-0.382	-0.491
	-0.276	-0.373	-0.489
80-20 CuNi	-0.276[a]	-0.359	-0.478
	-0.280	-0.378	-0.485
70-30 CuNi	-0.280	-0.401	-0.468
	-0.279	-0.375	-0.484
50-50 CuNi	-0.268	-0.356	-0.484
40-60 CuNi	-0.285[a]	-0.403	-
	-0.288	-0.412	-0.511
10-90 CuNi	-0.264	-0.404	-0.471

a = 28°C.

Table 11. The Apparent Activation Energies for Several Materials in Deaerated 1m NaCl Flowing at 4 fps

Material	Apparent Activation Energy, Kcal/mole -0.450v vs SCE	-0.550v vs SCE
Copper	17.5	19.9
	17.2	19.5
90-10 CuNi	19.7	22.0
	20.4	21.8
80-20 CuNi	16.9	19.1
	17.9	20.2
70-30 CuNi	16.9	20.1
	19.1	21.8
50-50 CuNi	19.6	22.0
40-60 CuNi	19.9	22.1
	18.1	20.1
10-90 CuNi	19.3	21.7
Nickel	9.2	14.2

Furthermore it was shown that δ was independent of temperature[9] so the velocity dependence should be the same at all temperatures, and this was at least approximately true for copper[9] and for 90-10 CuNi (Figs. 6 and 8). However as the nickel concentration of the alloy increased, the velocity dependence of the current density generally became less even at room temperature; as the temperature increased the effect of velocity diminished and in most cases at 100°C, and in some cases even lower, no effect of changing velocity was apparent. At present no explanation is available to account for this observation, particularly when one considers the similarity of the polarization curves of all alloys and copper at temperatures between 25 and 125°C at 4 fps.

The fact that the apparent activation energy for nickel is distinctly lower than that for copper or the copper-nickel alloys may at least qualitatively explain why at low temperatures the anodic process is diffusion controlled, whereas at sufficiently high temperatures the dissolution process is activation controlled. Figure 31 shows the anodic Tafel lines for pure nickel and pure copper at 75, 125, 150 and 175°C. At current densities greater than 10^{-7} amps/cm^2 at 75°C copper dissolution requires a higher potential than nickel. The same is true at 125°C at current densities greater than 10^{-6} amps/cm^2. At 150 and 175°C the cross-over point occurs at progressively higher current densities, 5×10^{-6} and 3×10^{-5} amps/cm^2 at 150 and 175°C, respectively.

Since the slopes of the copper and nickel Tafel curves are different, it is obvious that the Tafel lines would cross at some current density at all temperatures. Why the slopes of the experimental Tafel lines seemed to change at 150°C is not clear. Based on Fig. 31, one might expect a nickel slope at 150°C up to a current density of about 5×10^{-6} amps/cm^2 and then a change to a copper slope. In all of our experiments (except with 90-10 and 80-20 CuNi) however, the nickel slope at 150°C persisted at current densities well in excess of 5×10^{-6} amps/cm^2; in fact the same slope continued until passivation began. Thus, based on the higher activation energy for copper compared to that for nickel one might expect that at some high enough temperature the dissolution of nickel from the alloy would become rate limiting as is indeed observed. Why this temperature seems to be in the vicinity of 150°C for most of the alloys cannot be determined from our present knowledge.

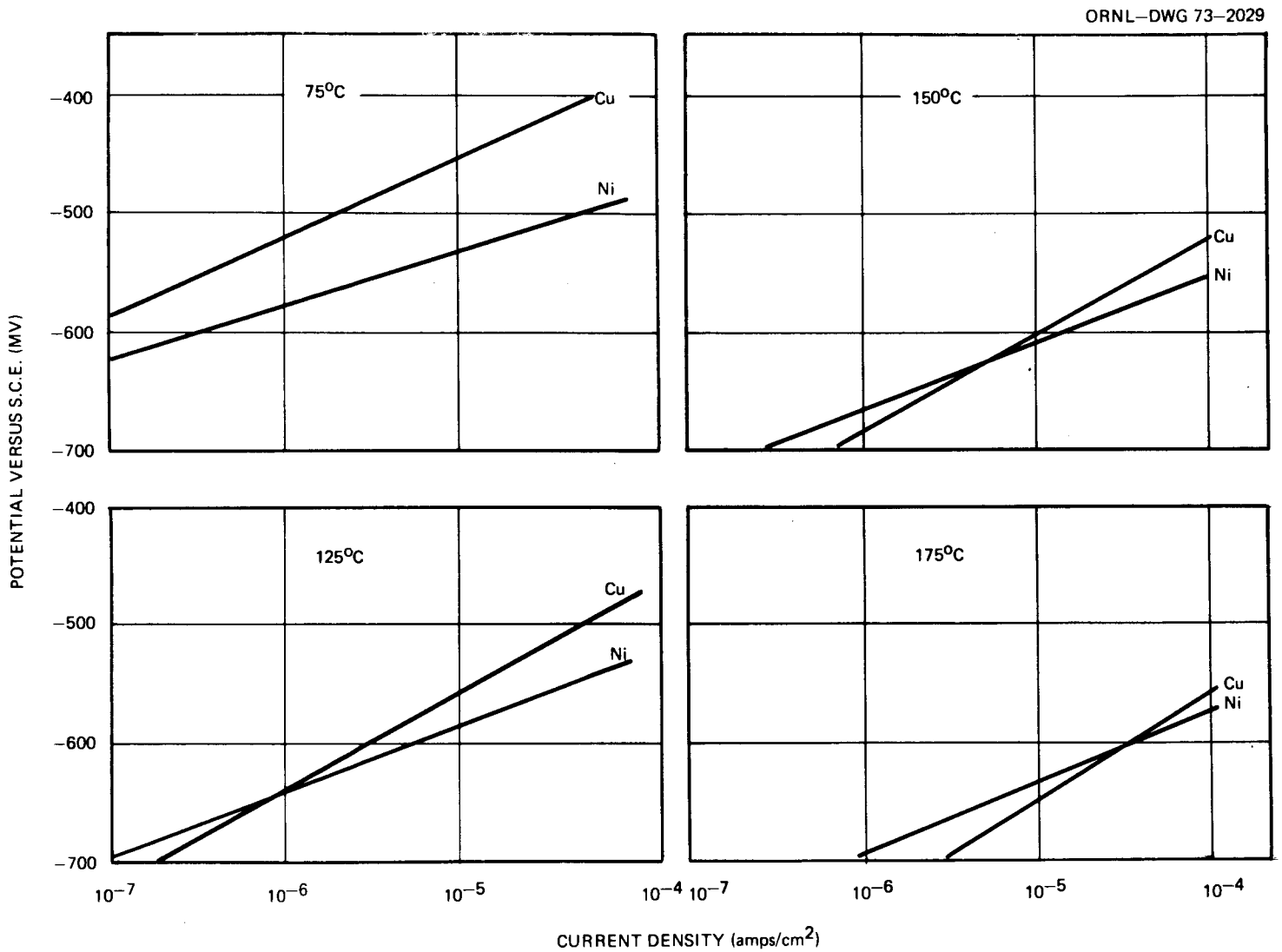

Fig. 31. Extrapolated Polarization Curves for Copper and Nickel in Deaerated 1m NaCl. Flow Rate - 4 fps.

From Fig. 31 and Tables 10 and 11 it is clear that up to 125°C the Tafel lines for the alloys are nearly the same as for copper. This fact is more clearly illustrated in Fig. 32 where the Tafel lines shown in the previous graphs have been reproduced and extrapolated. Except for 40-60 CuNi all alloys were no more than 15 mv from the line for pure copper, and the slopes of all lines range between 77 and 81 mv/decade. The line for pure nickel (slope of 55 mv/decade) is also included. Figure 33 shows a similar plot at 150°C for copper, nickel, and the copper-nickel alloys that changed slopes between 125 and 150°C. In this case all of the alloys had slopes close to nickel (52 to 58 mv/decade) and all were substantially above that for nickel. The slope for copper was 84 mv/decade. Thus the change in slope between 125 and 150°C is clearly distinguishable but the reason for the change is far from clear.

Not shown on Fig. 33 are the results for 90-10 and 80-20 CuNi. Neither of these alloys underwent a change in slope at 150°C; that is, both had polarization curves very similar to that for copper. At 175°C, the experimental slope of 80-20 CuNi was 55 mv, about the same as for pure nickel. The 90-10 alloy still had the copper slope, 89 mv/decade, at 175°C, the highest temperature investigated with this alloy. Thus at the low nickel concentrations there was evidence that higher temperatures were required before the transition in slope was observed. Similarly with the higher nickel alloys (40-60 and 10-90 CuNi) there was some indication, although not as clear as with 90-10 and 80-20 CuNi, that the transition might occur at temperatures somewhat lower than 150°C.

One interesting aspect of the polarization data of the alloys was the indication of an additional anodic process at low current densities at

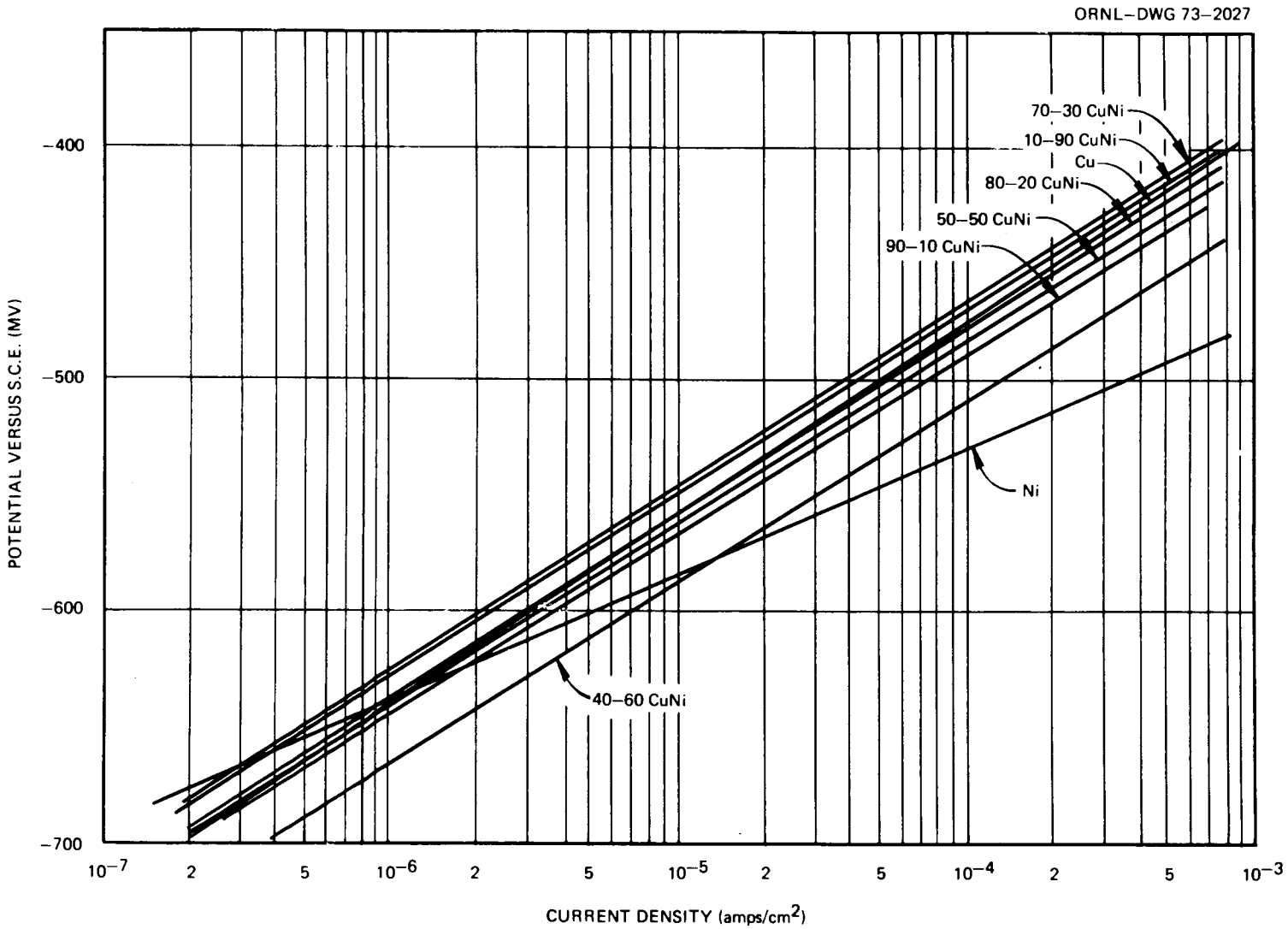

Fig. 32. Extrapolated Anodic Polarization Curves for Copper, Nickel and Copper-Nickel Alloys in Deaerated 1m NaCl at 125°C. Flow Rate - 4 fps.

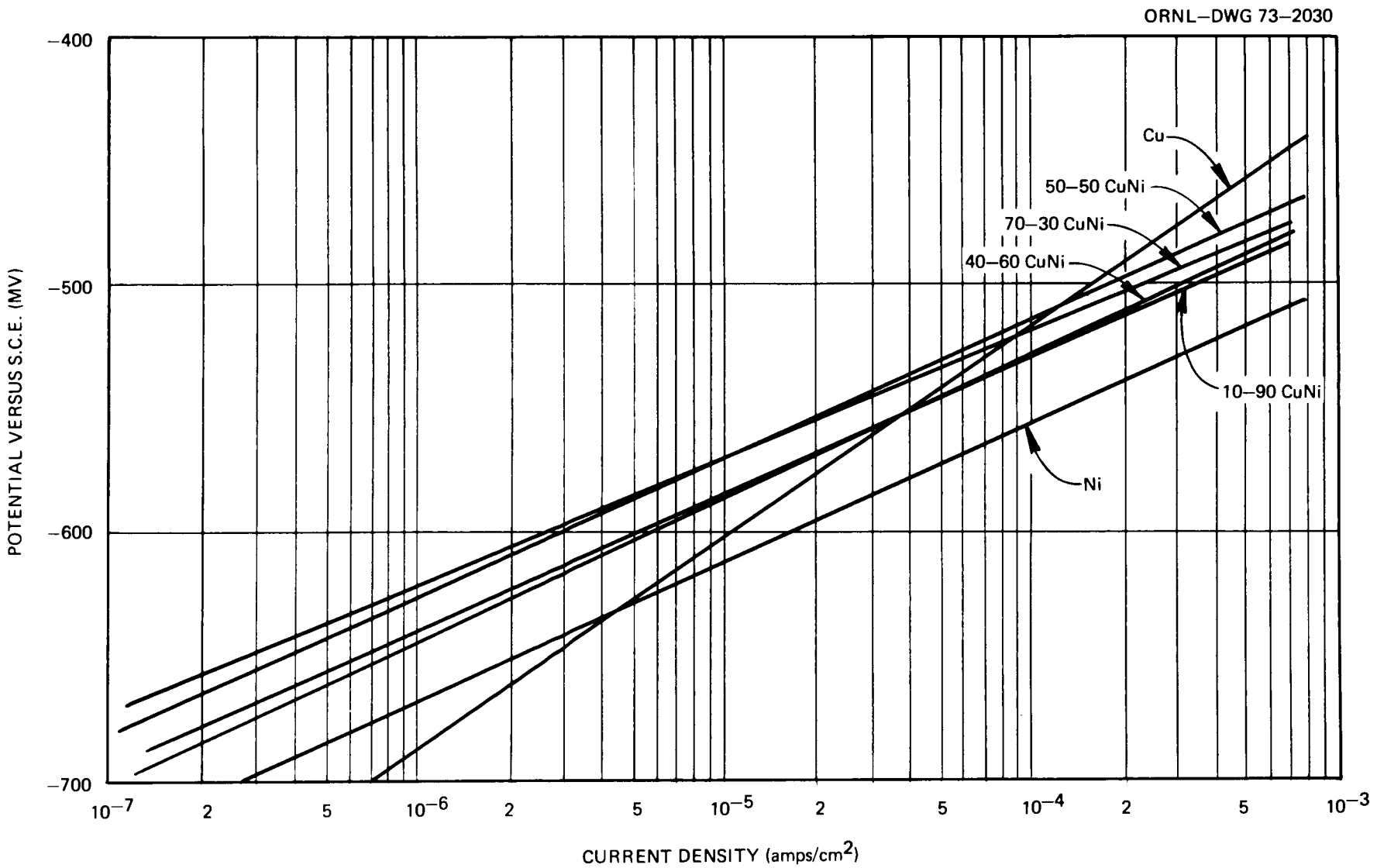

Fig. 33. Extrapolated Anodic Polarization Curves for Copper, Nickel and Copper-Nickel Alloys in Deaerated 1m NaCl at 150°C. Flow Rate - 4 fps.

temperatures of 150 to 200°C. There was a suggestion of the beginning of a Tafel line, followed by a region of unpolarizability, and this was followed by the Tafel slope discussed in the above paragraphs. In the case of the 70-30 CuNi data shown in Fig. 10 the additional process was not apparent, but on the other specimens of the same alloy it was noted. With 40-60 CuNi the additional process appeared as low as 100°C and was obvious on all curves up to 200°C. The open-circuit potential on the alloys varied somewhat from run to run which reflected the extent of the cathodic processes occurring on the specimen. However the region of unpolarizability appeared between -0.550 and -0.500v vs SCE in all cases. What anodic process is represented by the apparent Tafel behavior at low current density and how it affects corrosion of the freely corroding alloy have not been determined.

The examination of the surface films formed on 70-30 CuNi at different potentials produced an unexpected result. Below the passive potential either no oxide or a mixed oxide containing copper and nickel in the same ratio as in the alloy was present on the surface of the specimens. At or above the passive potential the surface film was composed largely, if not totally, of a nickel compound, probably an oxide or hydroxide. Since under the conditions of test the potential of formation of $Ni(OH)_2$ should be well below the passive potential, it seems likely that some higher valent oxide formed at the passive potential. However, the potential where passivation occurred did not correspond to any reported oxide or hydroxide of nickel. The photoelectron spectrum obtained from the surface of the specimen also showed the absence of chlorine, indicating that the deposit did not contain a basic chloride of either nickel or copper.

The passive potential, E_p, obtained for 70-30 CuNi in boiling 1.24m NaCl was related to the pH of the solution by

$$E_p = 0.19 - 0.076 \text{ pH}.$$

This equation was determined from anodic polarizations, that is on an electrode where the cathodic process was suppressed. We also showed that passivation could be achieved with oxygen at a sufficient concentration, in which case the above equation is not directly applicable. When the cathodic process is oxygen reduction, the pH at the reaction surface is greater than the pH of the bulk solution because of the hydroxide ions produced in the process:

$$O_2 + 2H^+ = 4e^- \rightarrow 2OH^-.$$

Thus E_p can be calculated by the above equation only if the pH at the solution-alloy interface is known. Although we did not investigate the passivation phenomenon at any other temperature, it appears possible that in ambient seawater the oxygen concentration may be sufficient to passivate 70-30 CuNi (and perhaps other nickel alloys) and this may account for the excellent corrosion resistance of the copper-nickel alloys in surface condensers.

The apparent absence of oxide on the 70-30 CuNi specimen at anodic potentials below E_p was in agreement with the anodic polarization curves which behaved in the same manner as pure copper on which no film formed under our conditions. On the other hand, cathodic data to be discussed later suggested the presence of some substance which appeared to inhibit the cathodic reduction of oxygen on 70-30 CuNi.

Time did not permit further investigation of the passivation phenomenon, but the data obtained in this study indicate that this is an area of great importance in understanding the corrosion of copper-nickel alloys in saline environments. One could speculate that if the potential of passivation could be lowered or the protectiveness of the passive film increased, for example by including another element in the alloy or in place of all or part of the nickel, a material with significantly better corrosion resistance in either aerated or deaerated seawater might be obtained.

Very few electrochemical data were obtained with the brasses (Cu-Zn alloys), but those that were obtained indicated that the anodic polarization characteristics were very similar to those of copper. The anodic polarization curves had the same slopes as copper up to 155°C, the highest temperature investigated. At sufficiently high current densities there were indications of passivation similar to that observed with the copper-nickel alloys.

The electrochemistry of the copper alloys in sulfide-containing chloride solutions was only investigated superficially at 125°C. The open-circuit potentials of copper, the copper alloys, and pure nickel were between -0.80 and -0.90v vs SCE and in all cases limiting diffusion current densities were noted in the anodic polarization curves. The data indicated that the diffusion limited current was not linearly related to the total sulfide concentration but was much less. The data presented in Fig. 17 show that as the nickel content of the alloy increased the current density at a given sulfide concentration decreased. Based on this information alone one might suspect that the effect of sulfide would be substantially

less on 70-30 CuNi than on 90-10 CuNi. However the data presented in Table 2 show that the two alloys actually corroded at about the same rate. The reason why the two corrode at the same rate appears to be that the rate in both cases is limited by the cathodic process, that is the reduction of water. This fact is illustrated for 90-10 CuNi in Fig. 24, and the same general behavior was noted for 70-30 CuNi. Table 2 shows that both Monel 400 and Admiralty brass had considerably lower corrosion rates than 90-10 and 70-30 CuNi in the presence of sulfide. Since Monel 400 is also a Cu-Ni alloy (∿ 69% Ni, 30% Cu, 1% Fe), it seems that at a sufficiently high nickel content the effect of sulfide on copper-nickel alloys is less than at lower nickel concentrations. In the case of Admiralty brass, not enough experiments were conducted to permit speculation about the reason for its good corrosion resistance in sulfide-contaminated saline water.

Although the anodic polarization data obtained with 70-30 CuNi indicated the absence of any film at potentials below the passivation potential, cathodic polarizations in oxygen-containing solutions certainly gave evidence of inhibition of the oxygen reduction process. This fact is illustrated in Fig. 22 where under similar conditions the limiting current density for oxygen reduction on 70-30 CuNi was about 100 times less than that for copper. A similar but lesser effect was noted on 90-10 CuNi and Admiralty brass. The reason for this effect is not known for certain, but it may be related to the fact that the oxygen concentration was sufficient to passivate these alloys. With the nickel alloys passivation produces a film highly enriched in a nickel compound (probably an oxide) and such films are not easily reduced as pointed out by Postlethwaite and Sephton.[17]

The presence of this type film may have been responsible for the low efficiency for oxygen reduction on the nickel alloys.

Although in neutral aerated solutions the cathodic process was much less efficient on 70-30 CuNi than on copper, the reverse was true in deaerated acid solutions. Proton reduction on 70-30 CuNi required less overvoltage than on copper in the pH range of 0.6 to 4.0. However, the kinetic order for the reduction of protons was 1.0 on 70-30 CuNi and only 0.7 on copper. Thus, at sufficiently high pH reduction of protons would be easier on copper than on 70-30 CuNi. Our data indicated that this would occur at about a pH of 8. Since the corrosion of copper and the copper alloys is usually controlled by cathodic processes, one would expect 70-30 CuNi to corrode at a greater rate in deaerated acid chloride solutions than would copper.

When this program was initiated, we stated that a basic understanding of corrosion mechanisms of the alloys, as well as the elements composing them, was essential if the corrosion of existing alloys was to be efficiently controlled or if new, more resistant alloys were to be developed. The results of our studies reinforce this view. Obviously there are gaps in our knowledge and understanding of the corrosion mechanisms; but we have developed information that shows at least qualitatively why some alloys behave as they do and that points to fruitful areas of future research. Furthermore, we showed that in the case of the copper-nickel alloys data developed at relatively low temperatures cannot be reliably extrapolated to high temperatures.

ACKNOWLEDGEMENT

The authors would like to acknowledge J. F. Winesette and A. L. Sutton for help in conducting the experiments and to Dr. R. E. Meyer for useful discussion concerning interpretation of the data. This work was sponsored by the Office of Saline Water, U.S. Department of Interior, under Union Carbide's contract with the U.S. Atomic Energy Commission.

References

1. L. L. Shrier, Corrosion, vol. 1, p. 4.13, John Wiley and Sons, Inc., New York, 1963.
2. ibid, p. 8.22.
3. ibid, p. 4.41-2.
4. J. C. Griess, Jr., Corrosion, 24, 96-109 (1968).
5. T. W. Bostwick, Corrosion, 17(8), 12-19 (1961).
6. R. F. North and M. J. Pryor, Corrosion Science, 8, 149-57 (1968).
7. D. B. Anderson, "Factors Affecting Corrosion of Copper and Copper Alloys in Hot Sea Water," Paper presented at Nat. Assoc. of Corrosion Engineers Meeting, Chicago, Ill., March 22-26, 1971 (Paper No. 61).
8. W. E. Berry, Corrosion in Nuclear Applications, pp 136-41, John Wiley & Sons, Inc., New York, 1971.
9. A. L. Bacarella and J. C. Griess, Jr., J. Electrochem. Soc., 120, 459-65 (1973).
10. N. Sato and G. Okamoto, J. Electrochem. Soc., 110, 605-14 (1963).
11. M. Pourbaix, Atlas of Electrochemical Equilibria in Aqueous Solutions, (translated from the French by J. A. Franklin), pp 330-32, Pergamon Press, New York, 1966.
12. A. J. de Bethune and N. A. Swendeman Loud, Standard Aqueous Electrode Potentials and Temperature Coefficients, Clifford A. Hampel, Skokie, Ill., 1964.
13. L. D. Hulett et al., J. Electron. Spectrosc., 1, 169-78 (1972).
14. I. M. Kolthoff and J. J. Lingane, Polarography, vol. 2, pp 559-60, Interscience Publishers, New York, 1952.

15. F. A. Posey, private communication (calculated from conductivity data using Nernst-Einstein Relationship).

16. K. J. Vetter, Electrochemical Kinetics - Theoretical and Experimental Aspects, pp 191-2, Academic Press, New York, 1967.

17. J. Postlethwaite and J. Sephton, Corrosion Science, 10, 775-84 (1970).

Appendix

Oak Ridge National Laboratory Water Research Program comprehensive reports to the Office of Saline Water, U.S. Department of the Interior:

First Biennium (March 15, 1962 to March 15, 1964)

ORNL-CF-67-8-55, issued as OSW R & D Progress Report 302

Second Biennium (March 15, 1964 to March 15, 1966)

Properties of Solutions, ORNL-CF-70-6-30, issued as OSW R & D Progress Report 685
Reactions and Transport Phenomena at Surfaces. Corrosion Studies, ORNL-TM-4097 (in preparation)
Separations Processes, ORNL-CF-69-5-41, issued as OSW R & D Progress Report 508

Third Biennium (March 15, 1966 to March 15, 1968)

Properties of Solutions, ORNL-TM-4096
Reactions and Transport Phenomena at Surfaces, ORNL-TM-4099
Separations Processes, ORNL-TM-4000

Fourth Biennium (March 15, 1968 to March 15, 1970)

Properties of Solutions, ORNL-TM-4214
Reactions and Transport Phenomena at Surfaces (to November 1, 1970), ORNL-TM-4145
Separation Processes, ORNL-TM-4001

Fifth Biennium (from March 15, 1970 to close of interagency agreements)

Properties of Solutions, ORNL-TM-4213 (in preparation)
Corrosion Studies (from March 15, 1966), ORNL-TM-4340 (this report)
Separations Processes, ORNL-TM-4236 (in preparation)

Crevice Corrosion of Titanium in Aqueous Salt Solutions*

JOHN C. GRIESS, Jr.*

Abstract

Crevice corrosion of titanium in high temperature sodium chloride solutions was investigated. Corrosion occurred only in very restricted crevices and attack was greater the higher the salt concentration. It was shown that crevice corrosion occurs because of the development of a low (~ 1) pH in the solution within the crevice and is not specific to chloride solutions. Crevice attack was demonstrated in iodide, bromide and sulfate solutions.

An electrochemical polarization technique was used to determine the effect of temperature and hydrogen and chloride ion concentrations on the corrosion of titanium and to determine the corrosion characteristics of several titanium alloys. Results indicate that titanium alloys containing sufficient molybdenum, nickel, or palladium are more resistant to nonoxidizing acid solutions than commercially pure titanium and, therefore, should be more resistant to crevice corrosion.

Titanium has a high degree of resistance to corrosion by neutral salt solutions even at relatively high temperatures. For this reason it is a potentially useful material for construction of desalination plants. In fact, one plant utilizing large amounts of titanium is presently in operation.[1] However, under certain conditions titanium is susceptible to severe crevice corrosion in aqueous salt solutions. Gleekman[2] and Sheppard et al.[3] referred to cases of service failures due to crevice corrosion in sodium chloride or chlorine environments. Turnbull[4] noted slight crevice attack in concentrated neutral brine solutions and the absence of such attack in similar alkaline brines (pH > 12). Shimose and Takamura[5] demonstrated crevice corrosion of titanium in hot concentrated magnesium or ammonium chloride solutions. Crevice corrosion in either synthetic seawater or sodium chloride solutions also was reported by Bohlmann and Posey.[6] In the latter paper no incidences of attack were observed at temperatures below 100 C (212 F), but frequency of attack increased as temperature increased. Crevice corrosion of a number of titanium alloys was observed.

This paper describes experiments carried out to determine the cause of titanium crevice corrosion and to attempt to find alloys more resistant to this form of attack than pure titanium. Successful solution of the problem of crevice corrosion would remove one major barrier to the use of titanium in large scale desalination plants.

Experimental

Experiments were carried out either in conventional glass laboratory equipment or in titanium autoclaves. The autoclaves were heated electrically and the temperature was controlled within ± 3 C in most cases; in those cases where the pressure was monitored, the temperature was controlled to ± 1 C. When electrochemical polarizations were carried out in the autoclaves, the head was modified to provide for two electrically insulated leads and a salt bridge to an external saturated calomel electrode (SCE) at room temperature. The methods of introducing the leads and the salt bridge were identical to those described by Bacarella and Sutton.[7]

All electrochemical polarizations were carried out potentiostatically allowing 3 to 5 min at each potential before changing. Generally the procedure was to start at the open-circuit or corrosion potential and proceed either anodically or cathodically. The volume of solution per cm^2 of exposed area was at least 250 ml. In solutions where titanium and its alloys were passive, open-circuit potentials usually were not constant but varied slowly in an irregular manner. In such cases the specimen was allowed to remain at the test condition for at least 15 min before beginning the polarization. When titanium corroded actively in the environment reasonably constant open-circuit potentials were obtained within a few minutes; random variations seldom exceeded 20 mv.

All solutions were prepared using reagent grade chemicals and deionized water with a specific resistance greater than 10^6 ohm-cm. Throughout the report concentrations are expressed as molarity or normality at room temperature. As the density of the solution decreased on heating, these concentrations decreased. At 150 C (302 F) the actual concentrations were only about 92 percent of those listed.

The commercially pure titanium used in this investigation was obtained from different fabricators either as rod or plate. Based on mill analyses other elements ranged between 0.01 and 0.03 percent carbon, 0.007 and 0.018 percent nitrogen, 0.04 and 0.18 percent iron and 0.002 and 0.006 percent hydrogen. Both electrochemical polarization curves obtained in several different environments and actual crevice corrosion tests showed no significant differences among these materials so they were used interchangeably. The titanium alloys were

* Submitted for publication August 14, 1967. Research sponsored by the Office of Saline Water, U. S. Department of Interior, under Union Carbide Corporation's contract with the U. S. Atomic Energy Commission.

* Oak Ridge National Laboratory, Oak Ridge, Tenn.

acquired either from commercial vendors or prepared in small heats by the Metals and Ceramics Division of Oak Ridge National Laboratory. Nominal compositions of the commercial alloys are shown in Table 2. Alloys made locally were prepared by nonconsumable are melting of appropriately weighed quantities of the pure elements in an argon atmosphere until homogeneous and casting them in a cylindrical mold. The casting was cold or warm swaged to a diameter of ¼ in. The alloy was then machined to a ⅛-in diameter to remove surface inclusions. All specimens were either abraded with fine grit paper or lightly pickled in an aqueous solution of nitric and hydrofluoric acids (300 ml 70% HNO_3 – 30 ml 48% HF – 670 ml H_2O) and rinsed in deionized water before test. The surface area exposed to the solution in the polarization tests was known to an accuracy of about ± 5%.

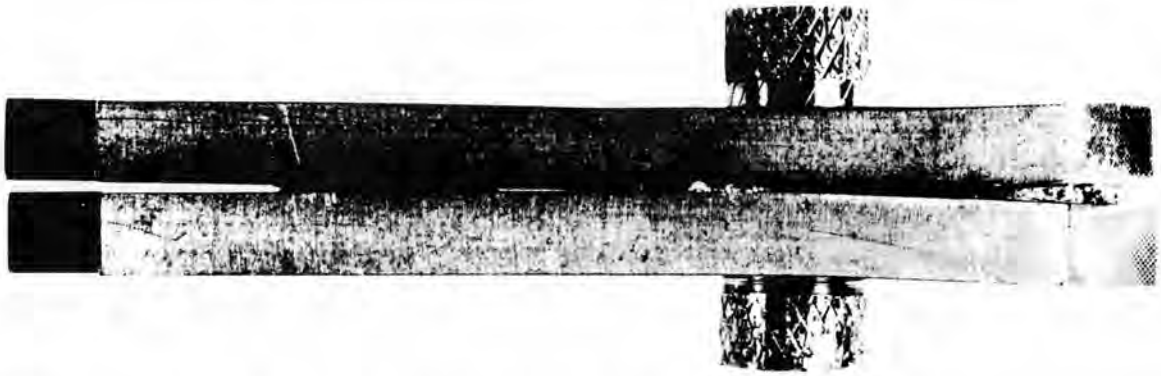

FIGURE 1 — Corrosion observed in a titanium crevice after an exposure of one week to aerated 1 M NaCl at 150 C.

Table 1 — The Extent of Crevice Corrosion Observed in 1 M NaCl.

Initial Conditions	Time (hr)	No. of Curve in Fig. 2	Calculated TiO_2 Formed (gm)	Gram Equivalents of :		Percent of Cathodic Reaction	
				H_2 Formed	O_2 Reduced	H_2	O_2
150 C 15 psia air (25 C) pH = 3.0	124	1	1.36	0.0620	0.0064	91	9
150 C 30 psia O_2 (25 C) pH = 3.0	246	2	2.24	0.059	0.053	53	47
150 C Deaerated pH = 3.0	142	3	0	0	0	0	0
150 C 15 psia air (25 C) pH = 6.0	171	4	0.02	0.0002	0.0008	20	80
150 C 30 psia O_2 (25 C) pH = 6.0	229	5	2.68	0.069	0.065	52	48
150 C 200 C 150 C 30 psia O_2 (25 C) pH = 3.0	68 195 76	6	4.63	0.158	0.074	68	32

Table 2—The Corrosion Potential and the Critical Current Density of Several Commercial Titanium Alloys in a 0.9 M NaCl—0.1 M HCl Solution at 98-100 C.

Elements Alloyed with Titanium (wt. percent)	Corrosion Potential (v vs SCE)	Critical Current Density (microamps/cm^2)
4 Mn + 4 Al	-0.69	210
5 Cr + 3 Al	-0.75	300
4 V + 6 Al	-0.73	190
14 V + 11 Cr + 4 Al	-0.68	240
2.5 Sn + 5 Al	-0.67	150
2 Nb + 1 Ta + 8 Al	-0.64	230
8 Zr + 1 (Nb + Ta) + 8 Al	-0.74	48
0.15 Pd	-0.34	-
None	-0.73	130

Experimental Results

Corrosion Tests

Corrosion tests were carried out to determine qualitatively the effects of several variables on the crevice corrosion of titanium in solutions of sodium chloride. In these experiments crevice specimens were suspended from insulated hangers in titanium autoclaves which were heated to the desired temperatures. The specimens consisted of two flat titanium plates bolted tightly together with titanium nuts and bolts. In some cases a small strip of 8-mil-thick titanium was placed between the plates near one end to form a tapered crevice.

When corrosion occurred, the attack always initiated in the regions of closest contact and never in crevices with measurable clearance. Figure 1 shows the nature of the attack in one case where corrosion was extensive. The specimen was exposed to air-saturated 1 M NaCl at 150 C for one week. Initially the ends near bolts were in contact, but after the test the ends were wedged apart by the mass of corrosion products formed in the crevice. Although the plates were ¼-in thick, the force was great enough to bend them.

This series of tests indicated that reproducibility of attack from test to test was very poor in aerated 1 M NaCl at 150 C. Of approximately 30 specimens exposed, no more than half showed attack to varying degrees. Increasing the temperature to 200 C (392 F) had little effect on the percentage of specimens undergoing attack, but when attack did occur it was greater at the higher temperature. In similar tests at 150 C in which the pH of the solution was adjusted to 3 with hydrochloric acid, the frequency and extent of attack increased somewhat. Increasing the concentration of oxygen in the solution had a similar effect. In degassed solutions corrosion seldom occurred and when it did, attack in the crevice was very slight.

Other tests conducted in 4.5 M NaCl at 150 C with oxygen present showed that both the frequency and severity of attack were much greater than in 1 M solutions; 18 of 20 specimens showed very significant attack in crevice regions in a few days.

In nearly all cases where attack occurred, it was confined to the crevice region. In a few cases, however, corrosion that originated in the crevice extended beyond the confines of the crevice. In these cases heavy deposits of titanium dioxide (rutile) covered the attacked area and appeared to maintain the conditions necessary for the attack to continue. In all other cases the freely exposed surfaces developed thin tarnish-like films and showed no evidence of attack.

Other crevice corrosion tests were conducted in a titanium autoclave in which the pressure could be recorded. The reduction half of the corrosion reaction involves the formation of hydrogen and/or the consumption of oxygen, either of which causes a change in pressure in a closed autoclave. For these tests the temperature of the autoclave was held within 1 C of the desired temperature and pressure was measured and recorded by means of a Baldwin Cell [1] and a standard recorder. In all cases except two the room temperature gas phase volume was 200 cc; in the last two cases the gas phase volume was 620 cc.

At the end of a test the autoclave was allowed to cool to room temperature, the pressure was noted, and a sample of the gas was analyzed with a mass spectrometer. From the gas volume, temperature and changes in pressure and composition, total amounts of hydrogen formed and oxygen consumed were calculated and from stoichiometric considerations the amount of corrosion product (TiO_2) was calculated. Figure 2 shows how the pressure changed with time under different conditions. Table 1 shows the test conditions, the calculated quantities of titanium dioxide formed, the gram-equivalents of hydrogen produced and oxygen consumed and the percentage of the cathodic reaction supported by each process.

As shown in Figure 2 in all cases where corrosion occurred, hydrogen was produced and oxygen was consumed. Except for Curve 4 where only a very little corrosion occurred, most of the cathodic reaction consisted of the reduction of hydrogen ions to hydrogen. In those cases with a high initial oxygen over-pressure (Curves 2, 5 and 6), oxygen reduction constituted a greater percentage of the cathodic reaction than in cases where an atmosphere of air initially filled the gas space in the autoclave (room temperature). No attack and no change in pressure were noted in the deaerated system and less attack was found at a pH of 6 than at 3.

With the exception of one experiment (Curve 6), when corrosion occurred it began essentially immediately and in all cases the pressure increased at a constant rate for some initial period even though analysis of the final gaseous products showed both hydrogen formed and oxygen consumed. With the exception of the deaerated test (Curve 3), some oxygen remained in the system after completion of all tests. In one case (Curve 6) no pressure change was noted for 68 hr at 150 C at which time the temperature was increased to 200 C. After reaching the higher temperature, the pressure began to increase but in a more irregular fashion than in other

(1) Baldwin-Lima-Hamilton Corp., Philadelphia, Pa.

cases at the lower temperature. On lowering the temperature to 150 C no further change in pressure was noted for the final 76 hr.

This series of experiments generally confirmed the results of other crevice corrosion tests and demonstrated that the cathodic process involves both the reduction of hydrogen ions (or water) and oxygen.

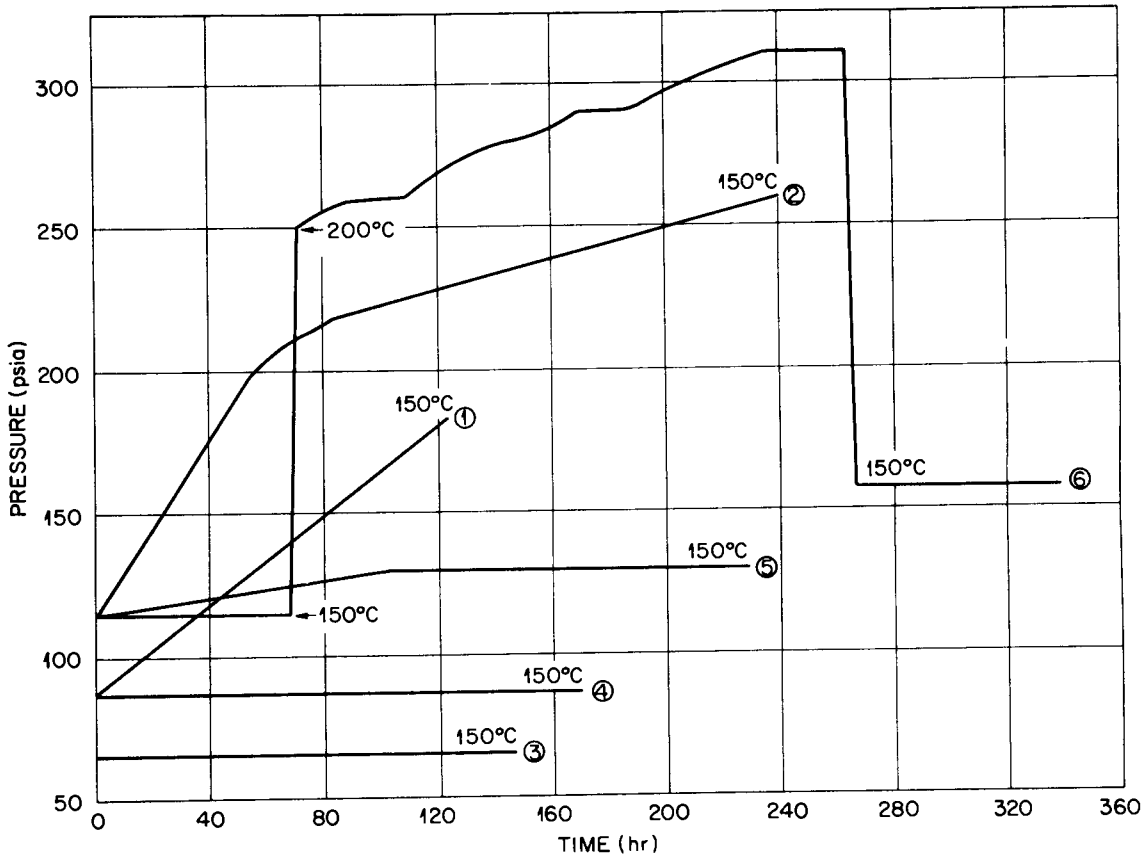

FIGURE 2—Pressures observed in autoclaves containing titanium crevice specimens corroding in 1 M NaCl.

Electrochemical Polarization Studies

To gain some insight into the corrosion processes, potentiostatic polarization curves were obtained with commercially pure titanium. The specimens were 1/16-in-diam wires inserted through the head of a titanium autoclave. Either the wall of the autoclave or another similar wire served as the counter electrode.

Figure 3 shows the effect of temperature on cathodic polarization of titanium in 1 M NaCl. The solution was air saturated and one atmosphere of air filled the free space of the autoclave at room temperature. Oxygen concentrations are those calculated from Henry's Law taking into account the expansion of water (and compression of the gas). The Henry's Law constants for pure water were used and the listed oxygen concentrations are undoubtedly somewhat higher than actually existed. The figure indicates that the reduction of oxygen occurred at less negative potentials as the temperature increased. The increase in limiting diffusion current density with temperature resulted from both the greater oxygen concentration and the greater diffusion rate of oxygen as the temperature was raised.

The data illustrated in Figure 4 obtained in 1 M NaCl at 150 C show that the limiting diffusion current is proportional to the oxygen concentration. Why the two curves obtained with the oxygenated solutions are separated by about 200 mv is not known. In the absence of oxygen the cathodic process is the reduction of molecular water.

Figure 5 shows the effect of pH on the cathodic process in oxygenated 1 M NaCl at 150 C. The polarization curve obtained with a platinum electrode also is included in the graph to illustrate the high overvoltage for the reduction of oxygen on titanium. As expected, increasing the hydrogen ion activity increased the ease of oxygen reduction, although the non-linearity of the titanium polarization curve at pH 3 is not understood. Curves of a similar shape were obtained sometimes in those cases where the hydrogen ion concentration was less than, but close to, stoichiometric for the reduction of oxygen to hydrogen peroxide or water.

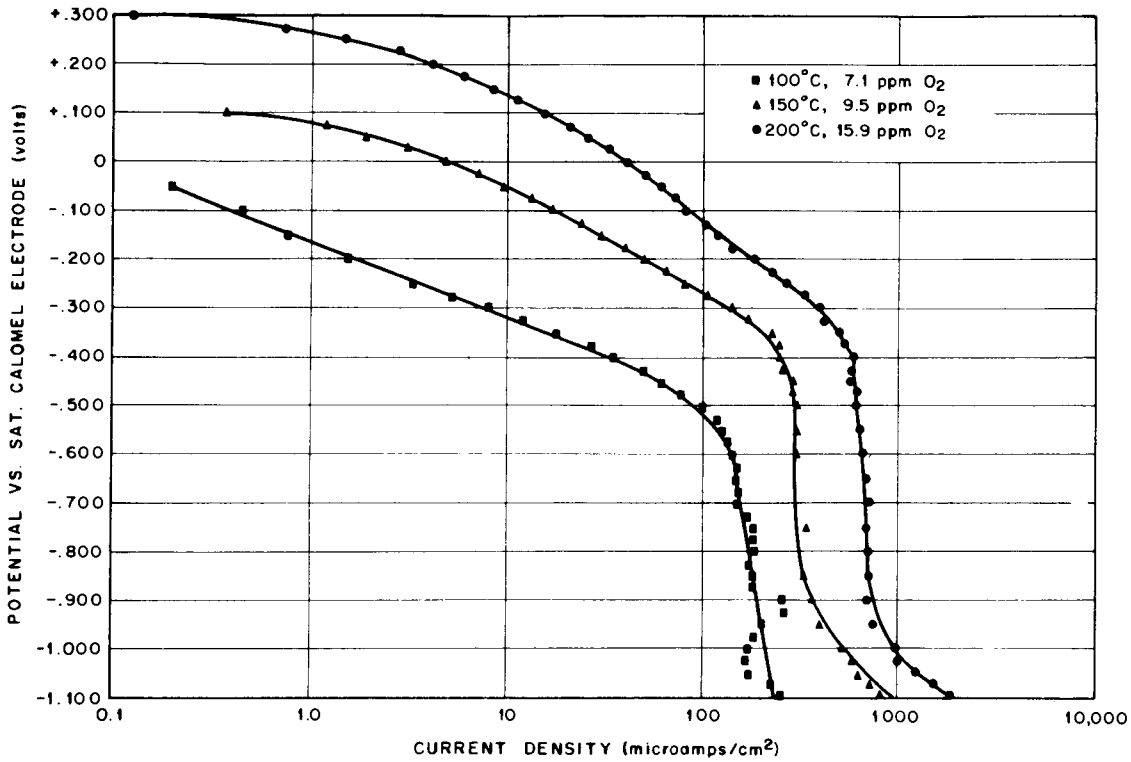

FIGURE 3—Cathodic polarization curves for titanium in 1 M NaCl.

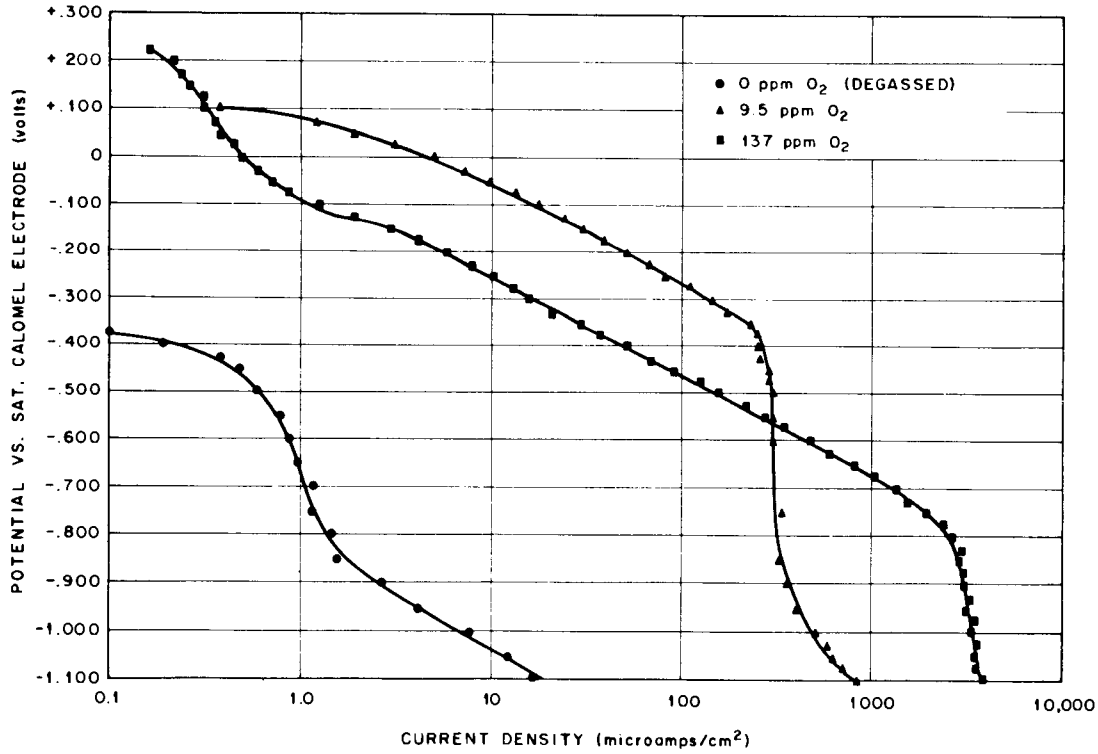

FIGURE 4—The effect of oxygen concentration on the cathodic polarization of titanium in 1 M NaCl at 150 C.

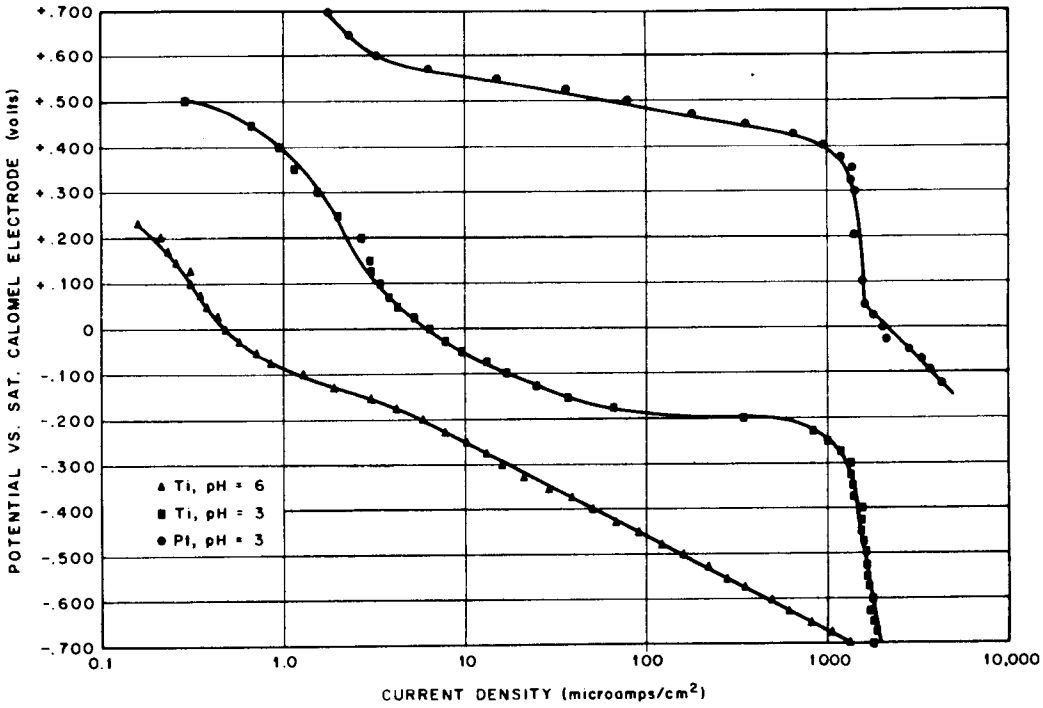

FIGURE 5—The effect of pH on the cathodic polarization of titanium in 1 M NaCl containing 137 ppm O_2 at 150 C and the polarization of platinum in the same solution at a pH of 3.

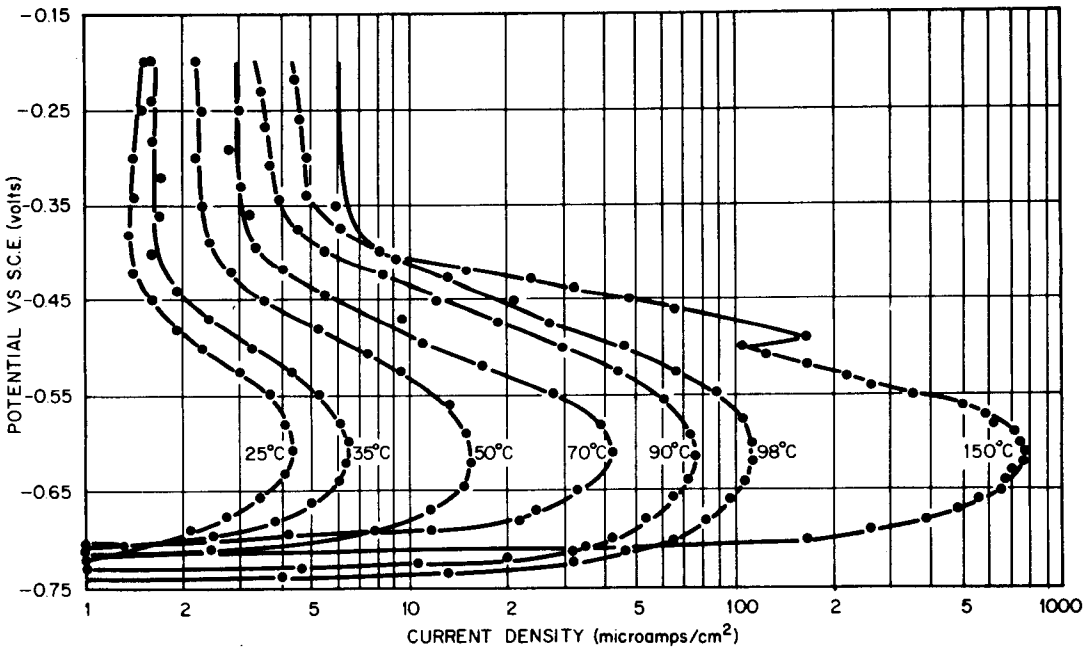

FIGURE 6—The effect of temperature on the anodic polarization of titanium in 0.9 M NaCl-0.1 M HCl.

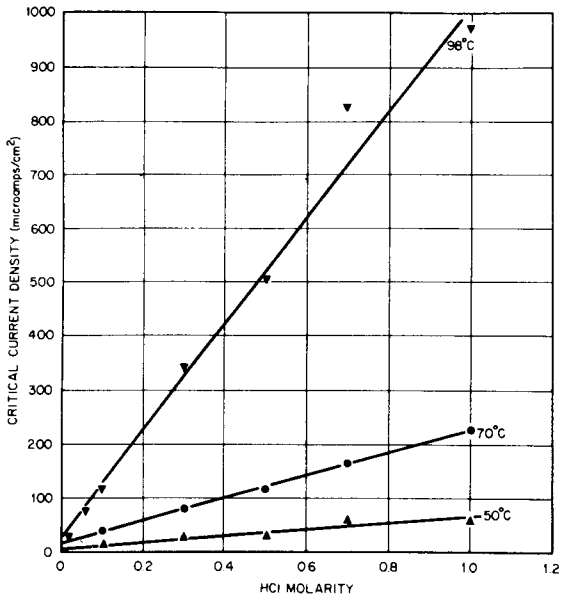

FIGURE 7—The effect of acid concentration on the critical current density for passivation of titanium in 1 M(Na + H) Cl.

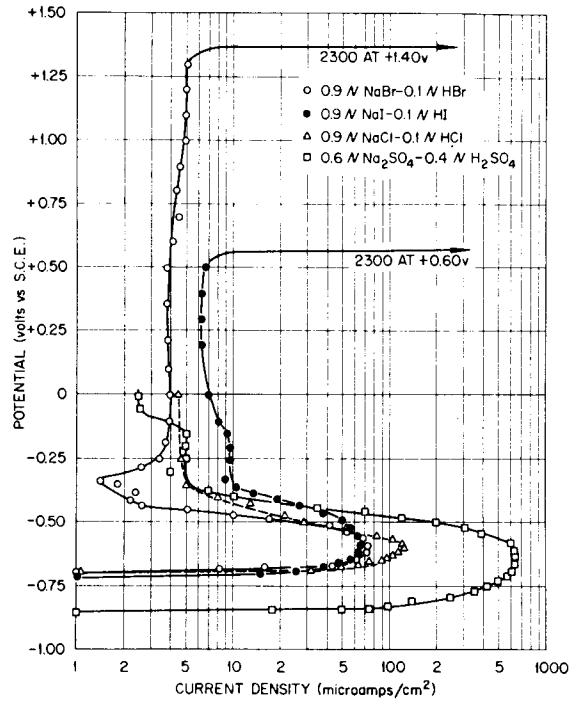

FIGURE 9—The anodic polarization of titanium in boiling normal solutions of bromide, iodide, chloride and sulfate adjusted to a pH of 1.

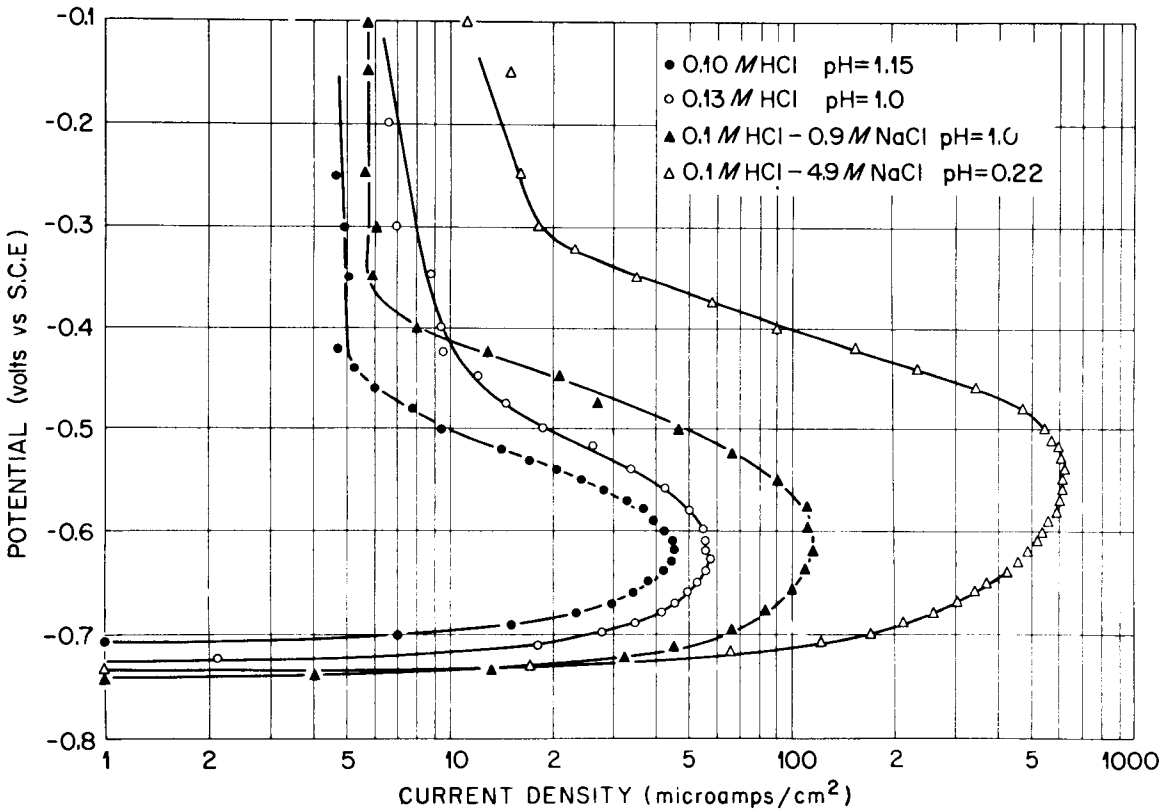

FIGURE 8—The effect of chloride and hydrogen ion concentrations on the anodic polarization of titanium at 98 C.

The reduction of oxygen on a titanium specimen which was first polarized to −1.2 v vs SCE or lower at 150 C required less overvoltage than on a new specimen not previously polarized. The effect produced by polarization to a low potential gradually diminished and after 10 to 20 hr, a polarization curve essentially identical to that obtained on a new specimen could be obtained. Polarization of the titanium to sufficiently low potentials produced a hydrided surface which had a lower overvoltage for the reduction of oxygen than the original titanium surface. With time the hydride apparently decomposed, leaving the surface with its original overvoltage characteristics.

Anodically titanium polarized very readily in 1 M NaCl. Current densities in the range of 10^{-6} amp/cm^2 were sufficient to polarize titanium to +1.0 v vs SCE or greater in neutral solutions or in those adjusted to a pH of 3 at either 100 or 150 C. At fixed potentials in the passive region anodic current densities decreased over long periods and steady-state values would have been even lower than 10^{-6} amp/cm^2 had potentials been maintained longer than 3 to 5 min. Neither anodic nor cathodic polarization activated titanium in the solutions tested, which were the same as those in which titanium undergoes crevice corrosion. It appeared, therefore, that for titanium to corrode in a crevice, the small volume of solution within the crevice must develop an acid concentration greater than 10^{-3} M.

The approximate pH of the solution in a corroding crevice was determined in the following manner. Specimens were prepared from two 1.5-in square titanium plates bolted together on each corner. In the center of one of the plates a small hole just large enough to accommodate a 0.020-in ID titanium capillary tube was drilled. The tubing was inserted flush with the inner surface of the plate and back welded in place. The capillary passed through the head of the autoclave and with appropriate valving a small volume of solution was withdrawn from the crevice while the specimen was at 150 C. The volume of solution in the sampling system was about 0.05 ml. The minimum pH of single small drops of solution obtained in this manner was about 1 in those cases where corrosion occurred and about 4 to 5 in those cases where significant corrosion was absent. The pH of the bulk solution was 6 to 7.

An anodic polarization curve of titanium was obtained at 150 C in a solution containing 0.9 M NaCl and 0.1 M HCl (pH = 1.0 at 25 C). For this experiment the autoclave was equipped with fluorocarbon liner and a piece of spectrographically pure graphite served as the counter electrode. The autoclave was degassed before the test. The specimen was polarized to the potential of the SCE during the heat-up period to minimize corrosion. At 150 C the open-circuit potential was −0.67 v vs SCE and the anodic polarization curve had the shape characteristic of an active-passive metal (see Figure 6). The critical current density for passivation was 7.6×10^{-4} amp/cm^2. Although not shown in Figure 6, the passive region extended to the pitting potential which is about 2.5 v vs SCE at 150 C for commercial purity titanium.[8] The current density of 7.6×10^{-4} amp/cm^2 corresponds to a corrosion rate of 350 mpy (based on the formation of trivalent titanium) which is close to, but somewhat less than, the highest corrosion rates observed in some crevices (~ 500 mpy) under the same conditions.

Effect of Temperature. The effect of temperature on the critical current density for passivity of titanium in a solution containing 0.9 M NaCl-0.1 M HCl is shown in Figure 6. In all cases except at 150 C, the solution was boiled for at least 2 hr with a stream of purified nitrogen passed over the surface to remove all oxygen from the system. With nitrogen flowing over the surface, the temperature of the solution was adjusted and the specimen was introduced. In all cases the specimen was pickled lightly in the HNO_3-HF solution and rinsed in deionized water before immersion. The critical current density increased with temperature at a rate corresponding to an activation energy of about 11 kcal/mol. On prolonged exposure of titanium the solutions developed a pink color, indicative of trivalent titanium.

In view of these results, the effects of several variables on the polarization curves of titanium were investigated at the boiling point or below because of the greater ease of conducting experiments at atmospheric pressure.

Effect of Acid Concentration. Anodic polarization curves were obtained in 1 M (Na + H)Cl solutions in which the acid concentration was varied from 0.02 M to 1.0 M at 98 C and from 0.1 to 1.0 M at 50 and 70 C (122-158 F). The critical current density required for passivation was directly proportional to the acid concentration at all temperatures as shown in Figure 7. The potential at which the critical current density occurred increased more or less regularly from −0.66 v in the solution with 0.02 M HCl to −0.53 v vs SCE in the 1 M HCl solution. The shift in critical potential with acid concentration was similar to that noted by Stern and Wissenberg.[9]

Effect of Chloride Concentration. Anodic polarization curves were obtained with pure titanium at 98 to 100 C in the following solutions: 0.10 M HCl, 0.13 M HCl and in a solution containing 4.9 M NaCl and 0.10 M HCl. These curves, as well as that obtained with 0.9 M NaCl-0.1 M HCl, are shown in Figure 8. The pH of each solution measured at room temperature is shown also. At first glance the curves indicate a significant effect of chloride ion concentration on the critical current density for passivation. However, comparison of pH values between the two most concentrated solutions indicates the activity of the hydrogen ion was six times greater in the more concentrated solution than in the 0.9 M NaCl-0.1 M HCl solution. Referring to Figure 7, it can be seen that the maximum current density at 0.6 M acid (1.0 M in total chloride ion) is 600 microamps/cm^2, which is about the same maximum current density as that observed in the more concentrated solution. These two curves then indicate that the chloride ion concentration was without significant effect on the critical current density. On the other hand, comparison of the curves obtained in 0.13 M HCl with that obtained in 0.9 M NaCl-0.1 M HCl (both at a pH of 1.0) indicates that about an 8-fold increase in chloride ion concentration increased critical current density by about a factor of two. Although these results do not fully delineate the effect of chloride ion concentration on critical current density for passivation, it is clear

that the chloride ion concentration is of lesser importance than the hydrogen ion activity.

Effect of Other Salts. The similarity of anodic polarization curves of titanium in acidified solutions of sodium chloride, bromide, iodide and sulfate is shown in Figure 9. In each case a 1.0 N solution of the salt was adjusted to a pH of 0.9 to 1.0 (room temperature) with a 1.0 N solution of the corresponding acid. In the case of the halogen salts the final acid concentration was about 0.1 N, but with the sodium sulfate solution the acid concentration had to be increased to about 0.4 N to obtain a pH of 1. All tests were conducted at the boiling point.

While all curves show a maximum current density at about the same potential, its magnitude varied from salt to salt. Curves obtained in the sodium chloride and sodium sulfate solutions were extended only to the potential of the SCE. In both of these solutions the passive region extends well beyond +2.0 v vs SCE. The passive regions are considerably narrower in the bromide and iodide solutions. In the iodide solution pitting began at about +0.6 v vs SCE. Although the curve indicates that pitting began at about +1.4 v vs SCE in the bromide solution, the true pitting potential is about +1.0 v under the test condition. The curve shown was obtained going from the open-circuit potential in a positive direction allowing 3 min at each potential. Retracing the curve in the opposite direction showed that pitting stopped at about +1.0 v.

If an acid environment develops in titanium crevices in solutions of sodium iodide, bromide or sulfate, crevice corrosion similar to that observed in chloride solutions should be expected. That such does occur was demonstrated by exposing four crevice specimens to aerated 1 M solutions of sodium bromide, iodide and sulfate at 150 C for 200 to 300 hr. In the case of the bromide and iodide solutions, all specimens exposed showed crevice attack to about the same extent as observed in chloride solutions. In the sulfate solution two of four specimens showed some attack in the crevice region.

Effect of Alloying Elements. The results support the hypothesis that corrosion observed in titanium crevices at high temperature is caused by the development of an acid environment in the crevice. It follows, therefore, that an alloy resistant to a relatively concentrated acid solution at the temperature of interest probably would be immune to crevice corrosion. The results also indicate that the degree of resistance to attack by acid chloride solutions can be determined from anodic polarization curves at temperatures below the point where crevice corrosion is a major problem (Figure 6).

Anodic polarization curves were obtained for a number of commercial titanium alloys in a solution containing 0.9 M NaCl and 0.1 M HCl at 98 to 100 C. The specimens were lightly pickled in the HNO_3-HF solution and rinsed in deionized water before immersion. The alloys tested, the corrosion potential and the critical current density for passivation are shown in Table 2. The cor-

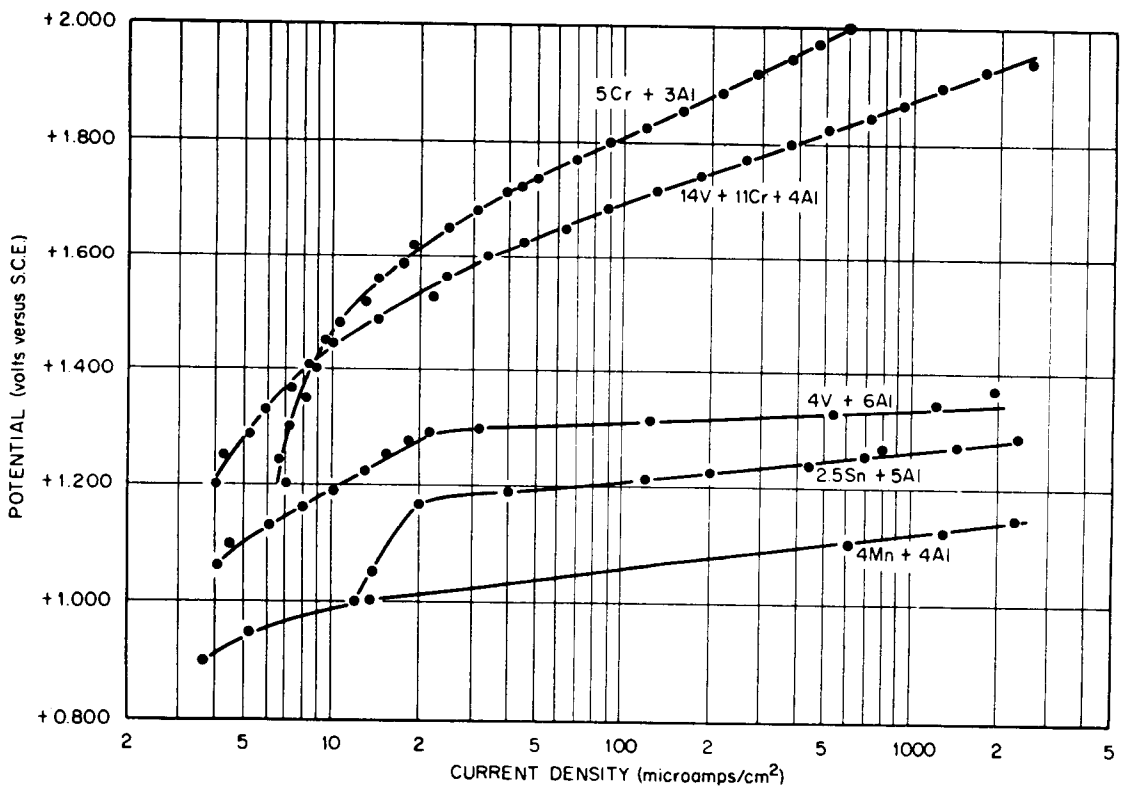

FIGURE 10—Anodic polarization curves of titanium alloys in 0.9 M NaCl—0.1 M HCl at 98 C.

rosion potentials were constant within ±20 mv for about 30 min before the polarizing current was applied. With the exception of the palladium alloy, all alloys had corrosion potentials comparable to titanium and demonstrated a similar active-passive behavior. The critical current density varied from alloy to alloy with the lowest value being observed with the alloy containing zirconium and the highest values with the two alloys containing chromium. Tomashov also noted a higher current density for chromium-containing alloys.[10] The corrosion potential for the palladium alloy was well above the potential of the active region and current densities of the order of 10^{-6} amp/cm^2 sufficed to polarize it to +2.0 v vs SCE, the highest potential to which any of the alloys were polarized.

All alloys except palladium showed a similar type of behavior in the potential range of −0.7 v to +1.0 v vs SCE, but significant differences were apparent at higher potentials. With pure titanium and the palladium alloy, the pitting potential is about 6 to 8 v vs SCE at 100 C (Ref. 8) and no evidence of pitting or significant current increase was apparent on polarizing these two alloys to +2.0 v vs SCE.

The behavior of the other alloys is indicated in Figure 10. Alloys containing 6% Al−4% V, 4% Al−4% Mn and 2% Nb−1% Ta−8% Al developed well-formed pits starting at potentials of +1.3, +1.0 and +1.0, respectively. No pits were found on the other three alloys although the curve for the 5% Al−2.5% Sn alloy was characteristic of pitting behavior and in other studies pitting of this alloy has been observed.[8] The two alloys containing chromium also did not develop pits and in general exhibited typical transpassive behavior, presumably due to the formation of chromate. It should be remembered that in this study the potential was held constant at each value for 3 to 5 min; had the time been increased, pits might have developed.

Small heats of titanium alloys containing individually 0.5% Ta, 0.5% Nb, 0.5% Cu, 1% Sn, and 1% Al were prepared and subjected to anodic polarization in a 0.9M NaCl-0.1 M HCl solution at the boiling temperature. In all cases the resulting polarization curves did not differ significantly from those obtained with pure titanium in the same environment. There was no evidence of pitting up to a potential of +2.0 v vs SCE.

Small heats of a series of titanium-molybdenum alloys with molybdenum contents ranging from 1 to 30 percent also were subjected to anodic polarization in boiling 0.9 M NaCl-0.1 M HCl solution. The 5 percent molybdenum alloy also contained 0.5 percent niobium. Alloy compositions and the anodic polarization curves are shown in Figure 11. The curve obtained with pure titanium is shown also for comparison. In this environment alloys containing 5 percent molybdenum or more showed no region of active corrosion; all had open-circuit potentials greater than the critical potential for passivation of pure titanium. The 1 percent molybdenum alloy showed an active region but the critical current density for passivation was about four times less than for pure titanium. The corrosion potentials of the alloys increased from − 0.55 v for the 1 percent alloy to − 0.30 v vs SCE for the 30 percent alloy.

Additional polarization curves for the same alloys in boiling 1 M HCl are shown in Figure 12 along with the polarization curve obtained with pure molybdenum. In this environment only the alloys containing 20 and 30 percent molybdenum had open-circuit potentials greater than the active region observed with pure titanium. For the other alloys the critical current densities for passivation were 86, 140 and 520 microamps/cm^2 for the 10, 5 and 1 percent alloy, respectively. All alloys showed a second active region in the vicinity of +0.1 v vs SCE. In this region the order of the current density maximum was: 10% alloy > 20% alloy > 30% alloy > 5% alloy >1% alloy.

Additional experiments with the 10% alloy showed that the second current maximum depended on the manner in which the curve was obtained. If the potential was held constant at a value above the second maximum,

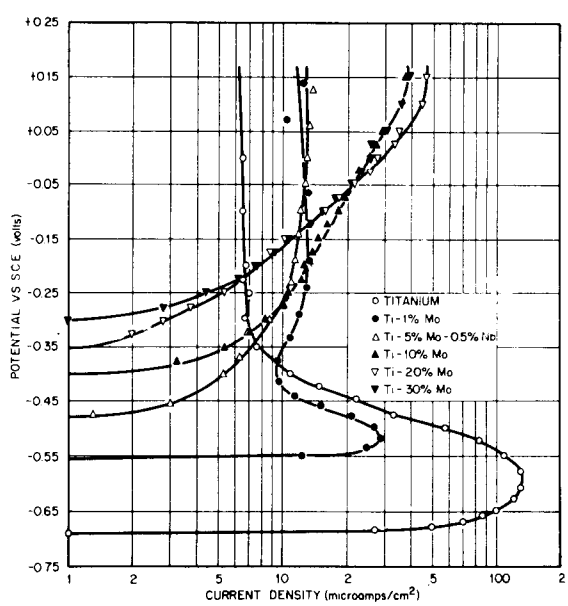

FIGURE 11—Anodic polarization curves of titanium-molybdenum alloys in boiling 0.9 M NaCl—0.1 M HCl.

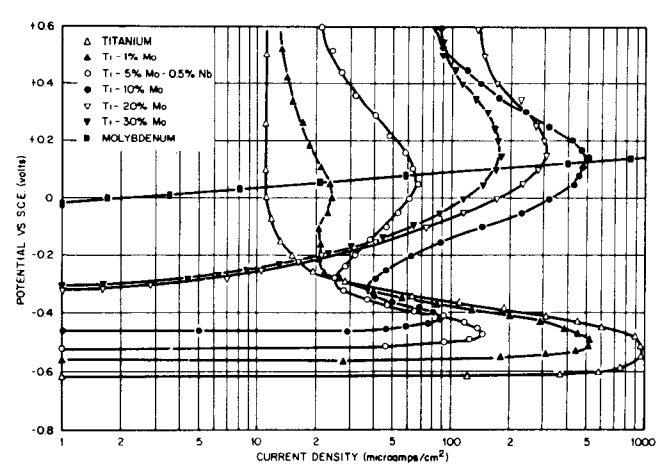

FIGURE 12—Anodic polarization curves of titanium-molybdenum alloys in boiling 1 M HCl.

the current gradually decreased and on retracing the polarization curve, the current maximum was much less pronounced. However, if the alloy was allowed to corrode freely at the open-circuit potential for some time, the pronounced second current maximum was again apparent on repolarization. These results plus the observation that the anodic polarization curve for molybdenum essentially passes through the second maximum, indicate that active corrosion of the alloy enriches molybdenum or a molybdenum compound on the surface which is oxidized when the potential is adjusted to about +0.1 v vs SCE.

Anodic polarization curves also were obtained with a series of titanium alloys containing nickel and in one case also molybdenum. Alloy compositions and polarization curves obtained in boiling 0.9 M NaCl-0.1 M HCl are shown in Figure 13. Alloys containing 0.2 and 0.5 percent nickel were supplied by Reactive Metals Inc.[2]; small heats of all others were prepared locally. All alloys containing nickel had open-circuit potentials well above the active potential for titanium. Exposure to the solution for as long as several hours produced no significant changes. Irregular curves were obtained in the passive region, but all points would have shifted to lower current densities had more time been allowed at each potential setting. Very large increases in anodic current were noted with all these alloys at potentials of +1.4 to +1.6 v vs SCE. The anodic current was not related to oxidation of the alloy but to the oxidation of chloride ions to chlorine. In this respect the nickel alloys differed from all other alloys tested. The anodic polarization of unalloyed titanium, which was typical of most of the alloys that did not have low pitting potentials, is also shown in Figure 13. Holding the potential of any of the nickel-containing alloys at +1.6 to +2.0 v for as long as a day resulted in no significant diminution in the current density and no detectable attack on the electrode. Although the highest current density was observed with the alloy containing the highest nickel content, the results generally indicated no direct relationship between nickel content and current density in this region.

(2) Reactive Metals, Inc., Niles, Ohio.

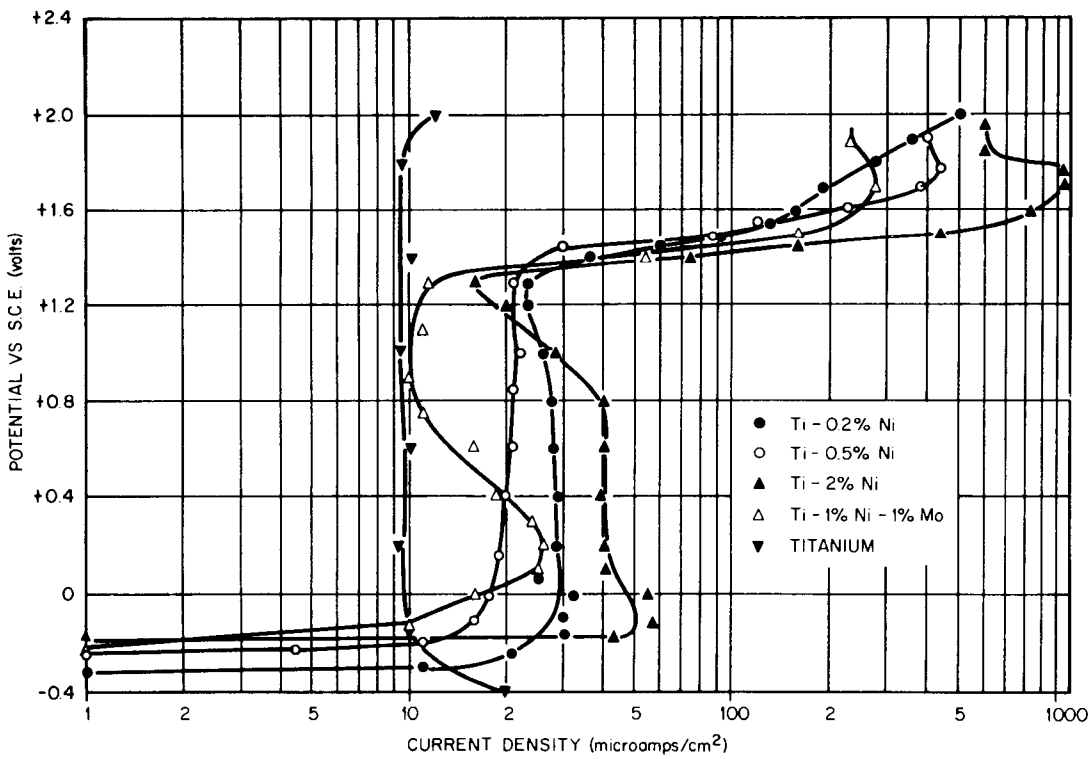

FIGURE 13—Anodic polarization curves of titanium-nickel alloys in boiling 0.9 M NaCl—0.1 M HCl.

The same nickel alloys and the titanium—0.15 percent palladium alloy were subjected to anodic polarization in boiling 1 M HCl. The results are shown in Figure 14. In this solution the alloys containing 0.2 and 0.5 percent nickel corroded actively with vigorous evolution of hydrogen. In both cases current density required to passivate the alloys was about 10^{-3} amp/cm^2, the same as for unalloyed titanium. Open-circuit potentials of the other alloys were above the active corrosion potential and remained reasonably stable for periods of at least several hours. However, cathodic polarization of the 2 percent nickel alloy at 5×10^{-4} amp/cm^2 for several hours activated the specimen. Following polarization, the open-circuit potential was −0.55 v vs SCE and hydrogen was evolved from the surface at a rapid rate. The anodic current density required to passivate the activated specimen was 5 to 6×10^{-3} amp/cm^2, significantly greater than for titanium. The observation that once activated the titanium-2% nickel alloy corroded faster than titanium is similar to that reported by Yoshida et al.[11] They noted that alloying titanium with 1 to 10 percent nickel improved corrosion resistance in 10 percent HCl but decreased its resistance in 20 percent HCl. Cathodic polarization of the titanium—0.15 percent palladium alloy under the same conditions had no effect on its open-circuit potential after the polarization was terminated.

Behavior of the alloy containing 1 percent nickel and 1 percent molybdenum following cathodic polarization at 10^{-3} amp/cm^2 for 16 hr in 1 M HCl was different from that of the 2 percent nickel alloy. Immediately after stopping the polarizing current, the potential was −0.29 v vs SCE. After about 15 min the potential decreased rather rapidly to −0.47 v and hydrogen was evolved from the surface of the specimen. During the next few minutes the potential increased to −0.32 v and remained there for 20 to 30 min during which time no visible gas evolution occurred. The potential of the specimen was recorded for 24 hr and the active-passive cyclic behavior continued throughout. The minimum potential was −0.470 ±0.005 v and the maximum was −0.315 ± 0.010. The time for a cycle varied between 19 and 30 min.

With all of the nickel-containing alloys chlorine was liberated at +1.4 to +1.6 v at approximately the same rate observed in the 0.9 M NaCl—0.1 M HCl solution.

Discussion

Results obtained in this investigation indicate that for titanium to corrode in crevice regions the solution within the crevice must become and remain significantly acid. The mechanism by which this condition is established appears to be the same as that described by Rosenfeld and Marshakov[12] for the corrosion of other metals in areas with limited access of electrolyte. The significant differences appear to be related to the chemistry of the corrosion products.

Where a titanium crevice is immersed in an aerated solution of sodium chloride, the concentration of dis-

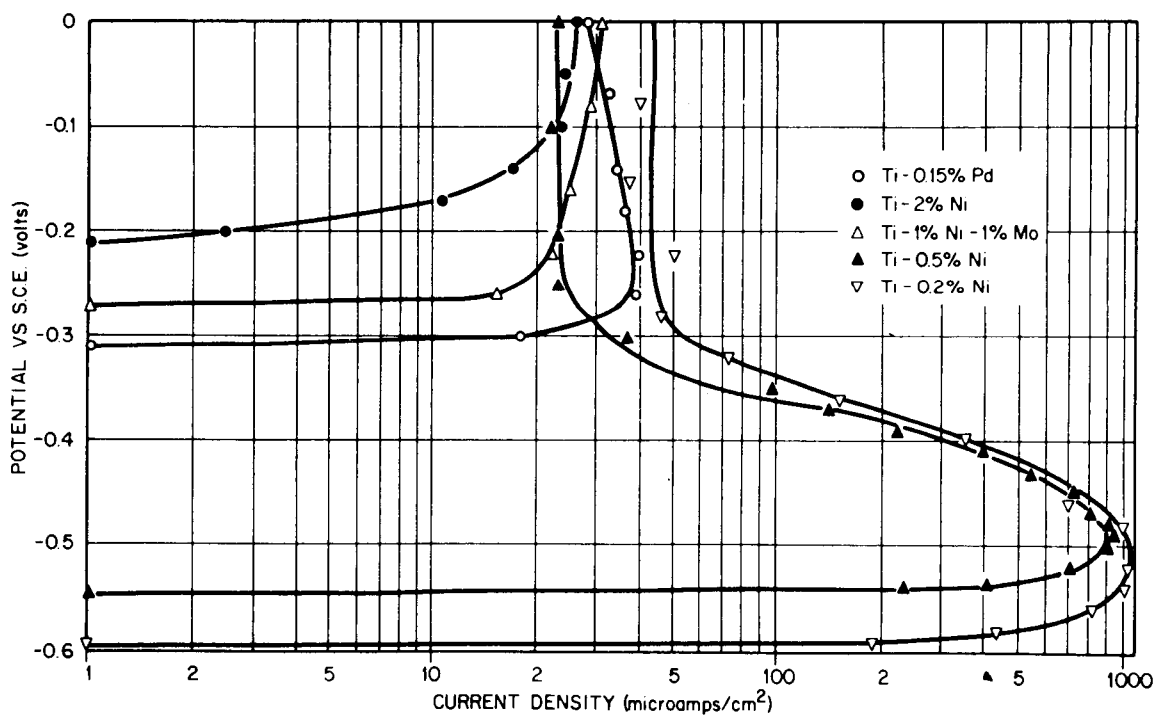

FIGURE 14—Anodic polarization curves of titanium-nickel alloys in boiling 1 M HCl.

solved oxygen in the solution is the same in the crevice as on the freely exposed surfaces. At room temperature and even at somewhat higher temperatures the corrosion rate of titanium is low enough so that the consumption of oxygen in the small volume of solution in the crevice is balanced by diffusion of oxygen from the bulk solution. As the temperature increases, the corrosion rate of titanium increases at a faster rate than the diffusion process and ultimately the solution within the crevice becomes depleted in oxygen. As noted by Rosenfeld and Marshakov[12] and as illustrated in Figure 4, anodic dissolution of the metal occurs at more negative potentials as the oxygen concentration diminishes.

Results of the present investigation showed that corrosion occurred only in very restricted crevices. If one assumes that the volume of solution in the crevice was 0.01 ml/cm^2 and that the solution contained 10 ppm of oxygen initially, then the formation of a uniform layer of TiO_2 only about 6Å thick could consume of the oxygen in the solution in the crevice.

Depletion of oxygen within the crevice causes the potential of the titanium to decrease, a condition necessary for the establishment of macrocells. The oxidation of titanium in the crevice is balanced by the reduction of oxygen or hydrogen ions at some distance from the crevice. To maintain electroneutrality in an operative macrocell, chloride ions must migrate into the crevice area and sodium ions to the bulk solution. Hydrolysis of the titanium ions causes the pH of the crevice solution to decrease. The actual concentration of acid developed depends on the buffering action of the hydrolyzed species and on diffusion of acid from the crevice to the bulk solution.

The corrosion of titanium in the active potential region forms trivalent titanium ions which are strong reducing agents and are capable of reducing hydrogen ions and water.[13] Both tri- and tetravalent titanium ions are appreciably hydrolyzed. It is reported that at room temperature $Ti(OH)_3$ is precipitated at a pH of 3 and $Ti(OH)_4$ at a pH of 0.7 (Ref. 14); at 150 C both would be expected to precipitate at significantly higher acidities. The fact that the corrosion product found within the crevice was rutile (TiO_2) indicates that titanium was oxidized to the tetravalent state and the high acidity of the solution removed from the crevice indicates, as expected, no significant buffering action of the rutile.

Gas analyses showed that in the system under study hydrogen was generated and oxygen was consumed when crevice corrosion occurred. Once a macrocell has formed, pH of the solution in contact with surfaces deep in the crevice is significantly lower than that of the bulk solution permitting cathodic formation of hydrogen. Escape of hydrogen bubbles from the edges of titanium crevices has been observed.[15] Rosenfeld and Marshakov[12] point out that macrocells may arise within a crevice itself due to differences in concentrations of depolarizers. In the present case, concentration of one of the cathodic depolarizers, hydrogen ions, would be relatively high in the anodic areas (as a result of hydrolysis of the corrosion products) and its reduction appears to account for at least part of the observed hydrogen. Additional hydrogen could be produced from the reaction of trivalent titanium with hydrogen ions and/or water.

Based on the above discussion which postulates the formation of macrocells as a result of differences of oxygen concentration, crevice corrosion should not occur in completely deaerated solutions of pure sodium chloride. This is in general agreement with results reported here. However, it should be pointed out that only very low concentrations of oxygen or other oxidizing agents in solution should suffice to initiate such a cell. While differential aeration appears necessary to establish such a cell, continued crevice corrosion can occur by an acid mechanism.[16] It should be pointed out also that substances other than oxygen can produce crevice corrosion in titanium. For example, chlorine presumably could act like oxygen and some of the cases of crevice corrosion observed in the chlor-alkali industry might be related to depletion of chlorine in the crevice areas, which would permit establishment of macrocells and result in significant corrosion within the confines of the crevice.

As indicated by Figure 8, it is the activity of the hydrogen ion rather than the concentration that apparently determines the rate of attack. At room temperature and undoubtedly at higher temperatures the activity coefficient of hydrochloric acid increases as the concentration of sodium chloride increases.[17] Therefore, in a macrocell the same net flow of current will produce a greater hydrogen ion activity the more concentrated the salt solution is. The greater frequency and extent of attack in titanium crevices observed in 4.5 M NaCl compared with that in a 1 M solution appear to be due to this fact.

Titanium is subject to pitting in halide solutions at relatively high potentials;[8, 18] in sulfate solutions titanium does not pit in the usual sense but dielectric breakdown of the oxide occurs at 80 v or higher.[19] That crevice corrosion is not related to this type of localized attack is illustrated by the fact that the pitting potential of titanium in the test solutions varied from less than a volt in iodide solutions to 80 v for sulfate solutions, yet crevice corrosion occurred to about the same extent in all solutions. The results show that crevice corrosion is caused by the development of an acid environment in the crevice. The anion associated with the acid seems to be of relatively minor importance.

From the above considerations it follows that an alloy which remains passive in acid solutions of the same concentration developed in the crevice should be immune to crevice corrosion. On this basis then titanium alloyed with sufficient palladium, molybdenum, or nickel would be expected to be immune or much less susceptible to crevice attack than pure titanium. Although insufficient materials were available to conduct actual crevice corrosion tests with these alloys, reported data indicate that the above conclusion is basically correct. Shimose and Takamura[5] indicated that in hot concentrated solutions of magnesium or ammonium chloride, titanium underwent crevice attack whereas a 0.2 percent palladium alloy was immune. Feige and Kane[20] reported that titanium alloyed with either 2 percent molybdenum, 0.2 percent palladium, or 2 percent nickel showed improved resistance to crevice corrosion and Bomberger[21] reported that alloying titanium with nickel significantly improves its resistance to crevice attack. Bohlmann and Posey[6] noted that 8 of 9 commercial alloys which are

listed in Table 2 were susceptible to crevice attack in either sodium chloride solutions or synthetic seawater at 150 to 200 C. The one exception was the 0.15 percent palladium alloy, which in similar tests appeared to be immune. However, incipient attack was noted on one specimen exposed in an operating desalination plant.

In summary, results of this investigation indicate that titanium crevice corrosion in salt solutions begins as a result of differential aeration and continues by virtue of the acid concentration developed in the small volume of solution within the crevice. The anion associated with the acid is relatively unimportant, but the actual salt concentration is important: The more concentrated the salt, the more severe the attack. Alloys which remain passive in nonoxidizing acid salt solutions should be much less susceptible to crevice corrosion than those which are readily attacked. Of the alloys investigated, those containing sufficient palladium, molybdenum or nickel should be the most resistant to crevice attack.

Acknowledgment

The author acknowledges the assistance of B. L. Johnson, Sr., and J. R. Hart in conducting experiments; R. E. McDonald for preparation of alloys and F. A. Posey and E. G. Bohlmann for many helpful discussions and much sound advice.

References

1. V. S. Ivins. *Power Engineering*, **69** (7), 52-53 (1965).
2. L. W. Gleekman. *Chem. Eng.*, **70** (23), 217-24 (1963).
3. R. S. Sheppard, D. R. Hise, P. G. Gegner and W. L. Wilson. *Corrosion*, **18**, 211t-218t (1962).
4. J. M. Turnbull. *Corrosion*, **16** (7), 11-16 (1960).
5. T. Shimose and A. Takamura. *J. Jap. Inst. Metals* **29** (4), 416-21 (1965).
6. E. G. Bohlmann and F. A. Posey. *Proceedings of the First International Symposium on Water Desalination*, Washington, D. C., Oct. 3-9, 1965, Vol. 1, pp. 306-25.
7. A. L. Bacarella and A. L. Sutton. *J. Electrochem. Soc.*, **112** (6), 546-53 (1965).
8. F. A. Posey and E. G. Bohlmann. *Desalination* (in press).
9. M. Stern and H. Wissenberg. *J. Electrochem. Soc.*, **106** (9), 755-59 (1959).
10. N. D. Tomashov, R. M. Altovsky and G. P. Chernova. *J. Electrochem. Soc.*, **108** (2), 113-19 (1961).
11. S. Yoshida, S. Okamoto and T. Araki. *J. Mechanical Laboratory*, **9** (2), 51-56 (1955).
12. I. L. Rosenfeld and I. K. Marshakov. *Corrosion*, **20** (4), 115t-125t (1964).
13. N. V. Sidgwick. The Chemical Elements and Their Compounds. Oxford University Press, London, 1950, p. 650.
14. J. Schmets and M. Pourbaix. International Committee on Electrochemical Thermodynamics. Proceedings of Sixth Meeting, Butterworth Scientific Publications, London, 1955, p. 167-179.
15. E. G. Bohlmann. Unpublished work.
16. G. J. Schafer, J. R. Gabriel and P. K. Foster. *J. Electrochem. Soc.*, **107** (12), 1002-1004 (1960).
17. H. S. Harned and B. B. Owen. The Physical Chemistry of Electrolytic Solutions. Reinhold, New York, 1950, p. 452.
18. I. Dugdale and J. B. Cotton. *Corrosion Science*, **4**, 397-411 (1964).
19. L. L. Shreir (ed.). Corrosion, Vol. I, J. Wiley and Sons, New York, 1963, p. 5.46.
20. N. G. Feige and R. L. Kane. Paper presented at the ASM session of the National Metal Congress, Chicago, Oct. 31-Nov. 3, 1966.
21. H. B. Bomberger. Private communication to E. G. Bohlmann.

ANALYSIS OF PROTECTIVE OXIDE FILMS ON COPPER–NICKEL ALLOYS BY PHOTOELECTRON SPECTROSCOPY*

L. D. HULETT, A. L. BACARELLA, L. LiDONNICI and J. C. GRIESS
Oak Ridge National Laboratory, Oak Ridge, Tenn. 37830 (U.S.A.)
(Received 24 April 1972)

ABSTRACT

Photoelectron spectroscopy was used to determine the elemental composition of thin films formed on 70:30 cupronickel exposed to sodium chloride solutions at different impressed electrochemical potentials. At anodic potentials below the passivation potential, −0.350 V versus SCE under the experimental conditions, either no film or a film containing copper and nickel in the same ratio as the alloy existed on the alloy. At the passivation potential the spectrum of the passive film indicated primarily nickel oxide and was very similar to the spectrum obtained from a pure nickel specimen passivated in the same environment.

INTRODUCTION

Alloys of copper and nickel find extensive use in saline water environments because the corrosion resistance of such alloys is usually superior to that of copper. The two most commonly used alloys in this class are alloys containing either 10 or 30% nickel and are usually referred to as 90:10 or 70:30 cupronickel. Both alloys contain small amounts of iron (1.0 to 1.8% for 90:10 and 0.4 to 0.7% for 70:30), the addition of which reportedly improves the corrosion resistance of the alloys to flowing salt water. Why the nickel-containing alloys have better corrosion resistance to salt water solutions than copper has not been fully established. Electrochemical studies have indicated that the presence of thin films on the surface of the alloys are primarily responsible for the excellent corrosion resistance of the nickel alloys, but the composition of the initial films that form on the alloys on exposure to salt water solutions has not been experimentally determined.

* Research sponsored by the Office of Saline Water, U.S. Department of the Interior, and the U.S. Atomic Energy Commission under contract with Union Carbide Corporation.

Recently the photoelectron spectroscopy technique has become available for examining very thin films on surfaces. It is the purpose of this paper to describe the experiments that have been conducted to determine the nature of the initial films formed on 70:30 cupronickel in salt water solutions.

DISCUSSION OF TECHNIQUES

Because the application of photoelectron spectroscopy in the examination of solid films has not received extensive use, and since at least some knowledge of the electrochemistry of copper and copper–nickel alloys is necessary to understand the purpose of the present investigation, the following brief discussions are given.

Photoelectron spectroscopy

It has been shown by Carlson et al.[1] and other workers that photoelectrons, ejected from metal oxide surfaces by soft X-rays, escape from depths of only 10–20 atom layers. This feature, coupled with the well-known capabilities to do elemental analysis and to determine chemical states of elements, makes the photoelectron spectroscopy technique very valuable in studies of protective films on metals.

For nickel compounds, chemical shifts of core binding energies (Ni $2p$) have been reported by other authors[2]. Satellite peaks have also been seen in many spectra. Their intensities and degree of separation from the parent peak are also functions of chemical state. Satellites are usually ascribed to electron shake-up processes or to multiplet splitting. In this work, satellites as well as chemical shifts have been seen.

Electrochemistry of copper and 70:30 cupronickel

Representative anodic polarization curves for copper and 70:30 cupronickel are shown in Figure 1. Both curves were obtained in oxygen-free 1.24 M NaCl at 100°C, but similar behavior is noted under other conditions. These curves were obtained potentiostatically; that is, the potential of the specimen was held constant until the current became constant, at which time the potential was increased to successively higher values. It should be noted that in the case of copper the current increased exponentially with no inflection in the curve. On the other hand, the current density of the 70:30 cupronickel began to decrease at a potential of about -0.350 V versus the saturated calomel electrode (SCE), indicating passivation (oxide film growth) of the alloy. In fact, holding the potential at -0.350 V for six hours resulted in about a thousand-fold decrease in the current density.

Figure 1, as well as other experimental data, indicates that copper dissolved anodically without the formation of a protective film, whereas a film which decreased the anodic reaction rate began to form at about -0.305 V versus SCE on the 70:30 cupronickel specimen. From consideration of the complexing of cuprous ions by chloride ions, it is calculated that Cu_2O should not become stable[3] at the potentials shown in Figure 1. On the other hand, NiO should be stable[4] at potentials above

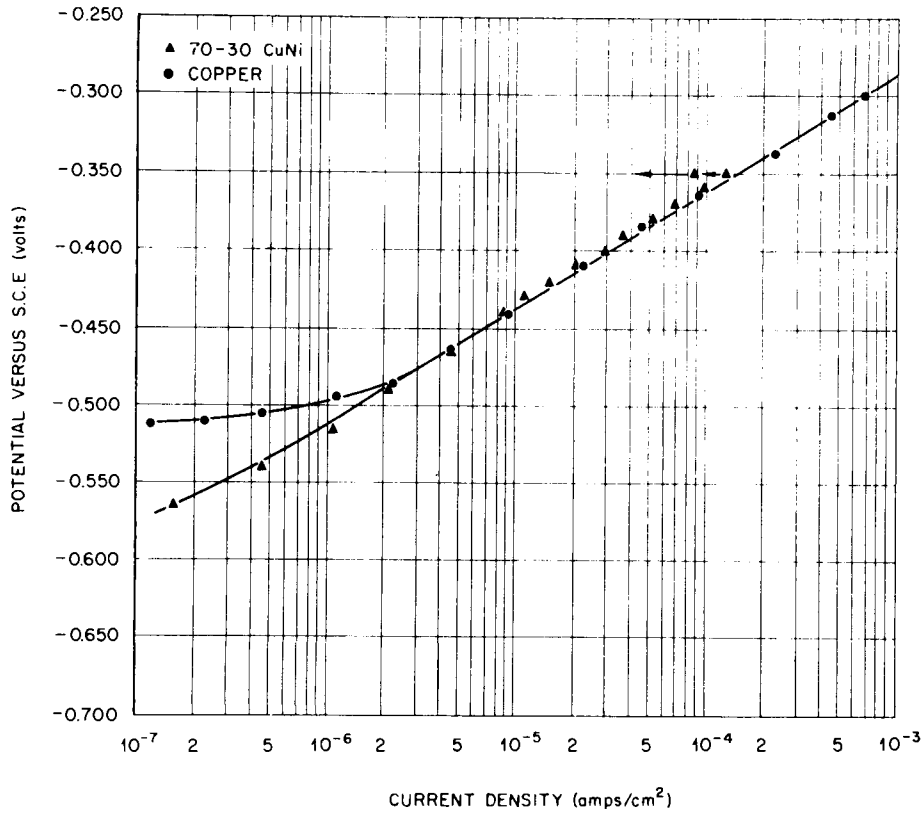

Figure 1. Anodic polarization curves obtained with copper and 70:30 cupronickel in 1.24 *M* NaCl at 100°C.

−0.65 V versus SCE; but Figure 1 indicates that, if it was present, it had no detectable influence on the anodic dissolution of 70:30 cupronickel up to −0.350 V versus SCE. At this potential, some higher valent nickel oxide may have become stable. The composition of films formed on 70:30 cupronickel at different potentials in chloride solutions has not been determined although this is an important aspect in understanding the corrosion process of the alloy in salt water.

EXPERIMENTAL PROCEDURES

Specimens used in the polarization experiments were machined from 1/16 inch-thick sheet stock. The 70:30 cupronickel was obtained from a commercial vendor and had the following composition: 68.86% Cu, 29.93% Ni, 0.67% Fe, 0.44% Mn, 0.10% Zn, and 0.005% Pb. The nickel specimen was made from nickel-200 (International Nickel Co.) which has a nominal composition as follows: 99.5% Ni, 0.25% Mn, 0.15% Fe, and 0.06% C. The 1.24 *M* NaCl solutions were prepared from reagent

grade material and triply distilled water. Polarizations were carried out potentiostatically in a 3-litre Pyrex flask under boiling reflux conditions. Purified hydrogen was bubbled through the solutions during the experiments. Potentials were measured with a high impedence electrometer using an external SCE bridged into the cell.

One 70:30 cupronickel specimen was anodized potentiostatically at −0.500 V versus SCE in the boiling solution. At this potential the alloy is in the active region. Over a period of 80 minutes the current was constant at 1.5×10^{-5} amps/cm^2. Another 70:30 cupronickel specimen was anodized at −0.350 V versus SCE, the potential where passivation began. Over a period of six hours the current density decreased from 1.5×10^{-4} to 2×10^{-7} amps/cm^2. A pure nickel electrode was anodized at −0.350 V versus SCE for 3 hr. Its current density decreased from 3×10^{-4} to 3×10^{-6} amps/cm^2. After anodization, all specimens were rinsed in distilled water and stored dry until examined.

An attempt was made to obtain a spectrum that would be representative of the unoxidized cupronickel substrate. The specimen was prepared by scraping the surface of a coupon of 70:30 cupronickel with the sharp edge of another piece of the same alloy. Exposure to air was allowed during the scraping.

Photoelectron spectra were measured with an electrostatic spectrometer developed by Pullen et al.[5] in the ORNL Physics Division. The instrument is double focusing with a mean radius of 20 cm for the spherical analyzer plates. A resolution of 0.05% could be obtained; however, for this work slit settings were chosen such that the resolution was 0.10%.

RESULTS

Figure 2a shows the spectrum of the surface of a 70:30 cupronickel specimen anodized at a potential of −0.500 V versus SCE which is well below the passivation potential. The peak, located at a binding energy of 75 eV, is due to electrons ejected from the $3p$ levels of copper, whereas the smaller peak, at a binding energy of 67 eV, is due to electrons ejected from $3p$ levels of nickel. The peak at a binding energy of 931 eV is due to electrons ejected from $2p_{3/2}$ level of copper, and that at a binding energy of 854 eV was caused by electrons ejected from the $2p_{3/2}$ level of nickel. In Figure 2a the copper peaks were more intense than the nickel peaks. This indicates that the composition of the surface layers is not greatly different from the bulk composition of the alloy. The ratio of the intensity of the Cu $3p$ peak to that of the Ni $3p$ peak for Figure 2a is about 2:1. If the surface layer had exactly the same relative metallic composition as the alloy, the ratio should be 7:3, assuming the cross sections for Cu $3p$ and Ni $3p$ electrons to be the same. Since the orbital configurations and binding energies are very nearly the same, this assumption should be valid.

Figure 2b is the spectrum of the surface of a 70:30 cupronickel specimen anodized in sodium chloride at the passivation potential, −0.350 V versus SCE. The nickel peaks in this spectrum are more intense than the copper peaks. Thus, it

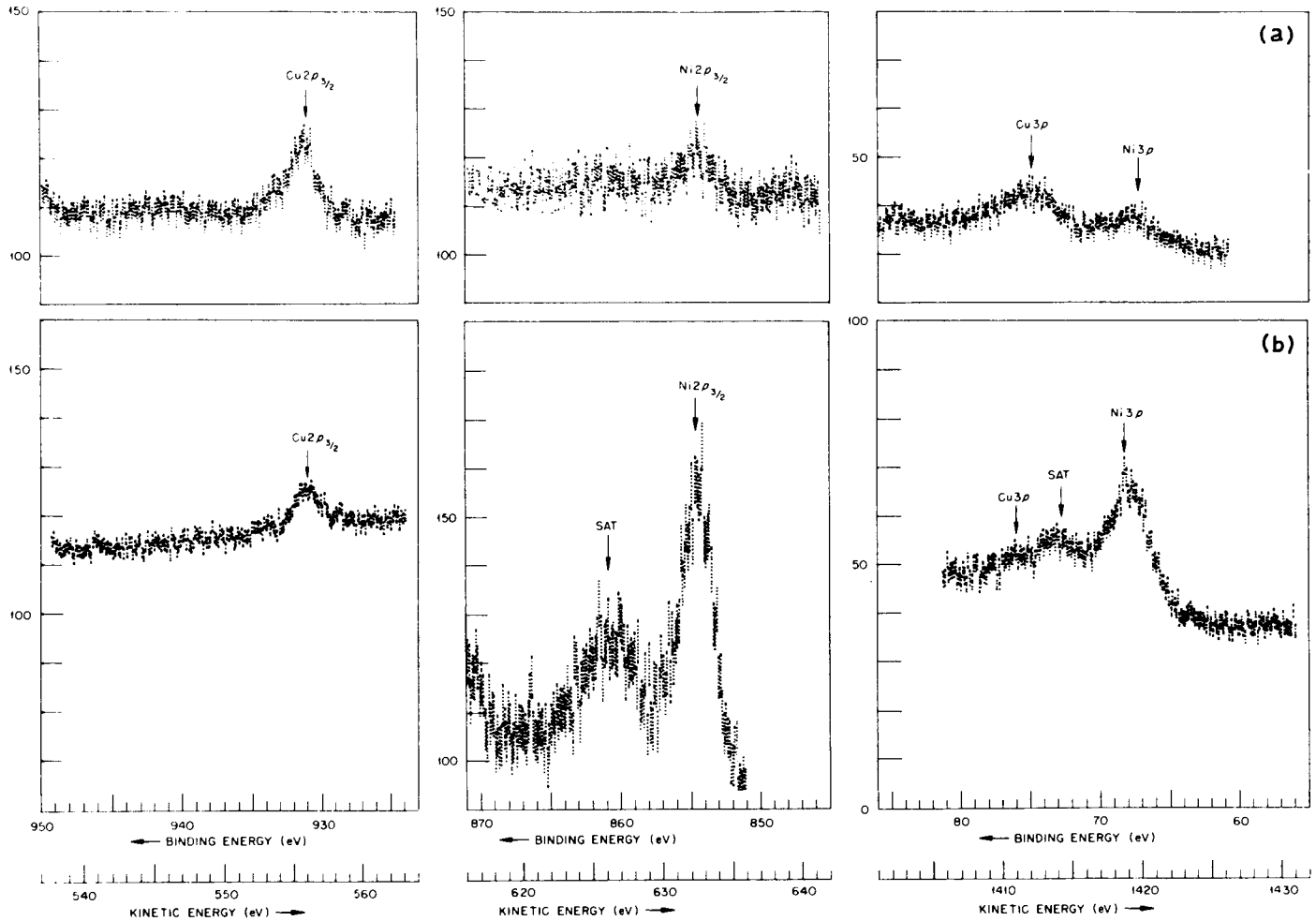

Figure 2. Photoelectron spectra of anodized 70:30 cupronickel alloy. (a) anodic potential = −0.500 V versus SCE, and (b) anodic potential = −0.350 V versus SCE.

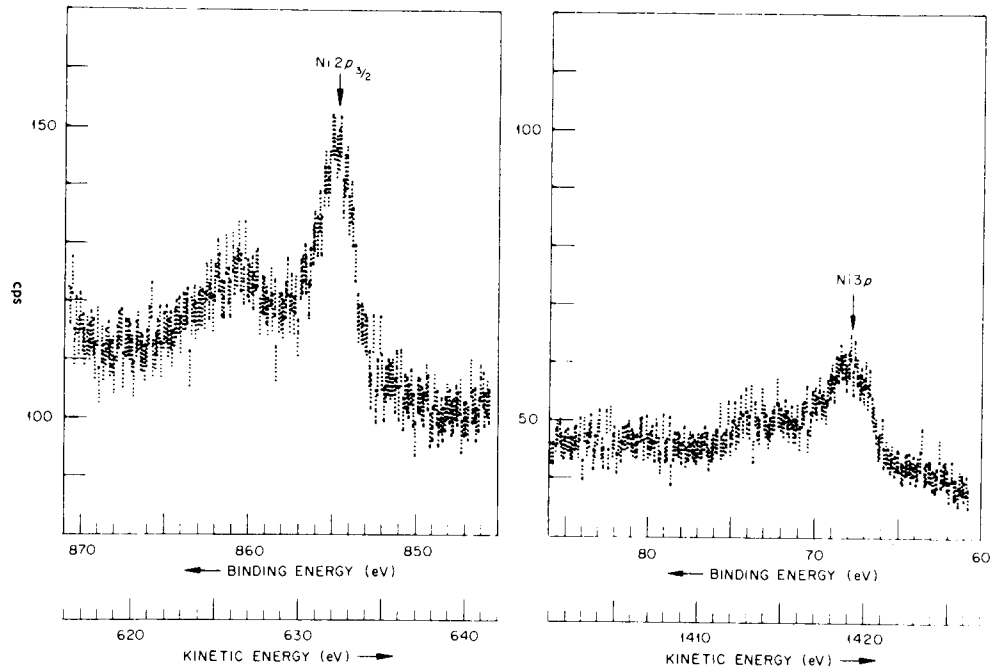

Figure 3. Photoelectron spectra of nickel anodized at −0.350 V versus SCE in 1.24 *M* NaCl at 100°C.

appears that the film on the passivated cupronickel contained predominantly nickel. The lower energy satellite (marked "SAT") to the Ni $2p_{3/2}$ peak is not due to a chemical shift or to another element. Also, the broadening of the Ni 3*p* peak (also marked "SAT") is not caused by the "normal" type of chemical shift. These satellite peaks will be discussed in the final section of this paper. The Cu 3*p* peak is barely resolved above the background of the Ni 3*p* satellites. The Cu $2p_{3/2}$ peak is more prominent above background, but its intensity, relative to the nickel peaks, is small. Figure 3 is the photoelectron spectrum of the pure nickel specimen passivated at −0.350 V versus SCE. The Ni $2p_{3/2}$ and the Ni 3*p* peaks are very similar to those of cupronickel in Figure 2b.

Figure 4 is the spectrum of the surface of the 70:30 cupronickel specimen that was freshly scraped with another piece of the same alloy. As expected, the copper peaks predominate. After correcting for the background the ratio of the intensities of the Cu 3*p* and Ni 3*p* peaks is very close to 7:3. The Ni $2p_{3/2}$ peak is slightly complicated because of chemical shifts. The peak with the binding energy of 851 eV is probably due to unoxidized metal. The peak with a binding energy about 4 eV higher is due to nickel in the oxide state. A thin layer of nickel oxide was present because the specimen was exposed to air during preparation. The third peak, located at a binding energy of 861 eV is a satellite peak. The Ni $2p_{3/2}$ oxide peak and its satellite resemble very closely the peaks of Figures 2b and 3.

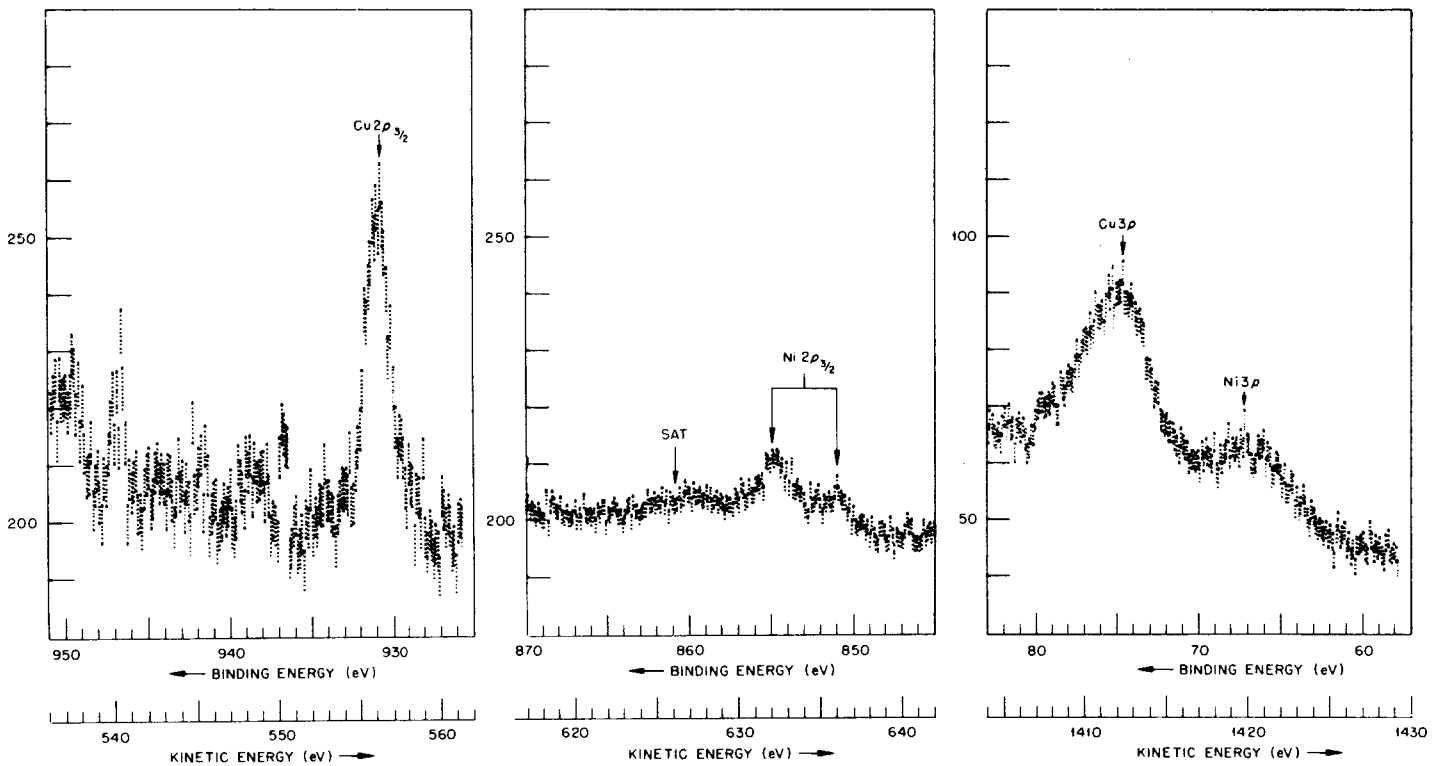

Figure 4. Photoelectron spectra of 70:30 cupronickel alloy.

Peaks due to silicon were noted in the spectra of all specimens exposed to the salt water solutions. The shift in binding energy indicated that the silicon was in the form of silicate, which probably originated from the pyrex flask that contained the solution. Sodium and chlorine, other possible contaminants, were not found.

DISCUSSION

The use of photoelectron spectroscopy in the study of thin solid films is a relatively new field and at this time the interpretation of such spectra is not completely clear in all cases. As pointed out earlier, the presence of elements is easily determined, usually without ambiguity, but some subtleties in the spectra are not always understood. The elements in the films examined in the study are clearly recognizable, but the significance or cause of the satellite peaks such as those associated with Ni $2p$ or $3p$ peaks is not clear. It is generally conceded, however, that these peaks are not the "normal" type of shift seen for light elements, which is due to changes in atomic charge densities. The "normal" type of shift does occur for heavy elements, but not to the extent of 6 eV or more seen in the spectra reported here. Rosencwaig et al.[6] reported Ni $2p$ satellites in many compounds other than nickel oxide. Their explanation involved the electron shakeup process. The satellites of the Ni $3p$ peaks could also be due to electron shake-up, but there is a possibility of multiplet splitting effects as reported by Fadley and Shirley[7] and Carver et al.[8].

Novakav and Prins[9] reported satellites to the Cu $2p$ peaks for copper oxide and showed that the satellite peaks were due to shake-up processes dependent on adsorbed oxygen or water vapor. He also reported the observation of satellite peaks for nickel oxide, but in this case it was not clear whether or not the satellites were due to absorbed oxygen.

A detailed explanation of the spectra obtained in this study is not possible at this time. Nevertheless the data show several aspects about the films formed on 70 : 30 cupronickel that were not generally known. At a potential below that of passivation, the relative concentration of copper and nickel at the surface is the same as in the alloy, indicating either the absence of a film or a film formed by uniform oxidation of the elements in the alloy. Since the anodic polarization curves of copper and 70 : 30 cupronickel are identical up to -0.350 V versus SCE, and since Cu_2O is thermodynamically unstable in this region, it seems probable that no film existed on 70 : 30 cupronickel below -0.350 V versus SCE. At -0.350 V versus SCE a film formed that significantly inhibited the anodic reaction. The photoelectron spectrum obtained from this specimen clearly showed that at least the outer portion of this film (perhaps up to 20 Å) was predominantly a nickel compound even though the alloy contains 70% copper. It should be noted that the spectrum of this film (Figure 2b) is very similar to that obtained from the passivated nickel surface (Figure 3), suggesting that the composition of the films on the two specimens were nearly the same.

We were hopeful that comparisons of the spectra obtained from the nickel

and cupronickel specimens with those of the bulk nickel oxide might provide some information on the chemical entities in the films. Spectra were taken of the black form of nickel oxide, which is believed to be nickel deficient and of the green form, which is more nearly stoichiometric. They were qualitatively different from the spectra of the protective oxide films. Kim and Davis[2] and other workers have also found that the NiO spectra vary strongly with the preparation history. It is clear that the base of fundamental information on nickel oxide spectra is not adequate. We therefore feel that a detailed interpretation of our spectra from thin films, with regard to valence states and defect structure, would be premature and probably incorrect. It is also clear, however, that NiO spectra are very rich in information about these details. After more fundamental work is done, we shall be able to extract considerably more knowledge from our spectra.

The fact that our data indicate no enrichment of copper on the surfaces of 70:30 cupronickel specimens regardless of polarizing potential was rather surprising in view of some results obtained by us (unreported) as well as by others[10]. Specimens of 70:30 cupronickel (as well as other alloys) exposed to salt water solutions for extended periods of time are usually covered with a thin film which has been shown by X-ray diffraction to be Cu_2O with no detectable nickel present in the film. It has been assumed, at least in some cases, that the *in situ* formation of Cu_2O and soluble nickel ions are the corrosion products. However, the present data show conclusively that the initial films that form on 70:30 cupronickel are not Cu_2O. Below the passivation potential the film, if it exists at all, contains nickel and copper in the same ratio as the alloy, whereas at the passivation potential, and presumably even at higher potentials (up to the pitting potential), the film contains predominantly nickel. Thus the presence of Cu_2O films on 70:30 cupronickel that has been exposed to sodium chloride solutions for long periods of time must be accounted for by a different mechanism. One possible explanation is hydrolysis of cuprous ions in the bulk solution with subsequent deposition on available surfaces.

ACKNOWLEDGMENTS

The authors are very grateful to T. A. Carlson and to the Physics Division, ORNL, for allowing us to use the double focusing electron spectrometer. The numerous discussions with T. A. Carlson, G. E. McGuire, and J. C. Carver were very helpful in the assimilation of ideas in this paper. We will also express our appreciation to K. S. Kim and R. E. Davis, Purdue University, for making available to us a preprint of their work on nickel–oxygen surfaces. Discussions with E. G. Bohlmann, Reactor Chemistry Division, ORNL, about corrosion problems have been very helpful in this work.

POSTSCRIPT

After this paper was submitted for publication, the work of Castle appeared in the literature[11]. He reports that oxide films formed on 70:30 and 50:50 cupro-nickel alloys are richer in copper than nickel. His treatment of the alloys was by high temperature oxidation in gas phase, however, rather than by anodization in liquid media.

REFERENCES

1 T. A. Carlson and G. E. McGuire, *J. Electron Spectrosc.*, 1 (1972/73) 161.
2 K. S. Kim and R. E. Davis, *J. Electron Spectrosc.*, to be published.
3 W. M. Latimer, *The Oxidation States of the Elements and Their Potentials in Aqueous Solution*, Prentice-Hall, New York, 1952, p. 186;
W. M. Latimer and J. H. Hildebrand, *Reference Book of Inorganic Chemistry*, The Macmillan Co., New York, 1947, p. 506.
4 H. J. de Bethune and N. H. Swendeman Land, *Standard Aqueous Electrode Potentials and Temperature Coefficients*, Clifford A. Hampel, Skokie, Ill., 1964.
5 B. P. Pullen, T. A. Carlson, W. E. Moddeman, G. K. Schweitzer, W. E. Bull and F. A. Grimm, *J. Chem. Phys.*, 53 (1970) 768.
6 A. Rosencwaig, G. K. Wertheim and H. J. Guggenheim, *Phys. Rev. Lett.*, 27 (1971) 479.
7 C. S. Fadley and D. A. Shirley, *Phys. Rev. A*, 2 (1970) 1109.
8 J. C. Carver, T. A. Carlson and G. Schweitzer, *J. Electron Spectrosc.*, to be published.
9 T. Novakov and R. Prins, in D. A. Shirley (editor), *Electron Spectroscopy (Proc. Int. Conf. at Pacific Grove, Calif., 1971)*, North-Holland Publ. Co., Amsterdam, 1972, p. 821.
10 R. F. North and M. J. Pryor, paper (No. 83) presented at *National Association of Corrosion Engineers Meeting, 1969, Houston, Texas.*
11 J. E. Castle, *Nature Phys. Sci.*, 234 (1971) 93.